THE UNIVERSITY OF CALGARY

Methane Oxidation in Soils as a Tool for Reducing Greenhouse Gas Emissions

by

Vincent Bradley Stein

A THESIS

SUBMITTED TO THE FACULTY OF GRADUATE STUDIES

IN PARTIAL FULFILMENT OF THE REQUIREMENTS FOR THE

DEGREE OF MASTER OF SCIENCE

DEPARTMENT OF CIVIL ENGINEERING

CALGARY, ALBERTA

JANUARY, 2000

Abstract

Current concern over the potentially negative impacts of climate change has brought attention to anthropogenic sources of methane, a primary greenhouse gas. Two such emission sources are methane leakage at heavy oil wells and sanitary landfills. At both of these sources, some quantities of methane could potentially be oxidised by methanotrophic microbes living in soils. Optimization of this phenomenon may serve as an inexpensive technique for reducing emissions from these sources.

Soil column and batch incubation experiments were performed to gain a better quantitative understanding of the biological and physical processes limiting CH_4 oxidation in soils. A numerical reactive-transport model was developed which, given soil biological kinetic parameters as input, can predict gas concentration profiles and CH_4 oxidation rates with a high degree of accuracy. The model was verified by reproducing the experimentally observed results of soil column experiments performed in this study and in those of an independent researcher.

ACKNOWLEDGEMENTS

This research was funded by Husky Oil Operations Ltd., the Canadian Association of Petroleum Producers, and a grant from the National Science and Engineering Research Council. The author also acknowledges the financial support provided by the University of Calgary in the form of an assistantship.

Thanks to my supervisor, Dr. Patrick Hettiaratchi, for his guidance and support in the development of this thesis and to Dr. Gopal Achari for assisting with the numerical modeling component of this research.

The machining of the soil columns was undertaken by Charlie Imer of the Engineering Faculty Machine Shop. Dave Dechka and Rob Scorey assisted with the design and construction of the laboratory apparatus. Harry Pollard and Heather Mills provided technical and logistical support. Wendy Morris and Susan Anand helped with the administrative aspects of this project.

Finally, thanks to my family, friends, and loving wife Nicole.

Table of Contents

List of Tables

List of Figures

Chapter 1. Introduction

1.1 General

Global climate change caused by anthropogenic emissions of radiatively active gases may present a serious threat to the future of the Earth's environment. Methane (CH_4) is a radiatively active trace gas whose concentration has increased significantly during the past few hundred years. Its relative contribution to the increase in radiative forcing since pre-industrial times is estimated to be about 19% (IPCC, 1996b).

Oxidation of methane by methanotrophic bacteria provides an important sink for methane that would otherwise escape from freshwater, soil, and marine environments to the atmosphere. While soils have not been considered as significant sinks for methane until recently, methane consumption has been reported in agricultural soils, forest soils, tundra, and bogs (Topp and Hanson, 1991). Methane oxidising activity, with a decrease in soil oxygen and an increase in microbial biomass, has also been demonstrated in soils around leaks in natural gas pipes (Adams and Ellis, 1969) and in landfill covers (Whalen et al., 1990).

The phenomenon of methane oxidation in soils could potentially have a strong mitigating effect on CH_4 emissions from sources such as heavy oil well sites and landfills, and the optimisation of this process may serve as an inexpensive strategy for reducing emissions of this potent greenhouse gas. Three options are available for exploiting this phenomenon at a variety of specific field sites:

1. optimisation of the CH_4 oxidation process through the selection, design and maintenance of soil covers.

2. manipulation of existing soil covers to increase their CH_4 oxidising potential;
3. the use of CH_4 oxidising biofilters for attenuating point source emissions. This could entail the use of an elaborate actively aerated biofilter, or simply channelling and distributing CH_4 gas through an existing layer of topsoil.

Before these techniques can be applied, however, some of the questions that need to be answered are:

1. what soil cover properties and minimum thicknesses are required to effect optimal CH_4 oxidation?
2. what are the maximum oxidation rates that can be expected in a biofilter or modified cover design?

To answer these questions, a thorough understanding of how environmental variables and soil properties limit a soil's CH_4 oxidation potential is needed. While work has been carried out to study the effects that environmental variables such as temperature, moisture content and oxygen concentration have on CH_4 oxidation, these studies have generally not included investigations into the effects that mass transfer limitations have on the overall CH_4 oxidation rate in soil covers.

1.2 Overall Approach

To provide a better quantitative understanding of the biological and physical processes related to CH_4 oxidation in soils than is currently available in literature, soil column

experiments were chosen for this study because they allow one to quantify the reductions in CH_4 oxidation associated with O_2 mass transfer limitations. Soil column experiments also present the opportunity to investigate whether the techniques used by others for estimating in situ CH_4 oxidation rates are valid.

In addition to soil column experiments, it was decided that a numerical reactive-transport model that is capable of estimating CH_4 oxidation rates in soils be developed, as it would also serve as a valuable tool for answering the two question posed above. In addition to providing greater understanding of the physical processes associated with CH_4 oxidation in soils, it could aid in the design of CH_4 oxidative soil cover systems by reducing the number of laboratory experiments required to determine the optimal soil properties and thickness for a given environment. Such a model could aid in the refinement of global landfill methane emission inventories. Most of the models used to estimate methane emissions from landfills assume that 100% of the methane generated within a landfill is emitted into the atmosphere. Those models that do account for methane oxidation merely assume that some constant fraction (usually 10%) of the methane is oxidised in the soil cover. At present, sufficient information is not available to accurately estimate the methane oxidation potential of methanotrophic microbes living in various types of soils and in various climates.

1.3 Specific Objectives

The specific objectives of this research are:

- To quantify the rate of biological CH_4 oxidation that would occur in a variety of soils using soil column experiments.
- To develop a numerical model that is capable of predicting soil gas concentration profiles and CH_4 oxidation rate as a function of soil physical properties and biological kinetic parameters.
- Use the numerical model to determine the theoretical maximum CH_4 oxidation rates that can occur in soil covers, based on O_2 mass transfer limitations associated with soil properties and the advective displacement of O_2 by migrating CH_4.
- Determine whether the techniques currently used for estimating in situ CH_4 oxidation give accurate results. Several authors have used batch incubation experiments for estimating in situ CH_4 oxidation in landfill soil covers, but it has yet to be determined whether the CH_4 oxidation rates of these disturbed soil samples are equal to their in situ rates.
- Determine whether a predictable relationship exists between a soil's gas composition and the biological kinetic parameters of its microbial populations.

Chapter 2. Literature Review

2.1 Methane and Climate Change

Methane has a global warming potential (GWP) of 21 with reference to a 100 year time horizon (IPCC, 1996a); i.e. over the course of 100 years, the cumulative direct effect on the atmosphere's energy budget resulting from a one-kilogram release of methane is 21 times the direct effect of a one-kilogram release of carbon dioxide (CO_2). Methane also has a much shorter atmospheric lifetime than CO_2 which means that its global warming potential is higher for shorter time horizons. For example, its GWP is 56 with reference to a 20 year time horizon (IPCC, 1996a). Therefore, the short term warming caused by a unit emission of CH_4 is much higher than the long term warming. On short time-scales, 1990's CO_2 emissions contribute over half of the direct effects of 1990's total GHG emissions, and methane almost 30% (Isaksen et al, 1992). Since methane's radiative forcing adjusts more rapidly to increases or decreases in emissions than does CO_2, its atmospheric concentration could be stabilised within a relatively short period with substantial near-term warming mitigation.

Anthropogenic CH_4 sources are estimated to contribute approximately 60-80% of the estimated 460-660 teragrams (Tg) of CH_4 emitted annually to the atmosphere (IPCC, 1996a). Based on a study which used the IPCC scenarios for future emissions of the greenhouse gases, the reductions in warming through the year 2050 that could be achieved by stabilising CH_4 concentrations would be similar to the reductions attainable through capping CO_2 emissions at 1990 levels (Hogan and Kruger, 1992). If CH_4

emissions were held constant at 1984-1994 levels, then methane levels would rise from 1720 to about 1850 ppbv over the next 40 years. However, if emissions were cut by 30 Tg (CH_4)/yr, about 8% of anthropogenic emissions, then methane concentrations would be stabilised at today's levels (IPCC, 1996b). Such efforts could produce positive results in a relatively short time frame.

2.2 Methane Emissions from Heavy Oil Production

Carbon isotope measurements indicate that about 20% of the total annual global methane emissions are related to the production and use of fossil fuel (IPCC, 1996a). One source of atmospheric methane emission related to the production of fossil fuel that has received recent attention is the methane leakage from outside the wellbore casings at oil and gas wells and from open hole abandonments. This leakage is caused by the disruption of the earth's surface associated with drilling, which allows gases held in the earth to migrate to the surface (see Figure 2-1) (Rich, 1995).

Current regulations in Alberta stipulate that any detectable gas leakage must be eliminated to satisfy the surface restoration requirements of well-site lease abandonment. Only under special situations, in which serious attempts by operators fail to completely eliminate the surface casing vent flow, will the Alberta Energy and Utilities Board reconsider its "zero tolerance" requirement for lease abandonment. Many wells in Alberta and Saskatchewan have reached the end of their economic lives. However, abandonment has been delayed for those wells with gas leakage, for lack of a technically reliable and economical way of stopping gas leakage (Schmitz et al., 1994). Schmitz et

al. (1993) have reported poor results with remedial work overs at 21 well sites with methane gas leakage.

Erno and Schmitz (1996) identify two types of CH_4 leakage: soil gas migration and surface casing vent flow.

Figure 2-1: Schematic of typical well completion

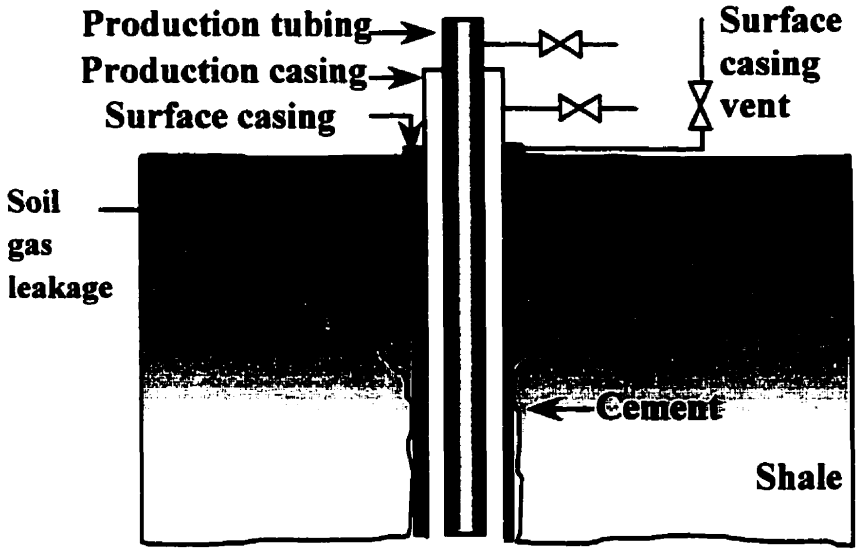

2.2.1 Soil Gas Migration

Methane gas has been observed to migrate in soils outside the outermost casing (either production or surface casing) of oil and gas wells, and escape into the atmosphere. These CH_4 emissions have not been accurately quantified, due to the lack of reliable well site emission monitoring data and effective reporting mechanisms. However, studies have been carried out to quantify the CH_4 gas migration from heavy oil production sites near Lloydminster, Alberta (Jocksch et al., 1993; Schmitz et al., 1994; Schmitz et al, 1993). Erno and Schmitz (1996) investigated CH_4 soil gas migration in the Lloydminster area,

and reported that 45% of the wells had detectable soil gas migration in the immediate vicinity of the well. Gas migration rates were mostly less than 0.01 m^3/day, and no well exceeded migration rates of 60 m^3/day. They indicated that gas leakage from soil was limited to an area near a well casing, and was rarely detectable beyond a 3m radius. Assuming that the CH_4 flux was uniformly distributed within this 3m radius, the maximum CH_4 flux at these sites would be 1400 $g*m^{-2}*day^{-1}$.

During the migration of CH_4 in soils adjacent to these wells, some quantities of methane could potentially be oxidised by methanotrophic microbes. Although this phenomenon is known to oil and gas operators, because of the lack of credible data, soil methanotrophy has not been used as a technique to control methane gas emissions at well sites.

2.2.2 Surface Casing and Production Casing Vent Flow

In wells completed with a surface casing, a vent flow can be detected in the annulus between the production and surface casing (see Figure 2-1). Erno and Schmitz (1996) investigated flow rates of surface casing vent flows in the Lloydminster area. They reported that 23% of the wells had surface casing vent flows. For the majority of wells, gas flow-rates ranged from 0.01 m^3/day to 100 m^3/day.

In a University of Calgary study that attempted to quantify production casing gas venting, 854 of the 953 wells for which data were available wells were determined to be venting production casing gas, with a total of emission rate of $3.94*10^5$ m^3 of gas per day. Flow-rates varied from 1 m^3/day to 25600 m^3/day. About 38% of the wells vented

less than 50 m^3/day. Two-thirds vented less than 300 m^3/day (Yang, 1999). Based on these figures, it is apparent that gas utilization at most well sites would be difficult due to the small volume of available gas, therefore inexpensive on-site treatment methods would be required. For a treatment technique to be economically feasible, the costs associated with reducing CH_4 emissions can not exceed a few dollars per equivalent tonne of CO_2 treated.

Recently, biological oxidation of CH_4 has attracted much attention from the research community due to a renewed interest in biofiltration as an inexpensive waste gas treatment mechanism and the potential benefits of oxidation of CH_4 by indigenous bacterial populations. Biofiltration is also seen as an attractive treatment technique in light of recent criticisms brought against flaring, which has been identified as a source of gaseous emissions capable of causing human health and environmental problems (Strosher, 1996). For these reasons, optimization of CH_4 oxidation for biofiltration applications is seen as a primary research need.

2.3 Methane Emissions from Landfills

Another significant source of anthropogenic CH_4 emission is the sanitary landfill, specifically, the ones accepting biodegradable municipal solid waste (BMSW). The anaerobic decomposition of landfilled BMSW generates large amounts of gas composed of approximately 50-60% CH_4 (by volume), 40-50% CO_2, and other trace gases such as nitrogen and volatile organic hydrocarbons (VOCs) (Kightley et al., 1995; Czepiel et al., 1996). Landfills are estimated to account for approximately 25% of annual

anthropogenic CH_4 emissions in the United States (Czepiel et al., 1996) and as much as 20% of the global anthropogenic CH_4 emissions (Nozhevnikova et al., 1993). Table 3 contains a list of the landfill CH_4 flux rates observed by several researchers. It can be noted that the maximum observed CH_4 flux rates of fugitive emissions from the soil surrounding heavy oil wells near Lloydminster is comparable to the maximum flux rates observed at landfills. For this reason, some of the research done on soil methanotrophy at heavy oil well sites may apply to landfills.

Table 2-1. Observed landfill CH_4 flux rates.

Landfill location and cover soil type	Observed CH_4 flux ($g*m^{-2}*day^{-1}$)	Reference
Illinois landfill with gas control system	0.003 – 20	Czepiel, et al.,1996a
New Hampshire landfill sandy clay loam	0 – 1495 (mean = 61.0)	Czepiel, et al.,1996b
Moscow landfill sandy clay mixture	0 - 31.2	Nozhevnikova et al., 1993
California landfill Unvegetated, granular soil	5.26 - 31.39	Bogner and Spokas, 1993
Essex landfill w/ 40-60 cm cover w/ sealing layer of clay	site 1 yearly average: 21.76 site 2 yearly average: 39.84	Jones and Nedwell, 1993
Various landfills in Illinois and California	0.003 – 1000	Bogner et al., 1995

Most of the global methane emission inventories are based on empirically derived mathematical models which assume that 100% of the methane generated within landfills is emitted into the atmosphere. The main argument against this assumption is that a significant proportion of the landfill methane could potentially be oxidised and converted to carbon dioxide by methanotrophic microbes living in soils used as cover material. By neglecting this potential source of methane conversion, many current global methane emission models over-estimate the contribution from landfills to the global methane

budget. Some laboratory studies of methane consumption by bacteria found in landfill cover soil suggest that 10% of methane gas is oxidised (Bogner and Spokas, 1993), while others have suggested that as much as 50% of methane is oxidised before reaching the surface (Whalen et al., 1990; Nozhevnikova et al., 1993). However, at present, sufficient information is not available to accurately estimate the methane oxidation potential of methanotrophic microbes living in various types of soils and in various climate conditions, therefore precluding incorporation of CH_4 oxidation in CH_4 emission models.

In addition to aiding in the refinement of global methane emission inventories, a better understanding of soil methanotrophy may serve as a means of mitigating landfill CH_4 emissions. When designing landfill covers, the potential exists to manipulate the soils in a manner that maximises CH_4 oxidation. Presently, landfills are designed with impermeable clay caps to "entomb" the waste. However, a permeable soil cap would be more effective in stimulating methane oxidation, for reasons previously mentioned.

In the past, two approaches for reducing CH_4 from landfills have been adopted:

1. recovering and using or burning the gas; and
2. reducing the source (e.g. recycling paper products, composting and incineration).

Only the first approach--recovering and using or burning the gas, reduces CH_4 emissions from existing landfills. Recovering and utilising landfill gas is an economically attractive option for reducing methane emissions, provided that the landfill is large enough. For initial screening purposes, the U.S. EPA considers only landfills containing more than 900,000 tonnes of waste to be capable of generating enough energy to support a CH_4

recovery project (Biggs and Bashki, 1996). For this reason, gas recovery would be economical only at landfills near larger urban centres.

Microbial CH_4 oxidation might provide a means of controlling CH_4 emissions at sites where landfill gas recovery is not practised. It may also serve as a means of complementing the emission control afforded by landfill gas recovery, as some researchers have found that conventional gas recovery systems are only capable of capturing between 50 and 95 percent of the generated CH_4 (Augenstein and Pacey, 1996).

2.4 Role of Methanotrophs in CH_4 Oxidation

2.4.1 Methanotrophic Bacteria

Methyltrophs are micro-organisms that can use one-carbon compounds which are more reduced than carbon dioxide (e.g. CCl_4, CH_4, etc.) as their sole sources of carbon and energy. Methanotrophic bacteria are the subset of methyltrophs that possess the specific enzyme methane mono-oxygenase which enables them to utilise methane as a sole source of energy and as a major carbon source, allowing them to catalyze the following oxidative reactions (Haber et al., 1983):

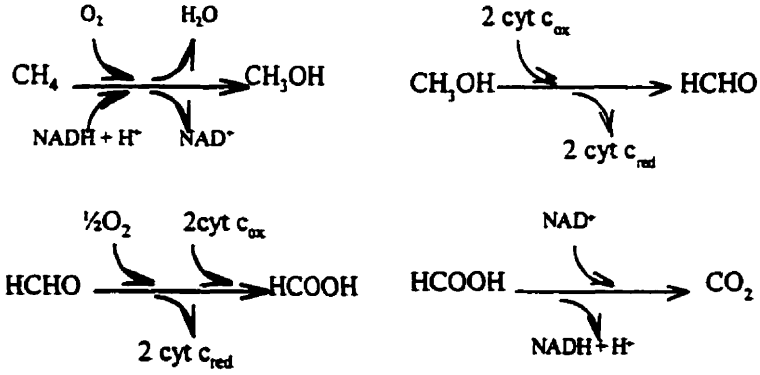

(2-1)

The methane monooxygenase enzyme system permits the introduction of an oxygen atom into the methane molecule, leading to the formation of methanol (the requirement for O_2 as a reactant in the initial oxidation explains why all methane oxidizers are obligate aerobes). They oxidise methane through methanol to formaldehyde, which they then either assimilate for the synthesis of cell material or further oxidise to carbon dioxide. All methanotrophic bacteria isolated and characterised to date have been gram negative, obligately aerobic, and have possessed intra-cytoplasmic membranes (Topp and Hanson, 1991). Most methane-oxidizing bacteria are obligate methyltrophs, unable to utilize compounds with carbon-carbon bonds. However, bacteria of one genus, *Methylobacterium*, are faculative methyltrophs, capable of utilizing organic acids, ethanol, and sugars (Brock, et al., 1984). Methanotrophs are also capable of oxidizing a larger number of substrates that do not serve as carbon and energy sources, a process known as "cometabolism" (Brock, et al., 1984).

There seem to be two types of methanotrophic bacteria that exist in soils (Bender and Conrad, 1994). They are:

1. *Low CH_4 oxidation capacity microbial populations*: This type of methanotrophic population is capable of oxidising methane when it is present in atmospheric concentrations (i.e. 1.7 ppm). These populations are characterised by a low capacity for CH_4 oxidation (i.e. a low V_{max}, where V_{max} is defined as the rate of CH_4 oxidation when CH_4 is not limiting). These populations are also characterised by a high affinity for CH_4 (i.e. a low K_{app}, where K_{app} is defined as the concentration of CH_4 which results in a CH_4

oxidation rate equal to one half of V_{max}). In environments with low CH_4 mixing ratios (e.g. atmospheric mixing ratios), no correlation has been observed between the CH_4 oxidation activity and the numbers of methanotrophs enumerated by the Most Probable Number technique (MPN) (Bender and Conrad, 1994). These bacteria have yet to be isolated in the laboratory.

2. *High CH_4 oxidation capacity methanotrophs*: This type is found only in soils that are, at least, temporarily exposed to elevated CH_4 concentrations, such as landfill covers, tundra soils and soils above natural gas reservoirs. These populations have a high capacity for CH_4 oxidation (high V_{max}) and a relatively low affinity for CH_4 (high K_{app}) (Bender and Conrad, 1992). They are the methanotrophic bacteria that have been isolated and characterised using standard techniques, such as plating serially diluted samples onto various agar media and counting the number of colonies formed following incubation under an atmosphere of methane and air (Topp and Hanson, 1991).

The remainder of this thesis is concerned with the latter type of methanotrophic bacteria and their potential for attenuating anthropogenic methane emissions such as those associated with landfills and heavy oil well sites. Maximising this potential necessitates a thorough understanding of how methanotrophs are affected by environmental conditions.

2.4.2 Factors Affecting CH_4 Oxidation

Proper environmental conditions are fundamentally important to microbial growth and survival. If environmental conditions such as temperature, moisture content and oxygen concentration are not suitable, microbial growth and survival will be adversely affected, resulting in non-optimal biodegradation. In soil systems, soil type also plays a significant role in determining the efficiency of biodegradation. Some studies have been conducted on how these and other factors influence methane oxidation in soils. The findings of these are briefly described below.

2.4.2.1 Methane Concentration

The CH_4 oxidation rate is a function of the CH_4 concentration, and exhibits typical Michaelis-Menten characteristics (Bender and Conrad, 1992; Czepiel et al., 1996b). The CH_4 oxidation rate versus CH_4 concentration is described by the following equation:

$$v = \frac{V_{max} \times [S]}{K_{app} + [S]} \qquad (2\text{-}2)$$

where:

v = CH_4 consumption rate ($g^{*}day^{-1}{}^{*}g$ dry $weight^{-1}$)

[S] = CH_4 mixing ratio [ppmv] in air

V_{max} = maximum CH_4 consumption rate ($g^{*}day^{-1}{}^{*}g$ dry $weight^{-1}$)

K_{app} = half saturation constant [ppmv]

The rate of oxidation is linearly proportional to the amount of CH_4 present when CH_4 concentrations are low (first order kinetics); the rate is independent of the amount of CH_4 present when CH_4 concentrations are high, but instead occurs at a maximum value, V_{max} (zeroth-order kinetics). The kinetic parameters of methanotroph populations observed by four authors are presented in Table 2-2.

Table 2-2: Kinetic parameters of methanotrophs exhibiting high CH_4 activity.

Soil origin and type	V_{max} (nmol*h^{-1}*g dry soil^{-1})	K_{app} (ppm)	Reference
Forest soil above natural gas source in Switzerland	44500	100 000	Bender and Conrad, 1994
New Hampshire landfill Sandy clay loam	40 - 2594	195-5847	Czepiel et al., 1996b
Essex, UK landfill Coarse sand	998	3793	Roslev and King, 1994
Moscow landfill Sandy clay mixture	5000 - 25000		Nozhevnikova et al., 1993

King (1992) reported that maximal oxidation rates (V_{max}) correlate well with methane flux rates. This suggests that the supply of methane to the zone of oxidation may determine V_{max}. However, it has yet to be determined whether there exists a predictable relationship between V_{max} and the rate of CH_4 flux among diverse sites. Czepiel et al. (1996) attempted to use linear regression techniques to represent the dependence of the V_{max} values at the depth of maximum oxidation on in situ CH_4 mixing ratios at that depth, and observed a linear relationship with a correlation coefficient of 0.68. The least squares fit of their data gives the following equation:

$$V_{max} = 50 * C_{CH4} \qquad (2\text{-}3)$$

Where:

V_{max} = Maximum CH_4 oxidation rate (nmol * hour^{-1} * g dry soil weight^{-1}) at the depth of maximum oxidation

C_{CH4} = The in situ soil gas CH_4 mixing ratio at a depth of 7.5 cm

Roslev and King (1994) demonstrated that methanotrophs could survive extended periods in the absence of CH_4. Methanotrophic cultures were seen to maintain oxidation activity after methane deprivation periods of up to 42 days. Kightley et al. (1995) observed that after interrupting the CH_4 supply to soil cores for eight days, the oxidation activity returned to previous steady-state rates almost immediately after CH_4 supply was re-established. Their findings show that a healthy population of methanotrophs would be maintained in a soil system subjected to intermittent methane flow. This is an important fact with regard to the control of surface casing vent gas, which typically exhibits intermittent flow-rates.

2.4.2.2 Oxygen Concentration

Methane oxidation by methanotrophic microbes occurs predominantly in environments where methane and oxygen (O_2) occur simultaneously. While there are some circumstances in which anaerobic methane consumption occurs, such as in sulphate reducing environments, methane oxidation is dominated on a global scale by aerobic consumption (King, 1992). Therefore in most situations, proper oxygen concentrations are essential for methane to be microbially oxidised. Methane oxidation activity has been observed to drop off at O_2 mixing ratios of less than 3%, but is only slightly sensitive to changes in O_2 concentrations at mixing ratios above 3% (Bender and Conrad, 1994; Czepiel et al., 1996b).

The potential for CH_4 oxidation in soils is therefore related to the depth of O_2 penetration, which regulates the areal extent to which the methanotrophic community can develop. The depth of O_2 penetration will depend on at least three factors: the gas permeability of the soil (which will depend on the soil particle size distribution, moisture content, and compaction status), the rate of displacement of the normal soil atmosphere by the upward movement of methane, and the microbial methane oxidation rate on a volume basis. For these reasons, the depth of O_2 penetration is highly site specific. The greatest depth at which CH_4 oxidation has been reported to occur in landfill soils is 70cm, indicating the presence of O_2 at such depths (Nozhevnikova et al., 1993).

2.4.2.3 Moisture Content

The response of soil CH_4 oxidation to varying moisture content has been investigated by several authors. They have observed a decrease in oxidising capacity at higher moisture contents, presumably due to a decrease in gas diffusion (CH_4 and O_2) between the soil and the gas phase (Whalen et al., 1990; Czepiel et al., 1996b; Adamsen and King, 1993; Koschorreck and Conrad, 1993). Gas diffusion at soil saturation is limited by the diffusion coefficient of CH_4 in water which is 4 orders of magnitude lower than in air.

These authors have also observed a decrease in oxidising capacity at lower moisture contents (e.g. 5% by weight), presumably due to a physiological response to water stress, resulting in lower microbial activity. Boeckx and Van Cleemput (1996) and Czepiel et al. (1996b) observed that the optimum moisture content for microbial methane oxidation lies between 10% and 20% (by weight) in sandy-loam and sandy-clay-loam

soils, respectively. Whalen et al. (1990) observed an optimum moisture content of 11% (by weight) in sand mixed with brown and grey clays.

2.4.2.4 Temperature

Several authors have quantified the response of microbial CH_4 oxidation to varying temperatures by manipulating temperature during soil sample incubations. This temperature response can be described by the Arrhenius relationship, in which oxidation increases exponentially to a distinct maximum, and then decreases with continued temperature increase (LaGrega et al., 1994). Optimum temperatures observed have been: 36°C (Czepiel et al., 1996), 31-36°C (Whalen et al., 1990), and 25-30°C (Boeckx and Van Cleemput, 1996). Nozhevnikova et al. (1993) observed that the methane consumption rate observed in enrichment cultures of methanotrophs at 6°C was 2.5 times lower than that of cultures developing at 25°C.

2.4.2.5 Soil Particle Size Distribution

The manner in which methane is microbially oxidised in soils is analogous to biofiltration. Biofiltration is a biological air-pollution-control technology that uses active microbial populations attached to a solid media to degrade gas-phase chemicals. When designing a biofilter, it is desirable to use a contact media consisting of finer particles, which have a high specific surface area. This maximises the attachment area, sorption capacity, and the number of reaction sites per unit volume (Swanson and Loehr, 1997). However, finer particles result in decreased gas permeability, which inhibits oxygen

penetration. For this reason, a trade off must be made between the microbial attachment area on the one hand, and maximising the gaseous diffusion and oxygen depth penetration on the other, in a manner which maximises overall methane oxidation. Therefore, an optimum particle size and pore space distribution must be determined.

After fractionating a forest soil into different grain size fractions, Bender and Conrad (Bender and Conrad, 1994) observed the greatest methanotrophic activity on particles of diameter between > 0.5 mm and < 2 mm. They concluded that aerated soils with a high content of sand should be the most favourable matrix for methanotrophic bacteria, possibly due to the facilitated gas diffusion in such "wide pore" soils with increased gas permeability. Kightley et al. (1995) found that porous, coarse sand soil developed a greater methanotrophic capacity than fine sand or clay soils. However, their coarse sand soil samples had previously been exposed to higher and more constant methane fluxes than their fine sand or clay samples, and may therefore have had larger, more active methanotrophic communities.

2.4.2.6 Nutrients

In addition to a carbon source, cellular metabolism requires numerous other elements as nutrients. The synthesis of cellular tissue requires much more phosphorous and nitrogen than other nutrients, so these macro-nutrients are often rate limiting. In engineered biological treatment systems, nitrogen and phosphorous are usually added as ammonia and orthophosphate. However, such conventional approaches may be ineffective with methanotrophic populations. Amending soil with ammonium ions (NH_4^+) has been

shown to substantially reduce CH_4 consumption (Steudler et al., 1989; King and Schnell, 1998). The exact mechanism responsible for this inhibition is controversial. Kightley et al. (1995) conducted experiments to determine the effects of nutrient amendments (specifically, NH_4NO_3, K_2HPO_4, and anaerobically digested sewage sludge) on CH_4 oxidation. Only the sewage sludge was observed to enhance methane oxidation (by 26%), whereas the NH_4NO_3 inhibited CH_4 oxidation, and K_2HPO_4 addition had no effect. Sewage sludge is a complex organic mixture consisting of various macro- and micro-nutrients. They concluded that the significant enhancement of CH_4 oxidation after amendment of soil with sewage sludge demonstrated that full development of the soil's methanotrophic community was limited by a lack of nutrient or nutrients. However, which specific micro- or macro-nutrients were rate limiting in their experiments is unclear. Hilger (1999) conducted experiments to test the effects of FeSO4, EDTA, a vitamin mix, and nitrate on CH_4 oxidation . Only nitrate showed stimulation of CH_4 oxidation in ungassed soil. However, when soil that had been gassed for several thousand hours and then retested with nitrate amendment, no stimulatory effect was observed.

Chapter 3. Experimentation

3.1 Overview

A primary objective of this study was to determine how to manipulate soils, such as those adjacent to heavy oil wells or those comprising landfill cover systems, in a manner which maximises their methane oxidation potential. To this end, laboratory experiments were carried out to investigate the effects of environmental variables and soil mass transfer properties on methane oxdidation and to provide data for the calibration and verification of a numerical reactive-transport model.

3.2 Soil Column Experiments

Most of the work performed to date investigating the factors which influence microbial methane oxidation in soils have relied on batch experiments in which soil is placed in jars which are then injected with methane. The problem with this approach is that it doesn't simulate the reduction in the areal extent of oxygen penetration caused by its advective displacement by methane and by its consumption due to microbial methane oxidation. For this study, it was decided that soil column experiments be used in addition to batch experiments to adequately simulate these mass transfer limitations. Soil column experiments also permit more thorough analyses of the interaction between the many variables which influence CH_4 oxidation rates. Also, the batch experiments performed to date haven't allowed the microbial populations to reach their potential and so do not indicate the maximum amount of methane that can be oxidized in soil systems

3.2.1 Soil Column Design

Figure 3-1 is a schematic diagram of the soil microcosms used for this research. Methane (99% purity) obtained from PraxAir was fed through the bottom of the columns, simulating the range of fluxes encountered at landfills and heavy oil well sites. Air was passed across the top of each column through ports in the head caps at a nominal flow rate of 300ml/min. This permited measurement of the methane flux from the soil surface, and also maintained natural oxygen concentrations within the soil.

Figure 3-1: Schematic of soil column

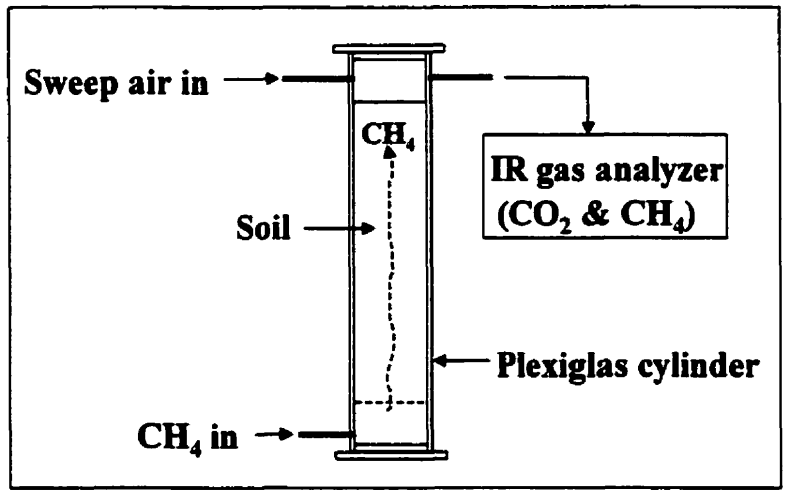

Since the maximum depth at which microbial methane oxidation has been reported is 70 cm (Nozhevnikova et al., 1993), the soil columns used in this work were designed with a height of 1m. Six columns were constructed from 1 m long Plexiglas tubes with a 6" outer diameter and ¼" thickness. Gas sample ports were drilled at 10cm intervals down the core and threaded for 1/8" NPT fittings (see Fig. C4, Appendix C).

The sample ports were fitted with ¼" Swagelok – 1/8" male NPT adaptors. The Swagelok end of the adaptors were fitted with 10mm silicone septa. Filters made of steel mesh were inserted inside of the male NPT end of the adaptors and secured with 1 cm long ¼" OD polypropylene tubes. A perforated plate covered with a fine steel mesh was located in the base of the column to support the soil, which was packed above it to a depth of 80 cm (see Figure C5, Appendix C).

The columns were closed at both ends with Plexiglas end caps fitted with rubber O-rings (see Figures C1 & C2, Appendix C). The end caps were fastened to the columns with 4 x ¼" threaded rods that ran the length of the column. The columns were supported in a steel frame (see Figure 3-2).

Figure 3-2: Photograph of soil column apparatus

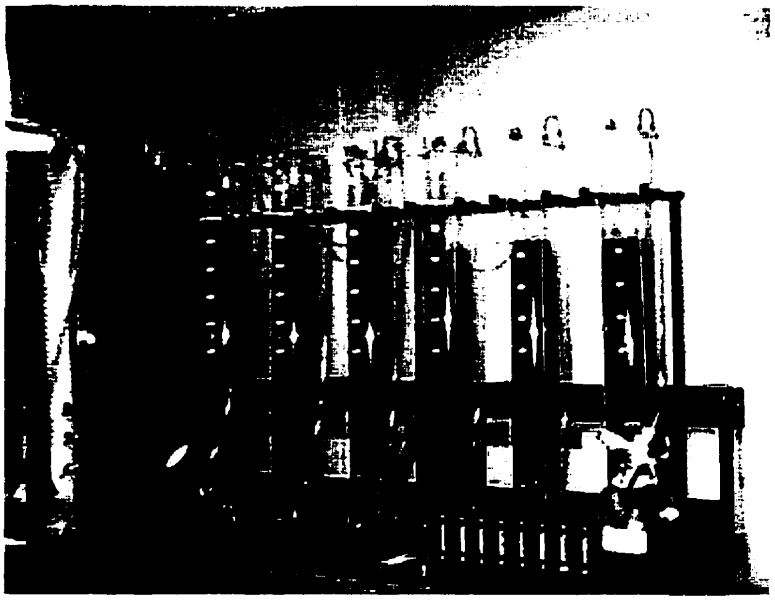

3.2.2 Methane Oxidation Efficiencies

The CH_4 flux from the surface of each soil column was calculated by measuring the CH_4 concentration and flow rates of the effluent air streams exiting each column. The difference between the CH_4 fed to the base of the column and the CH_4 flux from the surface of the column was then calculated. This difference was attributed to CH_4 oxidation within the soil. Thus the percentage of CH_4 oxidised was calculated with the following formula:

$$\%Oxidation = \frac{([Q_{CH4}]_{in} * 100\% - [Q]_{out} * [C_{CH4}]_{out})}{[Q_{CH4}]_{in} * 100\%} \quad (3\text{-}1)$$

Where:

$[Q_{CH4}]_{in}$ = flow rate of CH_4 entering at the column's base
$[Q]_{out}$ = flow rate of column's effluent
$[C_{CH4}]_{out}$ = CH_4 concentration in column's effluent

The CH_4 concentration in the column's effluent was measured using a GMI Land-surveyor I LEL meter calibrated for CH_4 (+/- 50 ppm accuracy). The CO_2 concentration was measured with a PP Systems EGM2 Infra-red CO_2 meter (accuracy = +/- 25ppm). The CH_4 flow rate at the base of the columns was controlled using needle valves and measured with Cole-Parmer 65mm variable area flow meters (reproducibility = 0.02ml/min). Calibration curves for each of the rotameters were generated using a Cole-Parmer digital flow meter (accuracy +/- 2%).

Experiments were performed without any soil in the columns to check the CH_4 balance in this system. The error in mass balance was between 2 and 5%.

3.2.3 Column Gas Concentration Profiles

Samples (2mL) were taken at each gas sample port and analyzed for CH_4, CO_2, O_2, and N_2 using a Hewlett Packard Micro-Gas Chromatograph with thermal conductivity detectors. CH_4, CO_2 and air were separated using a Poraplot-Q column (4m x 0.32mm I.D., 10μm df.). O_2 and N_2 were separated using an MS-5A molecular sieve (10m x 0.32mm I.D., 30μm df). The G.C. settings for both columns were: oven temperature= 100°C, injection time=100ms, and sample time=10 sec. A low detector sensitivity was used. All peaks were quantified with Hewlett Packared EZ-Chrom integration software on a personal computer. Gas sample concentrations were determined by comparison to standard gases obtained from Prax-Air Gases.

3.2.4 Soil Selection and Preparation

Soil column experiments were conducted using three soil types:

1. Sedge peat moss (PM)

   This soil was taken from a bog northwest of Cochrane, Alberta on March 27, 1998. It was believed that because this soil resides at the interface of an aerobic and anaerobic environment, it would likely contain a large number of methanotrophic bacteria, which could later serve as a seed material for further soil column experiments if necessary. A peat moss was also chosen because it is known to be an excellent bio-filter media, and might therefore give an upper range of the CH_4 flux rates that could be treated using biofiltration.

2. Springbank landfill loam (SB)

This soil was collected on April 28,1999 from the Springbank landfill (62Ave & 3rd St. SE Calgary, AB) from a location where the CH_4 concentration was 35% at a depth of 45 cm. The soil was gathered from the top 15cm of the landfill cover and immediately taken to the lab where it was passed through a 2.5mm sieve to remove large rocks, thoroughly mixed, and then placed in the soil columns. The columns were manually shaken during filling.

3. Agricultural Soil (Rocky View Dark Soil)

This soil is renowned for its high organic matter content and excellent agricultural properties. It was also chosen to represent soils found at abandoned oil well sites, which are often located on cultivated land. It was gathered from two farm fields east of Airdrie, Alberta. Rocky View soil one (RV1) was taken from the north-eastern corner of the Rge Rd. 284/Twp. Rd. 264 intersection. Rocky View soil two (RV2) was taken from a field located on the east side of Rge. Rd. 291, 2km north of Twp. Rd. 270 (immediately north of Stewart Rd.). Both soils were covered with grass.

3.2.5 Soil Column Operation

After placed in the columns, the soils were subjected to the CH_4 flow-rates and environmental or physical alterations listed in Table 3-1. A column flow-rate of 5ml/min corresponds to a CH_4 flux of 310 $g*m^{-2}*day^{-1}$.

Table 3-1: Column operation events

#days	SB1 Qch4*= 5ml/min	SB2 Qch4= 5ml/min	SB3 Qch4= 3ml/min	PM1 Qch4= 5ml/min	PM2 Qch4= 5ml/min	PM3 Qch4= 2.5ml/min	AS2 Qch4= 5ml/min
1	Began experiment	Began experiment	Began experiment	Began experiment	Began experiment	Began experiment	Began experiment
30							Moisture increased from 6% to 10% d.w.
32				Moisture reduced from 300% to 237% of d.w.			
160				Compacted to 66% of original volume.	Column experiment concluded	Placed in cold room at 5°C	
179						Returned to Laboratory	
266	Experiment concluded	Experiment concluded	Experiment concluded	Experiment concluded			

Methane flow rates were allowed to vary above and below the nominal flow-rates given in Table 3 in order to observe the effect variable flow-rate has on CH_4 oxidation efficiency.

3.3 Batch Experiments

After completing the soil column CH_4 purging experimments, soil samples were taken at 10-cm intervals along columns SB1-3 and PM1 to determine changes in moisture content and organic matter. In order to determine the effects of environmental variables on CH_4 oxidation potential, soil samples from columns SB1-3 were also subjected to various time series incubation experiments. Quantification of the effects of environmental variables is essential for developing of a CH_4 oxidation/transport model.

It was expected that a predictable relationship between the maximum oxidation rate (V_{max}) and soil gas concentrations could be established. These experiments also presented the opportunity to determine whether some of the previously unvalidated techniques used by others for estimating the in-situ CH_4 oxidation yield correct values.

3.3.1. General Procedure

Laboratory incubations were performed in 240 mL airtight glass bottles with teflon+silicone septa caps. For each incubation experiment, approximately 10 g of soil was placed in the bottle which was then sealed. A headspace methane concentration of approximately 4% was achieved by injecting CH_4 into the bottle with a syringe. A CH_4 concentration of 4% was used because investigations by Czepiel (1996b) and Kightley (1996) indicated that zero order CH_4 oxidation kinetics would be achieved when CH_4 headspace concentrations are greater than 2%. Incubations were performed at a nominal temperature of 22°C, unless temperature was the independent variable under investigation. Bottle headspaces were sampled a maximum of 5 times during the experiments by removing 2 mL of gas with a 5 mL gas tight syringe.

3.3.2. Analytical Techniques

Headspace methane concentrations were quantified using the Micro-Gas Chromatograph (see section 3.2.1.3 for details). Mixing ratios were determined by comparison to standard gases obtained from Prax-Air Gases. The minimum detectable rate of oxidation at an initial headspace CH_4 mixing ratio of 1.5% was 3 nmol CH_4 per hour.

3.3.3. Oxidation Kinetics

To determine the kinetic parameters for a given soil, varying quantities of CH_4 were supplied to the septum bottle headspaces. The resulting CH_4 draw-down rates were used to calculate the maximum rate of CH_4 oxidation (V_{max}) and the apparent half-saturation constant (K_s). Oxidation rate data were expressed in substrate saturation curves as a function of initial headspace CH_4 mixing ratio. Eadie-Hofstee plots were then use to linearize the data from which V_{max} and K_s were calculated. An Eadie-Hofstee plot is a graph of V vs. V/C, where V is the reaction rate and C is the concentration of the gas whose effects on kinetics is being determined. V_{max} is equal to the y-intercept of the Eadie-Hofstee plot, and K_s is equal to the inverse of its slope (Bender and Conrad, 1992).

3.3.4. Effect of Oxygen Concentration

Incubations to determine the effect of reduced O_2 concentration on CH_4 oxidation rates were performed on soil samples obtained from column 1 (Springbank loam) at depths of 35cm and 75 cm. Oxygen concentrations were adjusted by flushing the bottle headspaces with air+N_2 gas mixtures of varying ratios. Concentrations ranged from 1 to 20% O_2. Incubation of samples containing 5% O_2 were performed in triplicate to quantify error. Samples were allowed to equilibrate to their adjusted headspace atmospheres for 1 hour. Time series incubations were then performed as previously described.

3.3.5. Temperature Effect

The effect of soil temperature on CH_4 oxidation was determined by adjusting soil temperature and measuring the substrate-saturated CH_4 oxidation rate. Soil samples (10g, 12% moisture content) were acclimated for 4 hours to a range of temperatures from 4 to 40°C, and headspace CH_4 was adjusted to a nominal concentration of 2.5%. Time series incubations were then performed as previously described.

3.3.6. Effect of Moisture Content

The effect of soil moisture on CH_4 oxidation was determined by adjusting soil moisture content and measuring the substrate-saturated CH_4 oxidation rate. The moisture content of a composite soil sample was initially brought to 1% H_2O by air drying with intermittent mixing. The moisture content of the composite sample was increased in approximately 5% steps to 30% with a mist of distilled water, with 10g sub-samples being placed in septum bottles at each step. Samples were acclimated overnight to the changed moisture content. Headspace CH_4 was adjusted to a nominal concentration of 2%, and time series incubation experiments were performed as previously described. Soil moisture contents were then determined gravimetrically, by drying samples for 24 h at 104°C.

3.4 Soil Characteristics

3.4.1 Soil Textural Classification

Soil texture was determined by sieve analyses and classified in accordance with the U.S. Department of Agriculture classification system.

3.4.2 Bulk Density

The bulk density of the soils within the columns was determined by weighing soil-filled columns, subtracting the column weight, and dividing by the column volume that contained soil.

3.4.3 Moisture Content

Soil moisture content was determined gravimetrically by measuring the weight lost after heating at 104°C for 24 hours. Moisture content was expressed as percentage of dry soil weight.

3.4.4 Water Holding Capacity

The water holding capacity of the soils were determined by packing 1 kg of soil into a plastic funnel which was plugged with cotton wool. Water was slowly added to the soil without ponding until it began to drip out of the funnel (Wilson, 1998). Moisture content was then determined gravimetrically, as described in section 3.3.3.

3.4.5 pH

Soil pH was determined in a 1:2.5 soil-water mixture using a hand-held pH meter (Hanna Instruments, HI 9025 Microcomputer pH meter).

3.4.6 Intrinsic Permeability

The intrinsic permeability of the soils could be estimated experimentally for soil columns in which there was no microbial activity by solving the following set of equations:

$$-D_{CH4}\left(\frac{dC_{CH4}}{dy}\right)-\frac{k}{\mu}\left(\frac{dP}{dy}\right)C_{CH4}=FLUX_{CH4} \tag{3-2}$$

$$-D_{air}\left(\frac{dC_{air}}{dy}\right)-\frac{k}{\mu}\left(\frac{dP}{dy}\right)C_{AIR}=0 \tag{3-3}$$

$$D_{CH4} = 1.4\ D_{air} \tag{3-4}$$

where:

P = column pressure (Pa)

C_{CH4} = molar concentration of CH_4

D_{CH4} = diffusivity of CH_4 in soil

D_{air} = diffusivity of air in soil

k = soil's intrinsic permeability

μ = viscocity of gas mixture

The pressure (P) was measured using a water manometer attached to the base of the column, with the top of the column at atmospheric pressure. Its gradient (dP/dy) was approximated by dividing P by the column's length. The gas concentrations were

measured at the base of the column, and their gradients (dC/dy) were also approximated by dividing these measured concentrations by the column length. This would provide an accurate value for the gradients, provided that microbial activity was absent, in which case the gas concentration profiles were linear. Values for D_{air}, D_{CH4}, and k could then be obtained by solving the set of simultaneous equations.

Chapter 4. Presentation and Discussion of Experimental Results

4.1 Soil Properties

The properties of the soils used in the column experiments were determined using the methods described in section 3.4 and are presented in Table 4-1.

Table 4-1: Soil properties

Soil	Average CH_4 Flux ($g*m^{-2}*d^{-1}$)	ρ_{bulk} (g/ml)	Moisture Content (% d.w.)	W.H.C. (% d.w.)	Organic Matter % d.w.	pH	Total Porosity	Air-Filled Porosity
SB1	319	1.172	9.4	24.6	3.1	8.45	0.6	0.5
SB2	328	1.163	9.4	24.6	3.1	8.45	0.61	0.51
SB3	186	1.142	9.4	24.6	3.1	8.45	0.61	0.51
RV1	315	1.326	6.0	39.8	4.7	7.6	0.53	0.43
RV1*	315	1.38	10.0	39.8	4.7	7.6	0.53	0.40
RV2	-	-	10.2	-	10.9	-	-	-
PM1	320	0.54	316	505	79	6.5	0.9	0.49
PM2	320	0.54	316	505	79	6.5	0.9	0.49
PM3	160	0.55	316	505	79	6.5	0.9	0.49

*Properties of Rockyview soil RV1 after increasing moisture content to 10%

Rockyview soil 2 was not used in soil column experiments, but is included in Table 4-1 to illustrate the significant effect that a soil's organic matter content can have on its moisture content. RV1 and RV2 taken from locations that were only a few kilometers apart, and were likely exposed to similar climates. However, RV2 had over twice the organic matter content as RV1, and contained nearly twice as much moisture.

4.2 Soil Column Experiments

4.2.1 Methane Oxidation Rates as a Function of Time: Experimental Results

Tables giving the time course $\%CH_4$ oxidation rate and the equivalent CH_4 flux oxidized are located in Appendix A. Their values are plotted in Figures 4-1, 4-2 and 4-3.

4.2.1.1 Sedge Peat Columns

Two months after placing the sedge peat in the columns, the soil had settled by 10-15%. In all the soil column experiments using sedge peat, the flux of CH_4 from the surface of the soil decreased with time, indicating the growth of a microbial community capable of oxidising CH_4. Figure 4-1 illustrates the methane-oxidation rate for these columns.

Figure 4-1: Methane oxidation rate in sedge peat

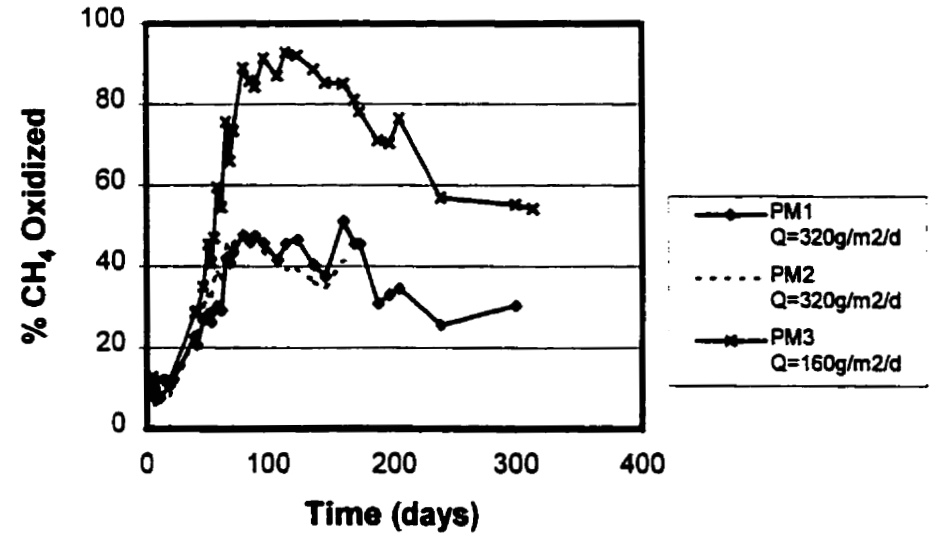

For the first 19 days, the methane-oxidation rate measured in all of the sedge peat columns remained approximately constant, demonstrating the existence of a small methanotrophic community prior to purging the soils with methane. During this time, the molar oxidation rate in each of the columns was a function of the methane flow rate into the columns, suggesting first-order growth kinetics. After 19 days the CH_4 oxidation

rate within the columns began to increase, and the growth kinetics began to shift from first-order to zero-order. By day 50, a shift to zero-order growth kinetics is complete, as the molar rate of CH_4 oxidation in columns purged with both low and high CH_4 flow-rates approach the same value. A plateau in the CH_4 oxidation rate was achieved after 80 days in all of the sedge peat columns. After 160 days, the rate of CH_4 oxidation had undergone little change, so it was assumed that a steady state had been reached. Consequently, one of the high CH_4 flow columns (PM2) was decommissioned and the other (PM1) was compacted by 30% to observe the effect of reduced intrinsic diffusivity on CH_4 oxidation. The low CH_4 flow column (PM3) was placed in a cold room at 5°C for 19 days. After removing PM3 from the cold room, its capacity for CH_4 oxidation had decreased from 85% to 71%, but then increased to 76% after more 18 days. After an additional 154 days of CH_4 purging, both of the remaining sedge peat columns saw a decline in their CH_4 oxidation rate to a lower steady-state value

4.2.1.2 Springbank Loam Columns

Figure 4-2 illustrates the methane-oxidation rate for columns SB1 (high CH_4 flow) and SB3 (low CH_4 flow). Column SB2 is not included in this graph for the sake of clarity.

Figure 4-2: Methane oxidation rate in Springbank soil

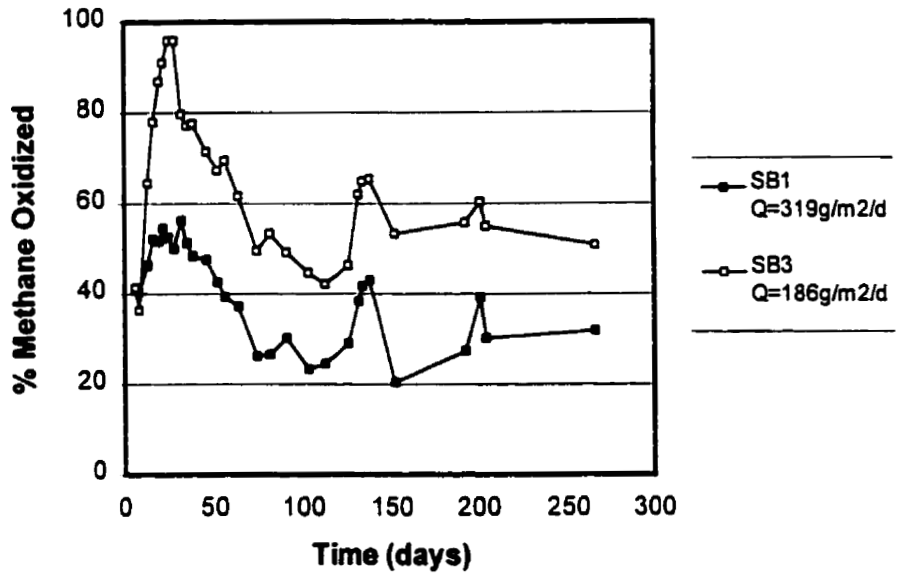

As in the sedge peat, a methanotrophic microbial community was initially present in the Springbank loam, albeit one capable of oxidizing four times more CH_4 than the initial sedge peat community. This community also initially exhibited first-order growth kinetics, which shifted to zero-order after being purged with CH_4 for 2 weeks. By day 28, both all of the Springbank loam columns achieved their maximum oxidation rate, with the high CH_4 flow-rate columns (SB1 and SB2) oxidizing 50% of the CH_4 and the low CH_4 flow-rate column (SB3) nearly 100 %, again indicating zero-order growth kinetics. After day 28, the oxidation rates for all three of the Springbank loam columns began to decline to their steady-state values. The steady-state oxidation rates eventually reached by columns SB1 and SB2 were 102 and 120 $g*m^{-2}*day^{-1}$, respectively (10-20%

below their initial oxidation rates). The steady-state oxidation rate for the low CH_4 flow-rate column was (93 $g*m^{-2}*day^{-1}$) 20% higher than its initial rate.

Contrary to King (1992) the rate of CH_4 oxidation in these soils did not seem to correlate with their rate of CH_4 flux; rather both the low and high CH_4 flux columns exhibited comparable molar oxidation rates.

4.2.1.3 Rockyview Dark Soil

As with the other soils, there was a low initial rate of CH_4 oxidation. However, after two months had elapsed, the CH_4 oxidation rate declined, unlike the oxidation rate in the other columns. Because the initial moisture content of this soil was only 6.1% (dry weight basis), it was hypothesised that microbial water stress was preventing the development of a larger methanotrophic community. The soil was removed from the column, and its moisture content was increased to 10% (d.w.) using a spray bottle while continuously mixing. Within a week of returning the soil to its column, the CH_4 oxidation rate climbed to 124 $g*m^{-2}*day^{-1}$ (40% oxidation efficiency).

Figure 4-3: Methane oxidation in Rockyview dark soil (RV1) vs. time

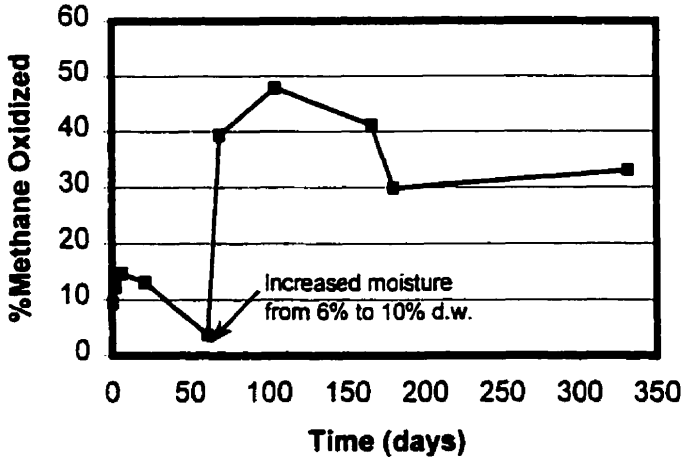

As observed in the other soils, the CH_4 oxidation rate increased to a maximum, only to decline to a somewhat lower, steady-state rate, in this case 103 $g*m^{-2}*day^{-1}$ (34% of the column's 310 $g*m^{-2}*day^{-1}$ CH_4 flux). This steady-state oxidation rate is close to those observed in the Springbank columns, which averaged 105 $g*m^{-2}*day^{-1}$.

4.2.2 CH_4 Oxidation as a Function of Time: Discussion

In all of the soil column experiments, with the exception of the high CH_4 flow-rate Springbank loam columns (SB1 and SB2), an increase in rate of CH_4 oxidation followed by a gradual decline to a lower steady-state value was observed. A similar pattern has has also been observed in the soil microcosm simulations of landfill soil covers performed by others (Hilger et al., 1999; Visvanathan et al., 1998). However, whether the reduction in oxidation efficiency observed in the peat columns was due to their microbial

community's natural course of development or to PM1's compaction and PM3's cooling cannot be unequivocally stated.

Hilger et al. (1999) suggest that exopolymer accumulation on microbial biofilm surrounding the soil particles could account for the gradual decline in biotic CH_4 oxidation levels. Exopolymer accumulation could limit gas diffusion to sites of active microbial activity. However, this hypothesis has yet to be proven.

Another possible explanation is that during long-term operation of a biofilter, the mandatory absence of net cell growth forces the cells into maintenance metabolism or the equivalent situation of balanced growth and death, which is of a relatively lower rate compared to substrate consumption during the exponential growth phase. A simple calculation confirms that bacteria must oxidize CH_4 while in a stationary phase. For example, assuming there is very slow net growth with a doubling time of 7 days, after one year, each active bacterium will have generated 2^{52} cells or about 5 kg of wet cell weight, which would be impossible to accommodate in the bed.

There are at least two scenarios that could account for the stationary phase with its maintenance kinetics. The first is that the microbial population enters a state of maintenance energy usage. Cells that are not growing and dividing still need to expend energy to maintain ion gradients across their membranes and to turn over their protein content through poteolysis and resynthesis. Because energy alone is needed for this, only a carbon source and oxygen are consumed.

The second possible scenario is that the maintenance energy usage actually reflects growth at a low rate; total cell mass does not increase because existing cells are

consuming nonviable biomass at the same rate as growth, which is known as endogenous metabolism. However, these two scenarios are mathematically equivalent

Further experiments should be performed to determine the exact cause for this rather significant decline in CH_4 oxidizing capacity. If, for example, it is merely a case of nutrient limitation, then this could be offset by facilitating the controlled extra release of mineral N into the soil, e.g. by adding an encapsulated form of N fertilizer or the addition of organic residue.

4.2.3 Oxidation Efficiency as a Function of CH_4 Flux

To determine the effect that the rate of CH_4 flux has on oxidation efficiency, the CH_4 flow-rates in both the low and high CH_4 flow columns were allowed to vary. The resulting data are pooled in Figures 4-4 and 4-5, and fit to logarithmic trendlines, as they resulted in the best fit.

Figure 4-4: Oxidation efficiency vs. CH_4 flux in sedge peat and Springbank loam under optimal conditions

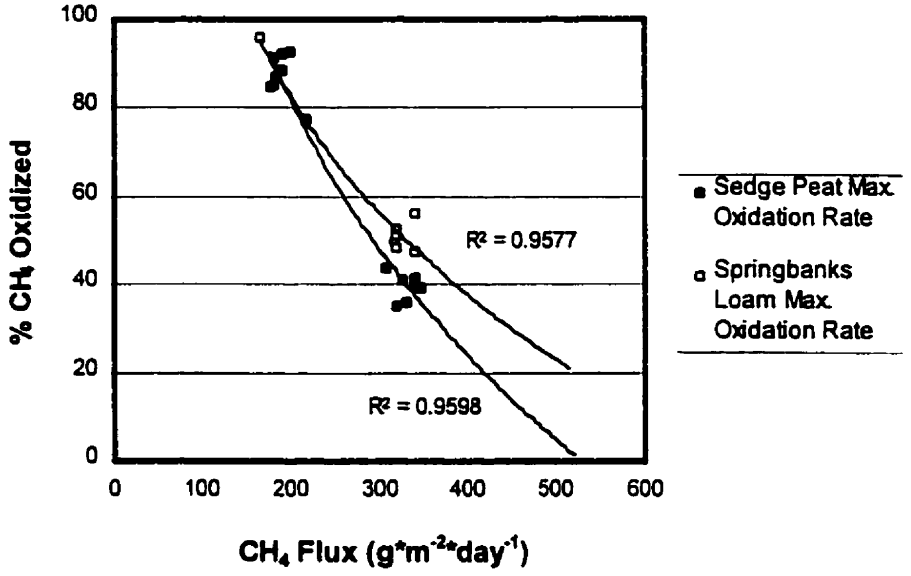

Figure 4-5: Decrease in oxidation efficiency in Springbank loam after reaching steady state

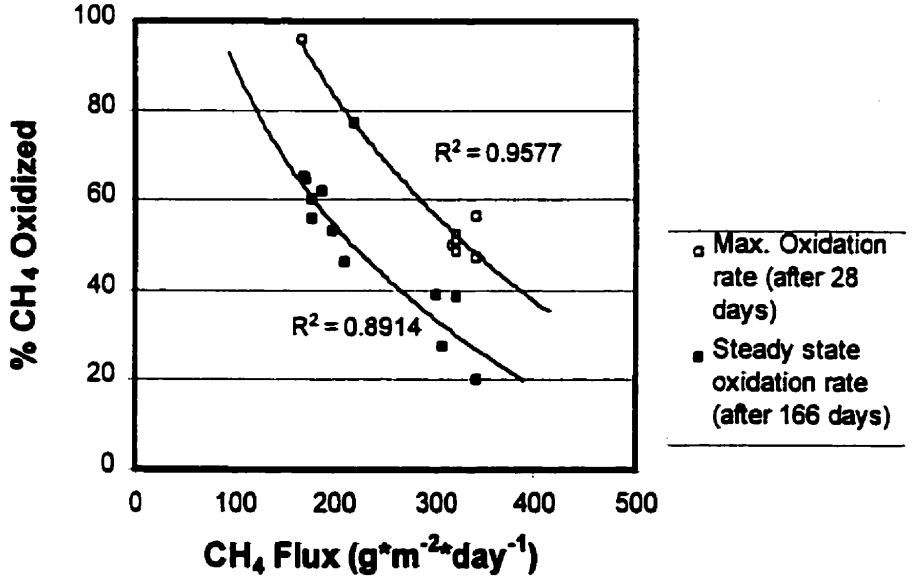

4.2.4 Steady State Gas Profiles

After the CH_4 oxidation rates in the columns achieved a steady state, vertical concentration profiles of the soil gases were obtained. Tables of the soil gas concentrations are located in Appendix A.

4.2.4.1 Sedge Peat

Figures 4-6 and 4-7 depict gas concentration profiles for two of the sedge peat columns (PM3 and PM1). Because a gas chromatograph was not available until the last four months of the soil column experiments, gas concentrations profiles are not available for column PM2, or for column PM1 prior to compaction.

Figure 4-6: Soil Gas concentration profile for low CH_4 flow sedge peat column PM3 (Q_{CH4} =160g*m^{-2}*day^{-1})

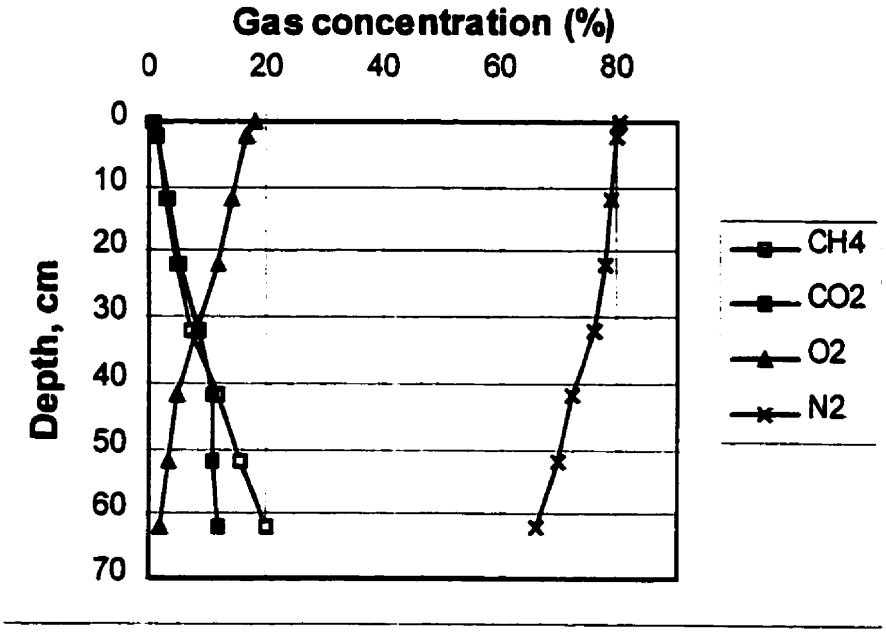

Figure 4-7: Soil gas concentration profile for compacted sedge peat column PM1 (Q_{CH4} =320 g*m^{-2}*day^{-1})

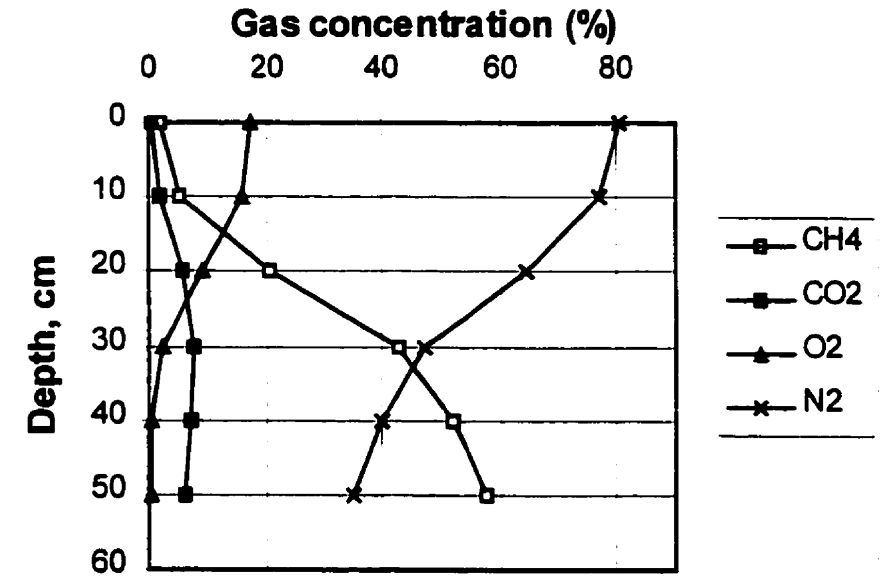

The compacted sedge peat (PM1) had a much steeper CH_4 concentration gradient than the uncompacted peat, which is to be expected since it has significantly less free-air space, and therefore a lower intrinsic diffusivity and gas permeability. A steeper gradient is therefore required to maintain its CH_4 flow-rate.

4.2.4.2 Springbank Loam

Figures 4-8 and 4-9 depict gas concentration profiles for two of the Springbank loam columns (SB1 and SB3). The gas concentration profile for the replicate column (SB2) resembled that of column SB1, and was therefore omitted.

Figure 4-8: Soil gas concentration profile for high CH_4 flow Springbank soil column SB1 (Q_{CH4} =319g*m^{-2}*day^{-1})

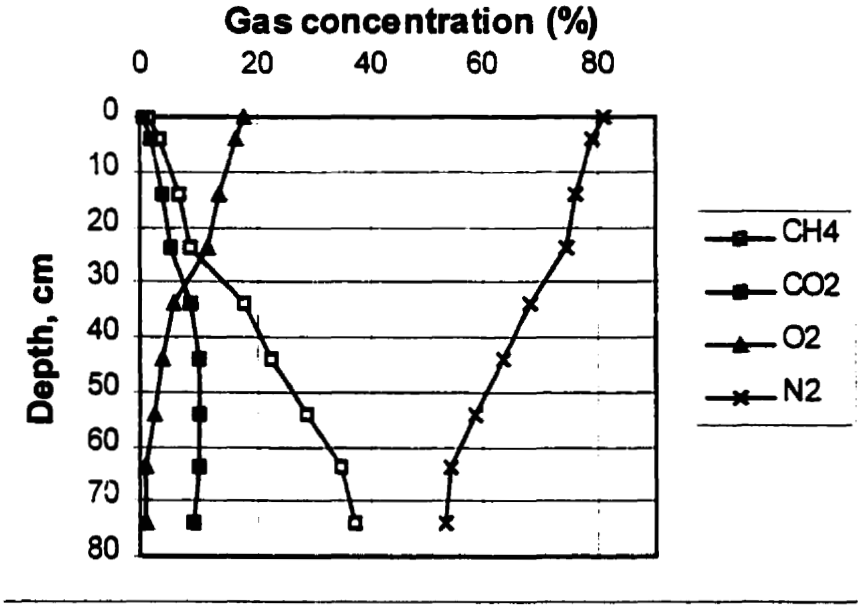

Figure 4-9: Soil gas concentration profile for low CH_4 flow Springbank soil column SB3 (Q_{CH4} =186 g*m^{-2}*day^{-1})

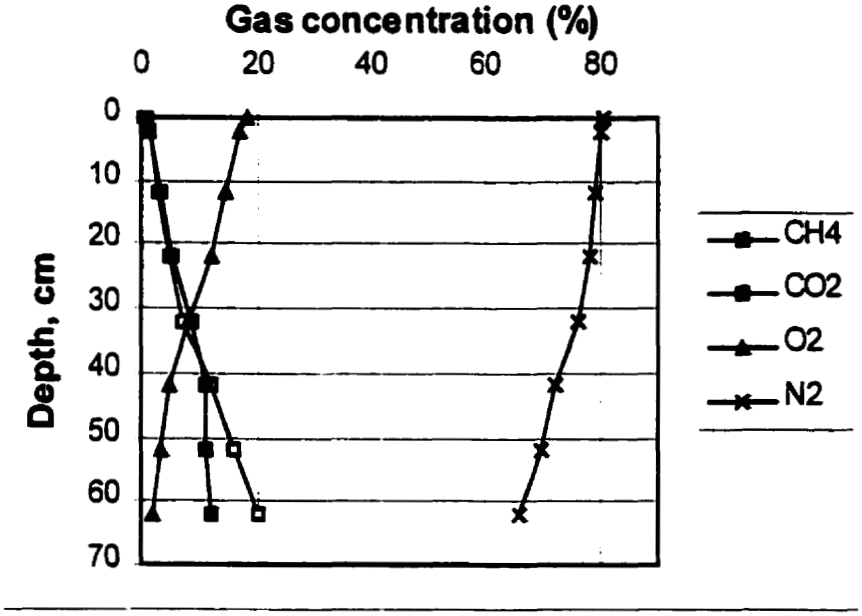

Oxygen profiles were similar in each of the Springbank soil columns, with aerobic conditions present throughout the columns' 80cm length. The O_2 concentration was 0.75% at the base of the high CH_4 flow column (SB1) and 1.8% at the base of the low CH_4 flow column (SB3). The CH_4 concentration at the base of the column SB3 was 67% of that of column SB1, which makes sense given that the low flow-rate column had a CH_4 flow-rate equal to 60% of that in the high flow-rate columns.

As previously stated, an 80cm soil depth was used in these experiments because 70cm was the greatest depth at which microbial CH_4 oxidation has been reported. However, the fact that the soils in this series of experiments were aerobic throughout their entire depth indicates that CH_4 oxidation could have occurred at a greater depth. It seems likely that the actual maximum CH_4 oxidation rate that could occur in a thicker cover consisting of the same soil was not achieved, especially for the low CH_4 flow-rate column. However, a field soil cover would be compacted to a greater degree, and would likely have a shallower aerobic depth.

4.2.4.3 Rockyview Dark Soil

Figures 4-10 depicts gas concentration profiles for the Rockyview dark soil.

Figure 4-10: Soil gas concentration profile for Col. RV1 (Q_{CH4}=310 g*m^{-2}*day^{-1})

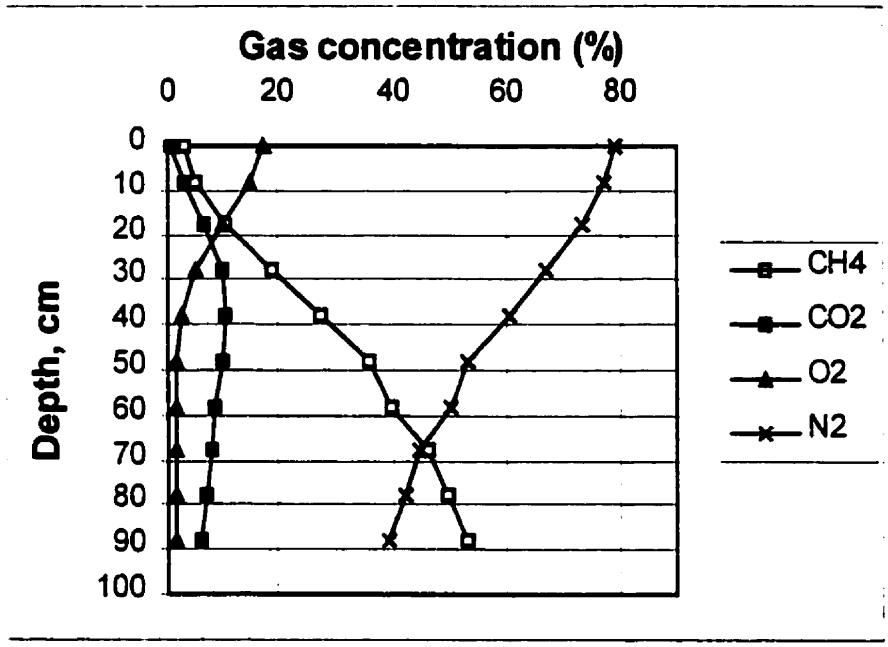

The Rockyview soil exhibited a steeper CH_4 concentration gradient than the Springbank loam. This can be explained by the fact that it has a higher bulk density than the Springbank loam, yet a similar moisture content, resulting in a volumetric air content that is 15% less than that of the Springbank loam. Since a soil's intrinsic diffusivity is proportional to the square of its aeration porosity, the Rockyview soil has a lower diffusivity, resulting in steeper concentration gradient in order to effect the same CH_4 flow-rate.

4.3 Batch Experiment Results

4.3.1 CH_4 Oxidation Rate as a Function of Column Depth

The batch experiments that were performed in empty bottles demonstrated that CH_4 leakage from the septum bottles was negligible. The drawdown of CH_4 in the headspace of the bottles was linear, as illustrated in Figure 4-11, and therefore indicative of the pseudo-zero-order kinetics expected in a maximum oxidation rate or substrate independent environment, according to Kightley (1997) and Czepiel (1997).

Figure 4-11: Sample graph of typical batch experiment CH_4 drawdown data from the 66cm depth of column SB1.

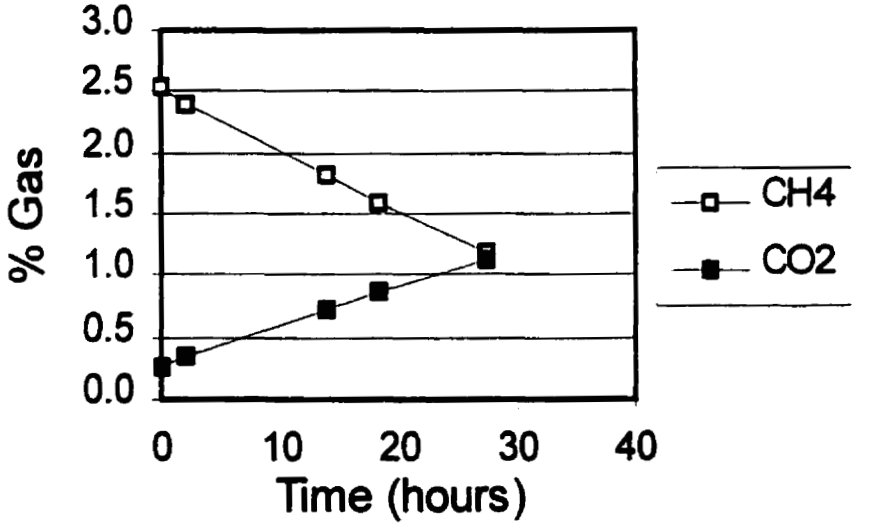

The CH_4 oxidation rate profiles for the Springbank loam columns obtained from incubation experiments are presented in Figure 4-12.

Figure 4-12: Springbank loam CH_4 oxidation as a function of depth

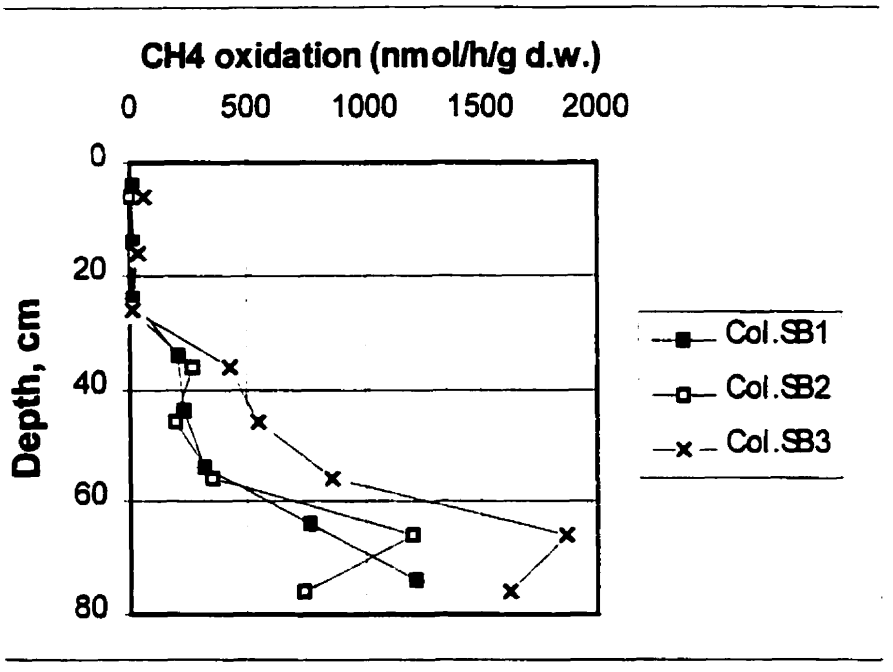

4.3.2 CH_4 Kinetic Parameters

The oxidation rate data from the incubation experiments performed on soil samples taken from the 76-cm depth of column SB1 exhibited typical Michaelis-Mentin characteristics, as illustrated in the following substrate saturation curve in which V_{CH4} is plotted as a function of initial headspace.

Figure 4-13: Substrate saturation curve – col. SB1, 76cm depth

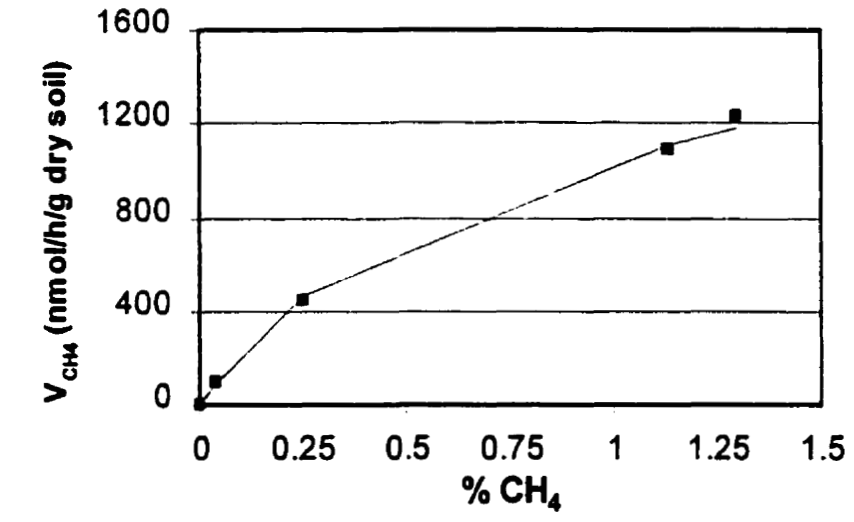

Using an Eadie-Hofstee plot to linearize this data, V_{max} and K_S can then be calculated (Figure 4-14).

Figure 4-14: Eadie-Hofstee plot for col. SB1, 76cm depth soil

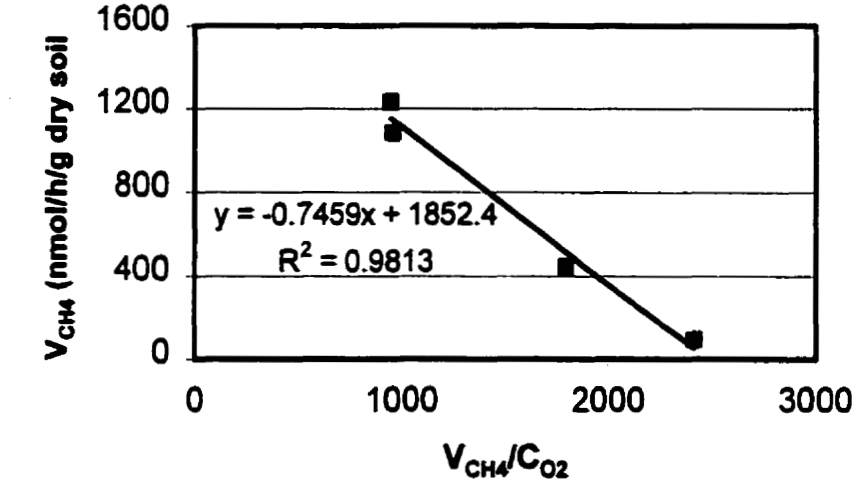

The quantity for K_s is equal to the inverse of the slope of this graph which in this case is 0.75% CH_4. The quantity V_{max} is equal to the y-intercept, which in this case is 1852 nmol/h/g d.w.. This is only 4% less than 1940 nmol/h/g d.w., the value calculated using a single batch test and applying the correction factor derived from K_s (see section 4.2.1). These kinetic parameters are similar to the maximum kinetic parameters determined by Czepiel et al. (1996b) for a sandy clay loam taken from a New Hampshire landfill, which were Vmax=2594 nmol/h/g d.w. and Ks = 5847ppm determined for column SB1 at the 76 cm depth.

Since the V_{max} value determined from the Eadie-Hofstee plot (1940 nmol/h/g d.w.) is considerably larger than that observed in the incubation experiment discussed in section 2.4.1, it was hypothesized that the initial 2.5% CH_4 headspace concentration used in the batch experiments was in fact somewhat lower than the amount required to effect a zero-order kinetic response in these tests, notwithstanding the observed linear draw-down. This was confirmed in a batch experiment that was later performed on a soil sample taken from the 56-cm depth of column SB1. An initial CH_4 headspace concentration of 3% yielded an oxidation rate of 311 nmol/h/g d.w. in the first set of incubation experiments, but an incubation experiment performed on soil from the same depth using an initial CH_4 headspace concentration of 10% resulted in an observed oxidation rate of 539 nmol/h/g d.w. Indeed, a straight forward calculation will show that the seemingly linear draw-down of CH_4 does not necessarily indicate substrate saturation, contrary to the claims made in two of the most widely cited papers on CH_4 oxidation in landfills (Czepiel et al., 1996; Kightley et al., 1995).

Consider, for example, the CH_4 drawdown data for the 66cm depth of column SB1 (Figure 4-11). A least squares fit of these data gives a correlation coefficient of 0.9989, indicating a straight line. The Vmax value determined from this graph's slope is 768 nmol/h/g d.w.. Using the half-saturation constant, K_s of 0.75% CH_4 (determined in section 4.2.2), one obtains the following theoretical drawdown curve, which has been superimposed on the experimental data:

Figure 4-15: Theoretical versus experimental CH_4 draw-down in SB1 Batch Test

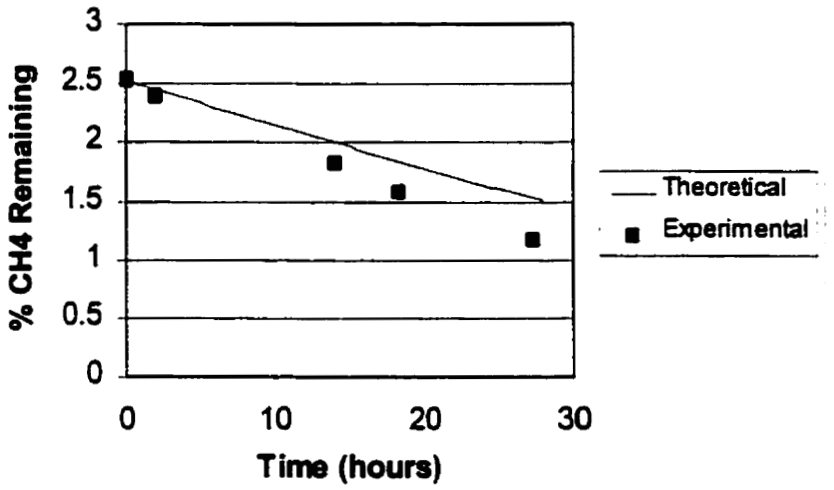

Since the theoretical draw-down curve does not coincide with the experimental data, the actual Vmax value is likely higher than that determined through regression analysis of the experimental data, and therefore the batch experiment was performed at a sub-saturating CH_4 concentration. One can manipulate Equation 2-2 to calculate correction factors that can be used to generate V_{max} values from batch experiment data acquired at sub-saturating CH_4 concentrations. The formula for the corrected V_{max} is:

$$V_{max} = \frac{V}{\left(\frac{C_{CH4}}{K_s + C_{CH4}}\right)} \qquad (4\text{-}1)$$

Where:

V_{max} = maximum CH_4 consumption rate (nmol*day^{-1}*g dry weight^{-1})
V = CH_4 consumption rate (nmol*day^{-1}*g dry weight^{-1}) determined from a batch experiment
C_{CH4} = average CH_4 head-space mixing ratio used in the batch experiment
K_s = half saturation constant (=0.75% CH_4)

Using the data given above (Column SB1, 66cm depth), namely C_{CH4}=3%, V=768 nmol/h/g d.w., one obtains a V_{max} of 1005 nmol/h/g d.w.. Using this V_{max} to again generate the theoretical CH_4 drawdown curve gives the following (again superimposed on the experimental data):

Figure 4-16: Modified theoretical CH_4 draw-down versus experimental draw-down

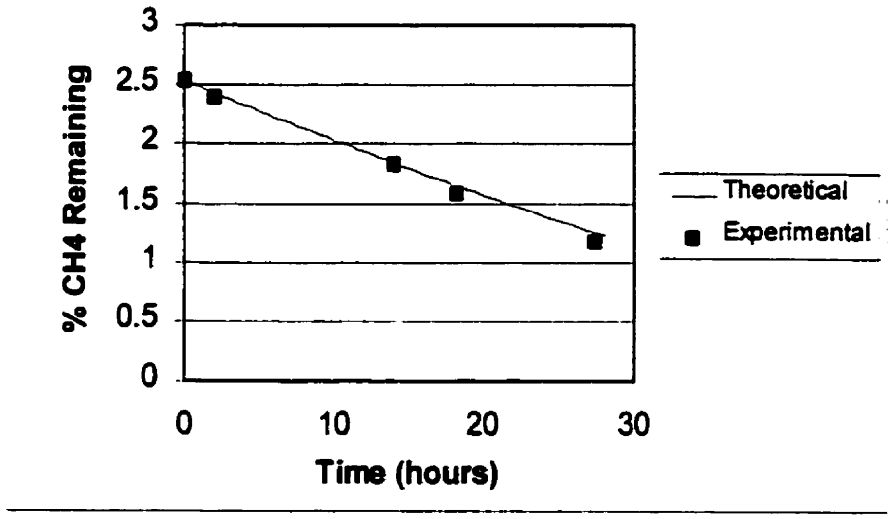

The correlation coefficient of the theoretical curve is $r^2 = 0.99993$ (i.e. a seemingly straight line). However, the actual V_{max} used to generate the curve is 31% higher than the V_{max} directly calculated from this straight line.

The error associated with the batch experiments performed on soil taken from the 76cm depth of column SB1 is even higher (64%) because that test was mistakenly performed at a relatively lower initial CH_4 concentration of 1.3%. The data from that experiment also exhibited an apparently linear decrease in the CH_4 headspace concentration (r^2=0.9997) until the CH_4 concentration was less than 0.25%.

Consequently, all of the V_{max} values calculated from batch experiment data were adjusted using the aforementioned correction factors for the purpose of modeling and for generating CH_4 oxidation depth profiles. The profiles are presented in Figure 4-17.

Figure 4-17: Springbank loam K_s-adjusted V_{max} CH_4 oxidation depth profiles

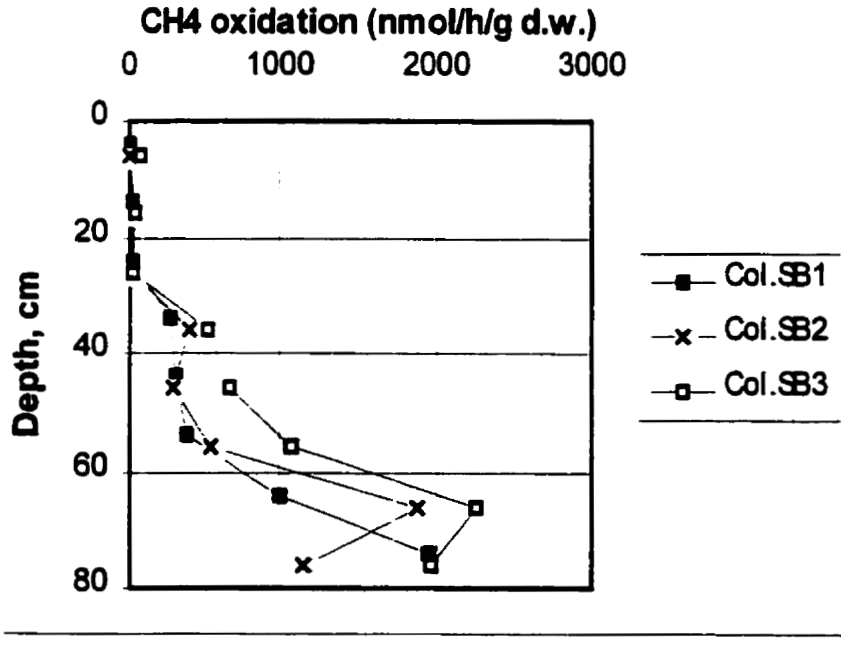

These profiles of CH_4 oxidation potential showed that the capacity for CH_4 oxidation was not uniform throughout the length of the columns. As can be seen in Figure 4-17, the distribution of oxidation potential in the low and high CH_4 flow Springbank soil columns are similar, with little oxidation occurring in the top 26cm. An appreciable increase in oxidation potential occurs at the 36 cm depth in all of these columns. This is likely due to sub-optimal moisture contents above the 26cm depth. In Column 1 (a high CH_4 flow), the maximum oxidation potential is seen at the bottom 10 cm interval (76 cm depth), whereas in Column SB2 (replicate high CH_4 flow column) and Column SB3 (low CH_4 flow), this maximum is seen at the 66 cm depth.

It was expected that a predictable relationship between the V_{max} values and soil gas concentrations could be established. However, Figure 4-18 indicates otherwise.

Figure 4-18: V_{max} vs. CH_4 concentration in Springbank soil columns

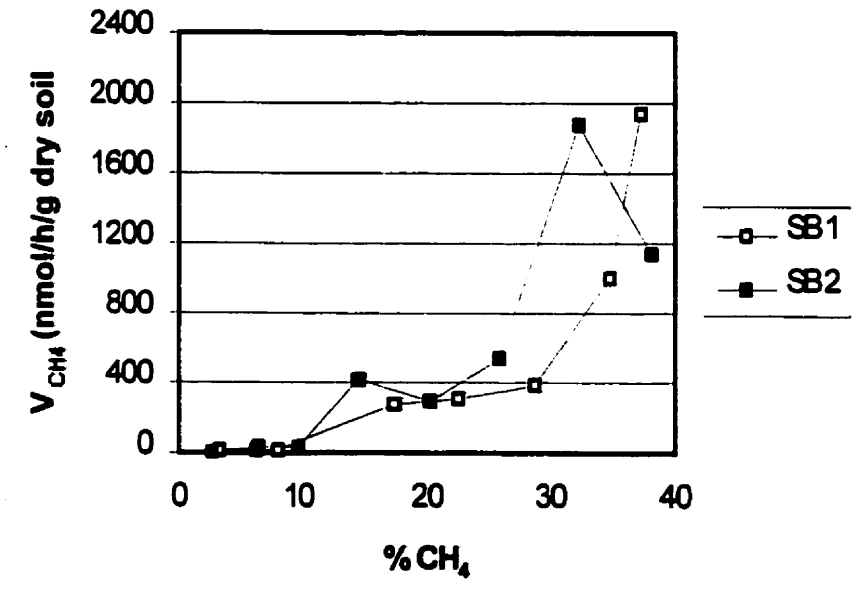

The V_{max} values did not exhibit a strong correlation with columns' historical CH_4 concentrations. However, the one thing that all three SB columns have in common is a low O_2 concentration at the depth of maximum V_{max} (<2% at the 66cm and 76cm depths). Cookson (1995) has noted that methanotrophs may grow more rapidly under reduced oxygen concentrations. Therefore, the depth of maximal V_{max} may coincide with the zone that has the lowest O_2 concentration that is not rate-limiting.

4.3.3 Effects of O_2 Concentration

Figures 4-19 and 4-20 present the CH_4 oxidation rates as a function of O_2 concentration for soil taken from the 36 and 76 cm depths of column SB1. The CH_4 oxidation rates remained relatively unchanged at O_2 concentrations above 2-3%. At O_2 mixing ratios below 2-3%, CH_4 oxidation rates decreased rapidly to zero. The solid lines in these figures represent a least-squares fit of the data to a Monod saturation curve.

Figure 4-19: CH_4 oxidation rate as a function of O_2 mixing ratio (SB1, 36cm depth)

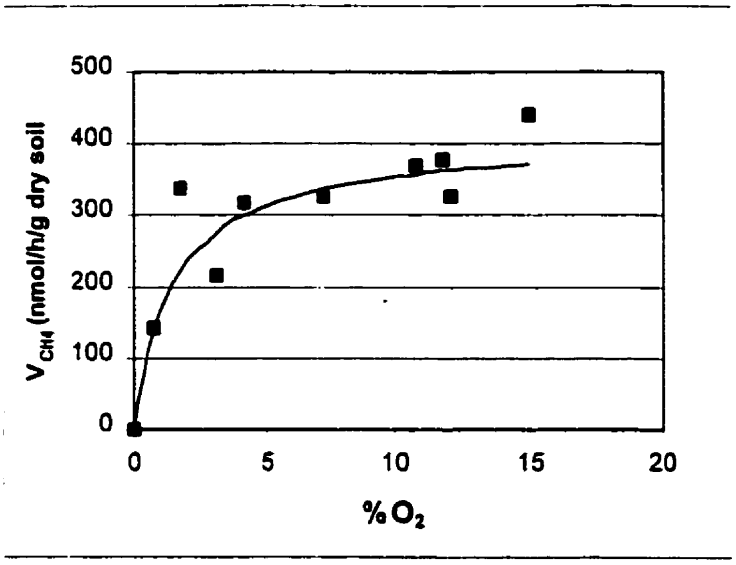

Figure 4-20: CH_4 oxidation rate as a function of O_2 mixing ratio (SB1, 76cm depth)

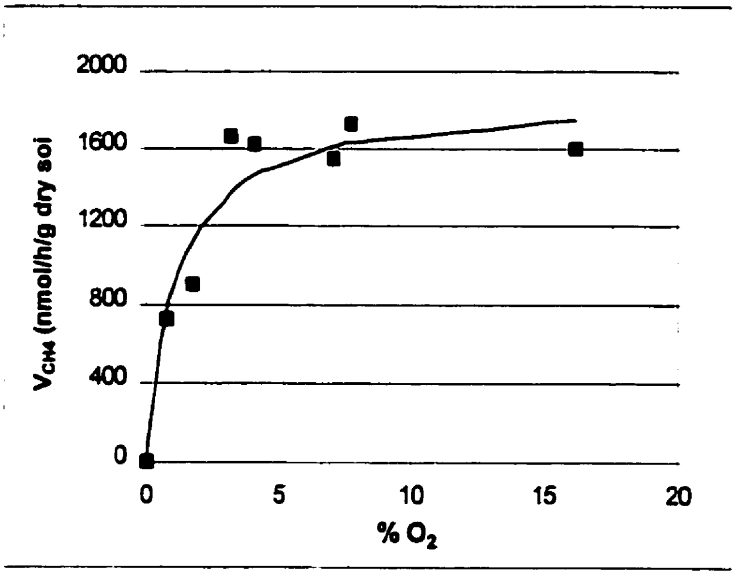

The apparent half-saturation constant for CH_4 oxidation as a function of O_2 concentration can also be estimated using an Eadie-Hofstee plot as illustrated in Figures 4-21 and 4-22.

Figure 4-21: Eadie-Hofstee plot for determining K_s due to O_2 at 36cm depth (SB1)

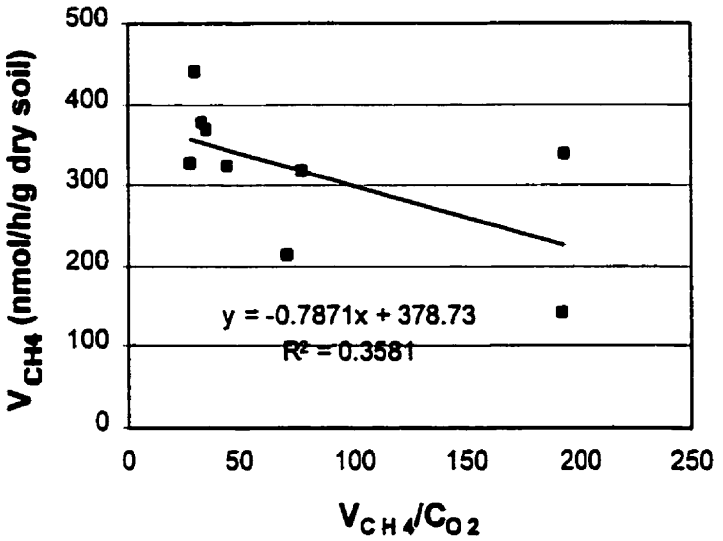

Figure 4-22: Eadie-Hofstee plot for determining K_s due to O_2 at 76 cm depth (SB1)

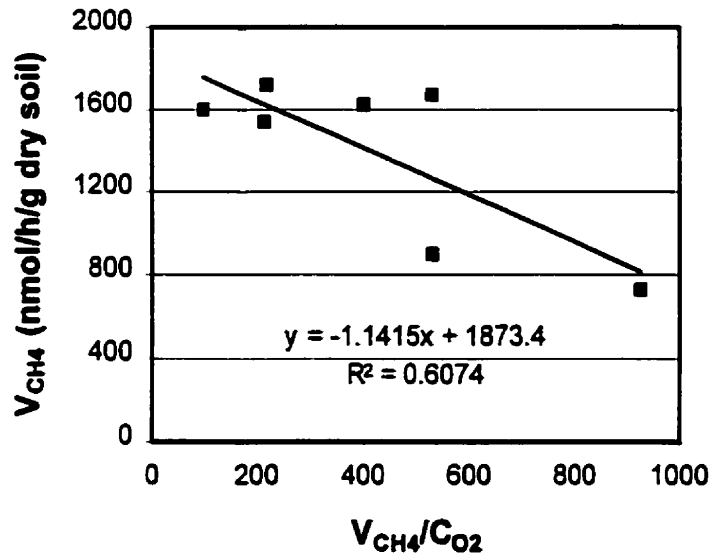

The quantity for K_s is equal to the inverse of the slope of these graphs. Because the correlation coefficient of the Eadie-Hofstee plot is low for the 36 cm depth, the K_s value determined for the 76cm depth is used in the numerical model developed in the next chapter. For the 76 cm depth, K_s was found to be 1.14% O_2, which is close to the value of 1.2% determined by deVisscher et al. (1999).

4.3.4 The Use of Batch Experiments for Determining Field CH_4 Oxidation Rates

The soil column experiments afforded the opportunity to evaluate whether the use of batch experiments for estimating in situ CH_4 oxidation rates in the field is a valid technique. This technique assumes that the in situ oxidation rates of a soil will equal those determined from a jar incubation experiment performed on a disturbed excavated soil sample.

Since the V_{max} values and CH_4 concentrations at various depths in the soil column are known, along with the half-saturation constants (K_s) for CH_4, the total CH_4 uptake rate in the soil column can be calculated. However, because batch experiments were conducted at almost atmospheric O_2 concentrations, and the local O_2 concentration in the soil air was much lower, the oxidation rates must be adjusted accordingly. The effect of sub-saturating O_2 concentrations on CH_4 oxidation can be explicitly accounted for with a modified Monod equation, which is:

$$V_{CH4} = V_{max}\left(\frac{C_{CH4}}{K_{CH4} + C_{CH4}}\right) * \left(\frac{C_{O2}}{C_{O2} + K_{O2}}\right) \qquad (4\text{-}2)$$

Where:

V_{CH4}, V_{max}, C_{CH4}, K_{CH4} as in Equation 4-1

C_{O2} = local O_2 concentration within the soil column

K_{O2} = kinetic half-saturation constant for O_2

Applying this equation to the three Springbank soil columns results in Figures 4-23, 4-24 and 4-25.

Figure 4-23: CH_4 oxidation rate profile column SB1

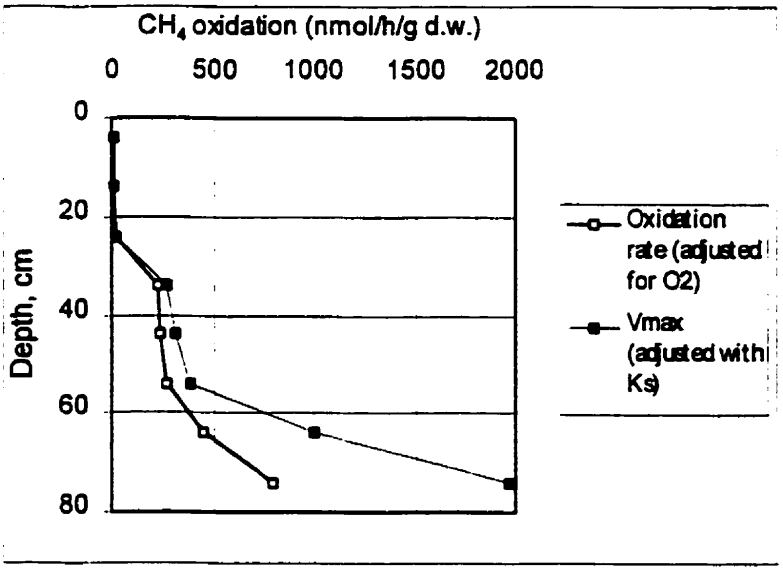

Figure 4-24: CH_4 oxidation rate profile in column SB2

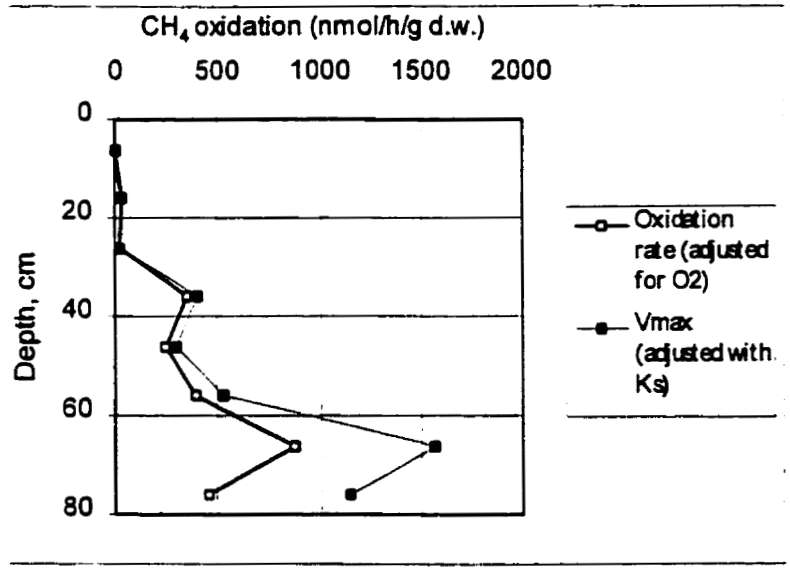

Figure 4-25: CH_4 oxidation rate profile in low CH_4 flow Springbank soil (SB3)

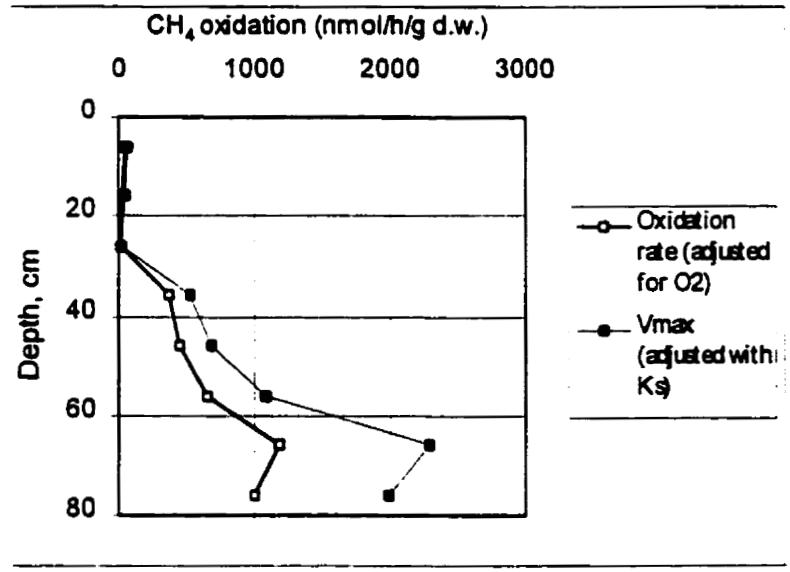

By integration along the entire column length, an estimate of the total CH_4 uptake of the soil column can be made. This estimate is compared with the CH_4 oxidation rates determined by mass balance (Equation 3-1) in Table 4-2.

Table 4-2: Comparison between batch test calculations and mass balance calculation of the overall column CH_4 oxidation rates.

Column	Q_{CH4} ($g/m^2/d$)	Tot. CH_4 Oxidation (batch tests) ($g/m^2/d$)	Tot. CH_4 Oxidation (mass balance) ($g/m^2/d$)	Oxidation efficiency (batch test) %	Oxidation efficiency (mass bal.) %	% Error
SB1	319.3	82.1	102.2	25.7	32.0	-19.6
SB2	333.3	104.8	120.0	31.4	36.0	-12.7
SB3	182.9	187.1	93.3	102.3	51.0	100.6

The estimates of the total CH_4 uptake based on batch experiments are reasonably close to those determined using a mass balance equation. However, there is a large discrepancy between the over all CH_4 oxidation rate calculated for column SB3 using batch experiments and the rate calculated on the basis of the column's mass balance. It was hypothesised that this was due to incorrect kinetic parameters being used for this soil column. Because the half-saturation kinetic constant (K_{CH4}) used to determine column SB3's V_{max} values was determined from experiments performed on column SB1 (a high CH_4 flow column), it might therefore be applicable only to the microbial population within column SB1. However, this alone cannot explain the discrepancy. For even if the correction for K_s given in Equation 4-1 were not applied, the overall CH_4 oxidation rate determined by integrating the local oxidation rates given in Figure 4-12 would still be 153 $g/m^2/day$ (64% more than the rate calculated using a mass balance). Only by assuming a K_{O2} value of 3.5% O_2 for the soil in column SB3 and not applying the K_s

correction would the batch test determined CH_4 oxidation rate equal the rate determined by mass balance. However, the K_{O2} values reported in literature are typically closer to 1%, and this author has never seen one that exceeded 2%. Therefore doubt is cast on the accuracy of the V_{max} values determined for column SB3.

4.3.5 Predicting V_{max} at the Depth of Maximum Oxidation

As was mentioned in Chapter 2, Czepiel et al. (1996b) observed a significant linear relationship between the maximum rate of CH_4 oxidation in a soil cover and the in situ soil gas CH_4 concentration, namely:

$$V_{max}=50*C_{CH4} \qquad (2\text{-}3)$$

As can be seen in Table 4-3, applying this equation to the CH_4 concentrations observed at the depth of maximum oxidation in the Springbank loam columns yields V_{max} values close to the values determined through batch incubation experiments, again with the exception of the soil from column SB3.

Table 4-3: Comparison between experimental V_{max} and V_{max} derived from Eqn. 2-3

Soil Column	Depth (cm)	V_{max} (Eqn. 2-3)	V_{max}(Experimental)
SB1	76	1861	1940
SB2	66	1907	1877
SB3	66	1006	2262

However, when considering some of the V_{max} values for CH_4 oxidation reported by others, it becomes apparent that Equation 2-3 must be applicable only to certain soil types. For example, Nozhevnikova et al. (1992) report a V_{max} of 25000 $nmol*h^{-1}*g^{-1}$. Substitution of their V_{max} value into Equation 2-3 would imply that their soil was exposed

to a CH_4 concentration of 500%, which is impossible. Bender and Conrad (1992) report an even higher V_{max} of 44500 $nmol*h^{-1}*g^{-1}$.

Another question that arises is how can the depth of the zone that has the highest V_{max}, or highest number of methanotrophs, be predicted for a given soil type and CH_4 flux rate? As was noted, methanotrophs seem to grow more rapidly under reduced oxygen concentrations. Therefore, the depth of maximal V_{max} may coincide with the zone which has the lowest O_2 concentration that is not rate-limiting. However, this depth would itself be a function of the number of methanotrophs present, as their consumption of O_2 limits its depth of diffusion. It might be possible to determine this depth by employing a numerical model that couples the growth and endogenous decay of biomass to the mass transfer of O_2 and CH_4.

4.3.6 Results of Temperature Manipulation Experiments

Methane oxidation rates were plotted against temperature to estimate the optimum temperature for CH_4 oxidation. The results of the incubation experiments performed on soil from the 36 cm depth of column SB1 are given in Figure 4-26. The error bars indicate the 90% confidence interval, based on the Student-t distribution.

Figure 4-26: Results of temperature manipulation experiments (SB1, 36 cm depth)

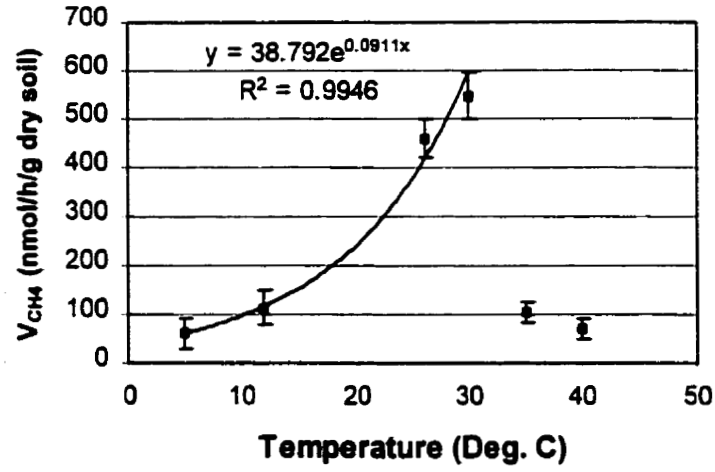

As the temperature is increased, CH_4 oxidation increased exponentially to a distinct maximum (in accordance with the Arrhenius relationship), and then decreases with continued temperature increase.

4.3.7 Results of Moisture Manipulation Experiments

All treatments gave linear decrease in headspace CH_4 concentration over 72 hours, which means that the consumption kinetics were zero-order and that oxidation rates were therefore moisture dependent rather than CH_4 dependent. The results of the moisture manipulation experiments on the soil from the 36 cm depth of column one are given in Figure 4-27.

Figure 4-27: CH_4 oxidation rate as a function of moisture (Col. SB1, 36cm depth)

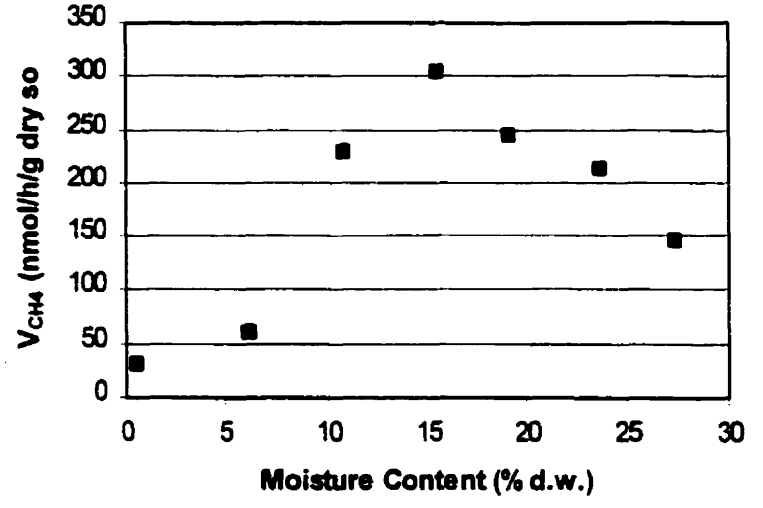

CH_4 oxidation rates decreased significantly after drying below field moisture contents, increased to an optimum value as water was added, and decreased with continued water addition. The maximum oxidation rate occurred at a moisture content of 15.4% (dry weight basis). The relatively low oxidation rate observed at a moisture content of 6% explains oxidation rates that were observed in the Rockyview dark soil prior to moisture addition.

This moisture response curve might also explain why Kightley et al. (1996) observed CH_4 oxidation rates that were 60% higher than those observed in this study. The Springbank soil columns had an average moisture content of 9.4% which, when compared with Figure 4-26, would indicate that the oxidation rate was approximately 66% of the potential rate. It is therefore conceivable that the Springbank columns could

have been oxidizing CH_4 at rates 50% higher than those observed, which would bring their oxidation rates close to those observed in the soil columns of Kightley et al. (1996).

4.4 Moisture and Soil Organic Matter Distribution Profiles

Moisture content was determined at each of the 10cm depths in all three Springbank loam columns (SB1-3). The results are presented in Figures 4-28, 4-29 and 4-30.

Figure 4-28: High CH_4 flow Springbank soil (column SB1) moisture content profile

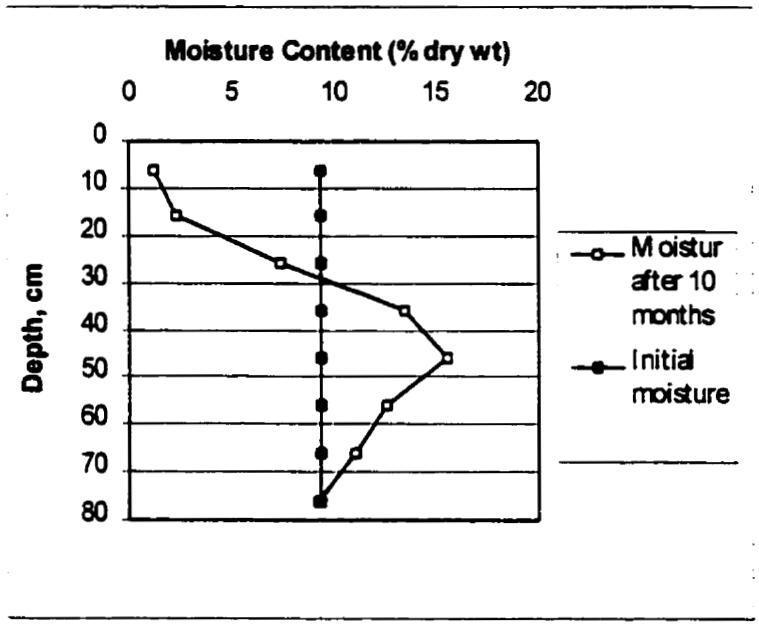

Figure 4-29: High CH_4 flow Springbank soil (column SB2) moisture content profile

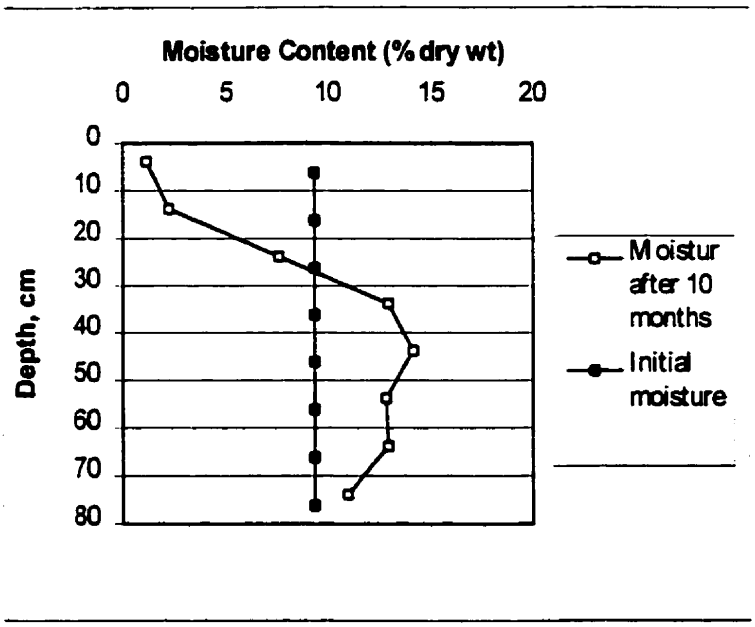

Figure 4-23: Low CH_4 flow Springbank soil (column SB3) moisture content profile

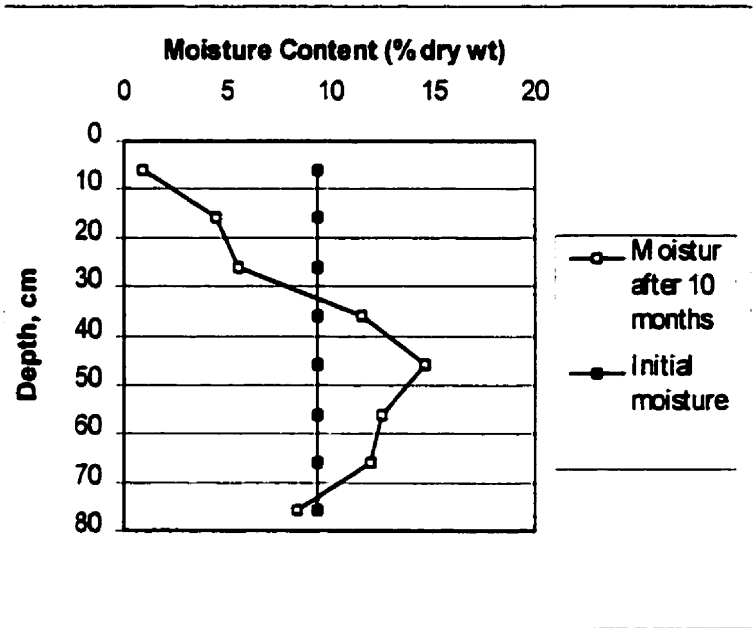

All three of the Springbank loam columns exhibited similar moisture content profiles after 10 months of operation. The top 26 cm exhibited significantly lower moisture contents, which was probably due to desiccation of the soil. It is unlikely that the accumulation of moisture at the 46 cm depths is due to the downward migration of moisture, for otherwise the lowest depth (76 cm) would have had higher moisture contents. Rather it is likely that a high moisture content is observed at the 46 cm depth because this was the region that saw the greatest amount of microbial CH_4 oxidation during the columns operative lifetime. Further evidence for this hypothesis is given by the higher amount of organic matter found at this depth, as illustrated in Figure 4-31.

The significantly lower moisture contents in the columns' top 26 cm might account for the notably lower CH_4 oxidation rates at these depths, in view of the CH_4 oxidation response to moisture content given in Figure 4-26.

The fact that column SB2 had a slightly higher moisture content than column SB1 at the lower depths might account for its slightly higher CH_4 oxidation rate. Alternatively, SB2's higher oxidation rate may instead be the cause of its higher moisture content at these depths.

Figure 4-31: Organic matter content profile of col. SB2 (after 10months)

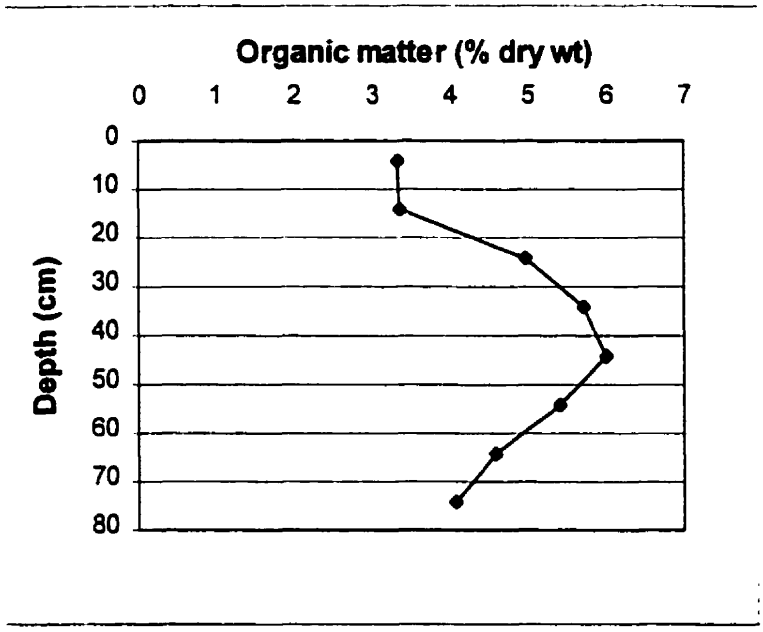

The depth containing the most organic matter (determined by loss on ignition at 550°C) corresponded to the depth with the highest moisture content. Since both water and bio-mass are products of the biological oxidation of CH_4, it is likely that this was the region that saw the greatest amount of microbial CH_4 oxidation.

However, this depth does not correspond to the location of maximal CH_4 oxidation indicated by the batch experiments. A possible explanation for this inconsistency is that the region of maximal oxidation had shifted downward during the column's lifetime. Further evidence for this is given by the vertical distribution of the carbon conversion coefficients (Y), which is the ratio of CH_4 converted to biomass, as determined in batch incubation experiments. Near the base of all of the columns, Y averages 0.5, and decreases toward the top of the column (see Table 4-4). As the

microbial population in a continuous growth reactor ages, Y tends to decrease (Gaudy and Gaudy, 1980). Therefore this vertical distribution of Y may indicate that the bacterial population at the bottom of the column was established more recently. Thus although the overall CH_4 oxidation rates within the columns have been at a steady state for several months, the depth at which most of the CH_4 oxidation occurs may have been shifting downward, perhaps due to the depletion of nutrients or the accumulation of exo-polymers.

Table 4-4: Carbon conversion ratios

Soil Column	Y at 46cm	Y at 76cm
SB1	0.12	0.65
SB2	0	0.42
SB3	0	0.51

Chapter 5. CH_4 Reactive-Transport Model

5.1 Introduction

The purposes of developing a numerical model that can predict the amount of methane that would be oxidised in a given soil cover are three-fold:

1. To provide a better quantitative understanding of the biological and physical processes related to CH_4 oxidation in soil covers than is currently available in the literature.
2. To aid in the design of CH_4 oxidative soil cover systems by reducing the number of laboratory experiments required to select the optimal soil type and thickness for a given environment. A soil methane reaction/transport model could be used in selecting the optimal soil type for a landfill or heavy oil well soil cover design.
3. To be able to estimate the methane oxidation potential of methanotrophic microbes living in various types of soils and in various climatic conditions in order to incorporate CH_4 oxidation into global emission models. Such estimations could also be used when claiming scientifically defensible carbon credits that arise from soil modification greenhouse gas offset projects.

All but one of the models presented to date have not considered the effects of mass transfer on limiting CH_4 oxidation. Rather they have been site specific models, and incapable of being applied to soils other than the ones for which they were developed.

Bogner et al. (1997) describes a 3-D model that does incorporate mass transfer equations, but does not offer any results. These models are briefly described below.

1. Czepiel et al.(1996b) developed a model that has no mass-transfer equations, but instead assumes that the zone of maximum CH_4 oxidation remains constant. It assumes V_{max} at the depth of maximum oxidation is directly proportional to CH_4 concentration. It does attempt to characterise the seasonable variability in CH_4 oxidation by interfacing with the BROOK90 soil/heat-flux model to determine soil moisture and temperature and then adjusts CH_4 oxidation rate accordingly.

2. Borjesson and Svensson (1996) developed a step-wise empirical regression model for predicting the CH_4 flux from a landfill which included the following variables: soil temperature, soil moisture at different depths, air pressure and the change in air pressure over time and partial pressures of CH_4, CO_2, N_2 and O_2. This model indirectly incorporates CH_4 oxidation, but does not allow one to quantify the magnitude of oxidation, and is entirely specific to the landfill for which it was developed.

3. Bogner et al. (1997) developed a 3D finite-difference model that simulates both the mass movement of methane through landfill cover materials and net emissions of CH_4 to the atmosphere. Their model simulates gas movement through a mass gradient approach based on the sum of the kinetic and

potential energy of the gas fluid. The soil matrix is modelled in each cubic node by assuming that all of the soil solids are present in a solid sphere in the node. The probability of collisional interactions between gas molecules and the solid sphere is calculated based on the ratio of the sphere's surface area in two dimensions (circle) to a node surface area. The transported CH_4 is the mass of CH_4 that completely passes through the node because of the mass transport gradient and which does not collide with the sphere (soil) within the node.

This model requires the input of gas concentration profiles through the cover for CH_4, CO_2, and O_2. Little information regarding the accuracy of their model's predictions has been provided, other than the vague claim of its order of magnitude predictive capability.

5.2 Model Development

The composition of the soil gas phase is determined by a combination of the physical transport of gases within the soil and the microbially mediated reactions of these gases.

5.2.1 Physical Transport Equations

The physical transport of gases in soil is mainly governed by diffusion and, to a lesser extent, advection (bulk flow). Field measurements performed by others indicate that the maximum pressure build-up in landfills is of the order of 0.3048 m of water. At such a

pressure, Mohsen (1980) has showed that mechanical dispersion is negligible. For this reason, mechanical dispersion terms have been omitted to simplify the model's equations.

The general flux equation for gas component i, taking into account diffusion and advection is:

$$J_i = -D_i \nabla C_i + \nu C_i \qquad (5\text{-}1)$$

Where:

J_i = the molar flux of gas component i ($mol*m^{-2}*s^{-1}$)

D_i = the diffusion coefficient of component i in soil ($m^2\ s^{-1}$)

∇C_i = the concentration gradient (the driving force of the diffusion) process) ($mol*m^{-2}$)

ν = the flow velocity of the gas mixture through the soil (m/s)

C_i = the concentration of component i ($mol*m^{-3}$)

5.2.1.1 Diffusive Transport of Gases in Soils

In soil systems, the efficiency of methane bio-oxidation is influenced by several factors, not the least of which is soil type. Soil texture and structure are extremely important parameters, as they determine a soil's gas diffusivity and water holding capacity.
The diffusion coefficient of a gas in a soil (D_i^s) is less than that in free air (D_i^a) because of the reduced cross-sectional area and increased path length caused by the presence of solid and liquid obstacles. To determine (D_i^s) one must determine (D_i^a) and then multiply it by the relative diffusion coefficient, ξ_g which is the ratio D_g^s / D_g^a. This ratio has been

shown to be independent of the nature of the gas or vapour (Yin and Jury, 1996) and is therefore a function of the physical properties of the soil alone. Several authors have attempted to find a relationship between ξ_g and the volumetric air content (a) of the soil (Freijer, 1994; Steele and Nieber, 1994). Although a simple and unique relationship between ξ_g and a that can be used for a variety of porous media has never been found, Jin and Jury (1996) have shown that the following Millington-Quirk model gives reasonable values, especially for disturbed soils:

$$\xi_g(a) = a^2 / \phi^{2/3} \tag{5-2}$$

Where:

ϕ = soil porosity

a = volumetric air content

So to determine (D_i^s) one must determine (D_i^a). Because the gas phase is a heterogeneous mixture consisting of four gases, the diffusion coefficient (D_i^a) will be a function of the mole fractions of the gases. Reid and Sherwood (1966) gave the following equation for the diffusion coefficient of component i (D_{im}) diffusing in a homogeneous mixture of m components:

$$D_{im} = \frac{(1 - y_i)}{\sum_{\substack{j=1 \\ i \neq j}}^{m} (y_j / D_{ij})} \tag{5-3}$$

Where:

y_i = mole fraction of the diffusing component i

y_j = mole fraction of component j

D_{ij} = diffusion coefficient for a binary mixture of component i and j

To use Equation 5-3 the binary diffusion coefficient for each combination of gases needs to be known (i.e. D_{CH4-N2}, D_{CH4-O2}, $D_{CH4-CO2}$, D_{N2-O2}, D_{N2-CO2}, and D_{O2-CO2}). Several correlations and methods for predicting binary diffusion coefficients in gas mixtures have been proposed over the years. A relatively simple yet accurate semi-empirical equation, which requires only the molecular weights and critical temperatures and pressures of the relevant gases was proposed by Chen and Othmer (1962). The diffusion coefficient $D_{1,2}$ for the diffusion of gas 1 in gas 2 at moderate pressures can be calculated from the following equation:

$$D_{1,2} = \frac{0.604 * 10^{-8} * T^{1.81} * \left(\frac{M_1 + M_2}{M_1 M_2}\right)^{0.5}}{P * (T_{C,1} * T_{C,2})^{0.1405} (V_{C,1}^{0.4} + V_{C,2}^{0.4})^2} \qquad (5\text{-}4)$$

Where:

M_1, M_2 = molecular weight of both components (kg/kmol)

$T_{c,1}$, $T_{c,2}$ = critical temperature (K)

$V_{c,1}$, $V_{c,2}$ = critical volume (m^3/kmol)

T = temperature (K)

P = pressure (bar)

$D_{1,2}$ = diffusion coefficient (m^2/s)

5.2.1.2 Advective Transport of Gases (Bulk Flow)

The advective transport of gases at a flow velocity, v, will occur as a result of gradients in total pressure. The equation for v is assumed to be Darcy's law, which, neglecting the gravitational term, is:

$$v = \frac{k}{\mu}\frac{\partial P}{\partial x} \tag{5-5}$$

Where:

μ = the gas-mixture viscosity

k = intrinsic permeability of soil

P = pressure

Pressure can be calculated using the ideal gas law if the concentration of each gas component is known.

$$P=(C_1 + C_2 + ... + C_n)*R*T \tag{5-6}$$

Where:

C_i = concentration of component i

R = universal gas constant

T = absolute temperature

The viscosity of the gas mixture (μ) can be expressed as a function of the viscosities of the individual gases using the following formulae (Reid and Sherwood, 1966):

$$\mu = \sum_{i=1}^{4} \frac{\mu}{1 + \sum_{\substack{j=1 \\ i \neq j}}^{4} \theta_{i,j} \frac{y_j}{y_i}}_{i} \tag{5-7}$$

Where:

μ = visocicity of gas mixture

y_i = mole fraction of gas i

$$\theta_{i,j} = \frac{\left[1+\left(\frac{\mu_i}{\mu_j}\right)^{1/2}\left(\frac{M_j}{M_i}\right)^{1/4}\right]^2}{\sqrt{8}\left(1+\frac{M_i}{M_j}\right)^{1/2}} \qquad (5\text{-}8)$$

Where:

μ_i = viscocity of gas component i

M_i = molar mass of gas i

The viscocities of the individual gases at standard temperature and pressure (in N-s/m^2 * 10^{-5}) are as follows: μ_{CH4} = 1.1024; μ_{O2} = 2.071; μ_{CO2} = 1.4995; μ_{N2} = 1.7865 (Reid and Sherwood, 1966). While these values can be corrected for temperature, the change in their magnitudes over the range of temperatures expected in soil covers are relatively small (< 6%).

The soil's permeability (k) was determined experimentally using the method outlined in Chapter 3. For the Springbank soil, k was found to equal $9.72*10^{-13}$m^2. This is close to the value one would expect for a loamy soil, based on the permeabilities reported in literature given in Table 5-1.

Table 5-1: Soil permeabilities

Soil type	Permeability, k (m^2)
Gravel	$10^{-9} - 10^{-7}$
Sand	$10^{-13} - 10^{-10}$
Silt	$10^{-15} - 10^{-13}$
Clay	$10^{-18} - 10^{-15}$

Source: Schnoor, 1996.

5.2.2 Biological Reaction

The biological oxidation of CH_4 can be modelled using the modified Monod equation given in section 4.2.3. Based on the work of Hoeck (1962) the rate of CO_2 production was assumed to be 0.8 times the rate of CH_4 consumption. The O_2 consumption rate was assumed to be 1.5 times the rate of CH_4 consumption, based on Equation 2-1.

5.2.3 Continuity Equation

The continuity equation for gas component i can be written as:

$$\phi \frac{dC_i}{dt} = -\nabla \bullet J_i + R_i \qquad (5\text{-}9)$$

where:

J = flux of gas i due to physical transport (advection and diffusion)

R_i = the rate of production of component i (due to chemical or biological reaction)

ϕ = soil porosity

Combining Equations 5-1 and 5-9 gives:

$$\phi \frac{dC_i}{dt} = D_i \nabla^2 C_i - \nabla(vC_i) + R_i \qquad (5\text{-}10)$$

Since this model is one-dimensional, Equation 5-10 can be rewritten as

$$\phi \frac{dC_i}{dt} = D\frac{d^2C_i}{dx^2} - \frac{d(vC_i)}{dx} + R_i \qquad (5\text{-}11)$$

5.2.4 Discretization

The systems of Equations 5-11 can be solved numerically using a finite difference scheme. The concentrations of all of the gases are calculated at a number of equidistant points, under the assumption that the concentrations vary linearly between these points (see Figure 5-1). The soil properties are also assumed to be homogeneous between these points.

Figure 5-1. Finite difference representation of concentration profile

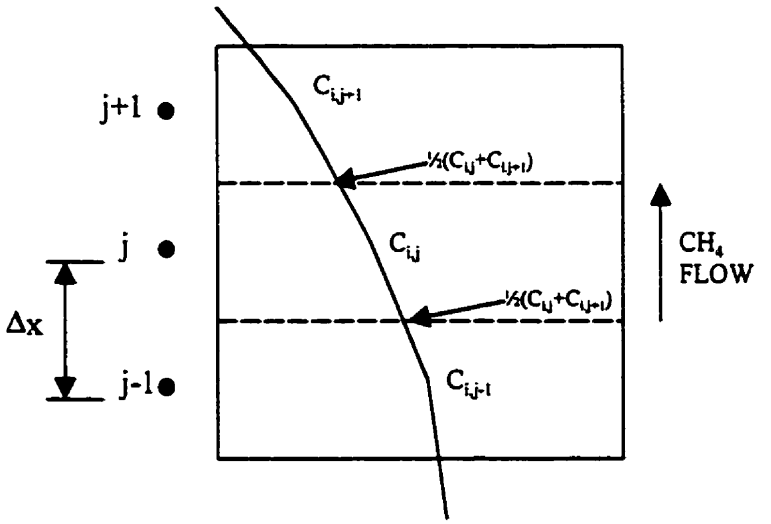

5.2.5 Steady State Solution

First, an attempt was made to find a steady-state solution to Equation 5-11, which when given a soil's mass transfer and biological kinetic parameters as inputs would output soil

gas concentrations and CH_4 oxidation rates. A steady state solution was seen as desirable for its computational speed. To obtain this model, the derivatives in the system of transport equations are set to zero, resulting in a simple 1-D boundary value problem. An equilibrium matrix was generated by lagging the coefficients, which was then solved using the Gauss-Siedel algorithm. However, this model failed to produce a physically meaningful solution, consequently its development is given in Appendix E.

5.2.6 Non-Steady State Model Formulation

The transport Equation 5-1 can be written as a finite difference equation by dividing the soil column into j segments centred at the nodes (as in the steady state case), and considering the continuity equation for each segment, giving:

$$\frac{dn_{i,j}}{dt} = J_{i,j-1/2} - J_{i,j+1/2} - \Delta x R_i \tag{5-12}$$

The number of moles of gas component i contained in segment j is:

$$n_{ij} = \varphi_j * \Delta x * C_{ij} \tag{5-13}$$

Therefore

$$\varphi_j \frac{dC_{i,j}}{dt} = \frac{J_{i,j-1/2} - J_{i,j+1/2}}{\Delta x} - R_i \tag{5-14}$$

This central difference approximation for the flux gradient results in second order accuracy.

Discretizing the time domain gives:

$$\frac{C_{i,j}^{k+1} - C_{i,j}^{k}}{\Delta t} = \frac{J_{i,j-1/2} - J_{i,j+1/2}}{\Delta x \varphi_j} - \frac{R_i}{\varphi_j} \tag{5-15}$$

$$C_{i,j}^{k+1} = C_{i,j}^{k} + \Delta t \frac{J_{i,j-1/2} - J_{i,j+1/2}}{\Delta x \varphi_j} - \frac{R_i}{\varphi_j} \Delta t \tag{5-16}$$

The flux of gas i through the lower boundary of segment j is:

$$J_{i,j-1/2} = -D_{i,j-1/2} * \frac{(C_{i,j} - C_{i,j-1})}{\Delta x} - \frac{k_{j-1/2}}{\mu_{j-1/2}} * \frac{(C_{i,j} + C_{i,j-1})}{2} * \frac{(P_j - P_{j-1})}{\Delta x} \tag{5-17}$$

The flux of gas i through the upper boundary of segment j is:

$$J_{i,j+1/2} = -D_{i,j-1/2} * \frac{(C_{i,j} - C_{i,j-1})}{\Delta x} - \frac{k_{j-1/2}}{\mu_{j-1/2}} * \frac{(C_{i,j} + C_{i,j-1})}{2} * \frac{(P_j - P_{j-1})}{\Delta x} \tag{5-18}$$

Substituting Equations 5-13 and 5-14 into Equation 5-17 gives:

$$\begin{aligned} C_{i,j}^{k+1} = C_{i,j}^{k} + \frac{D_{i,j+1/2}\Delta t}{\phi_j \Delta x^2}(C_{i,j+1}^{k} - C_{i,j}^{k}) - \frac{D_{i,j-1/2}\Delta t}{\phi_j \Delta x^2}(C_{i,j}^{k} - C_{i,j-1}^{k}) + \\ \frac{k_{j+1/2}\Delta t}{8\phi_j \mu_{j+1/2}\Delta x^2}(C_{i,j}^{k} - C_{i,j+1}^{k})(P_{j+1}^{k} - P_j^{k}) - \frac{k_{j-1/2}\Delta t}{8\phi_j \mu_{j-1/2}\Delta x^2}(C_{i,j-1}^{k} - C_{i,j}^{k})(P_j^{k} - P_{j-1}^{k}) - \frac{\Delta t}{\phi_j} R_{i,j} \end{aligned} \tag{5-19}$$

5.2.6.1 Solution Procedure

From the initial conditions, the soil gas concentrations are known for each node. Knowing these concentrations, the pressures can be calculated at each node using equation 5-6. These values can be substituted into Equation 5-19, giving $C_{i,j}^{k+1}$.

Predictor-Corrector Scheme

A commonly used approach for solving initial value problems is the predictor-corrector method. It is a two-step method which gives a more accurate and usually more stable result than the unmodified forward Euler method (Cheney and Kincaid, 1985). To implement it, one uses a two-step approach consisting of:

$$C^{P}_{n+1} = C_n + \Delta t * f_n \tag{5-20}$$

which is just a standard forward Euler step, followed by a corrector step where the reaction and transport rates are computed using the provisional value of the concentration, C^P:

$$C^{C}_{n+1} = C_n + (\Delta t/2)* (f_n + f^{P}_{n+1}) \tag{5-21}$$

Using this method instead of the explicit Euler method allowed the time step, Δt, to be increased by nearly a factor of ten, which significantly improved the computational efficiency of the program.

5.2.6.2 Solution Domain, Boundary Conditions and Initial Conditions

The solution domain and boundary conditions are identical to that of the steady-state problem, however a false node does not have to be created as in the case of the equilibrium method. For the initial condition, the concentrations for all of the nodes are set to 100% air. Again, the upper boundary is assumed to be at constant (atmospheric) concentrations, i.e. $C_{CH4} = 1.7$ppm; $C_{O2} = 20.9\%$; C_{O2}=330ppm; $C_{N2} = 79.0\%$

To ensure that the model would converge, a simplified version without biological oxidation of CH_4 was first programmed in MathCAD using the following constant parameters (obtained from the lab data for sedge peat column SP1):

$D_{CH4} = 7.0 * 10^{-6}\ m^2/s$

$D_{air} = 6.53*10^{-6}\ m^2/s$

$k_{air} / \mu_{air} = 3.12 * 10^{-8}\ m/s$

Results:

The simplified model converged, provided that the time interval used was small enough. Consequently, a complete version of the model was programmed in BASIC which included equations for CH_4 oxidation, algorithms for calculating diffusivities and viscosities as functions of gas mole fractions, and the effects of moisture content and porosity on intrinsic diffusivity. The model source code is given in Appendix F.

5.3 Comparison Between Experimental Results and Uncalibrated Model Results

5.3.1 Column SB1

The following soil properties and biological kinetic parameters from soil column SB1 were used as model inputs to assess the model's validity.

Model Inputs:

- $G_s = 2.5$ g/cm^3 (soil particle density)
- $\rho_{bulk} = 1.163$ g/cm^3
- CH_4 Flux = 319 g * m^{-2} * day^{-1}
- $k = 9.7 * 10^{-13}$ m^2 (intrinsic permeability)
- V_{max} = values given in Appendix B1
- Moisture contents = values given in Appendix B1
- μ_j = calculated with Equation 12
- $D_{i,j}$ = calculated with Equation 9
- $K_{O2} = 1.1\%$
- $K_{CH4} = 0.75\%$

Figure 5-2: Uncalibrated model results versus experimental results (Col. SB1)

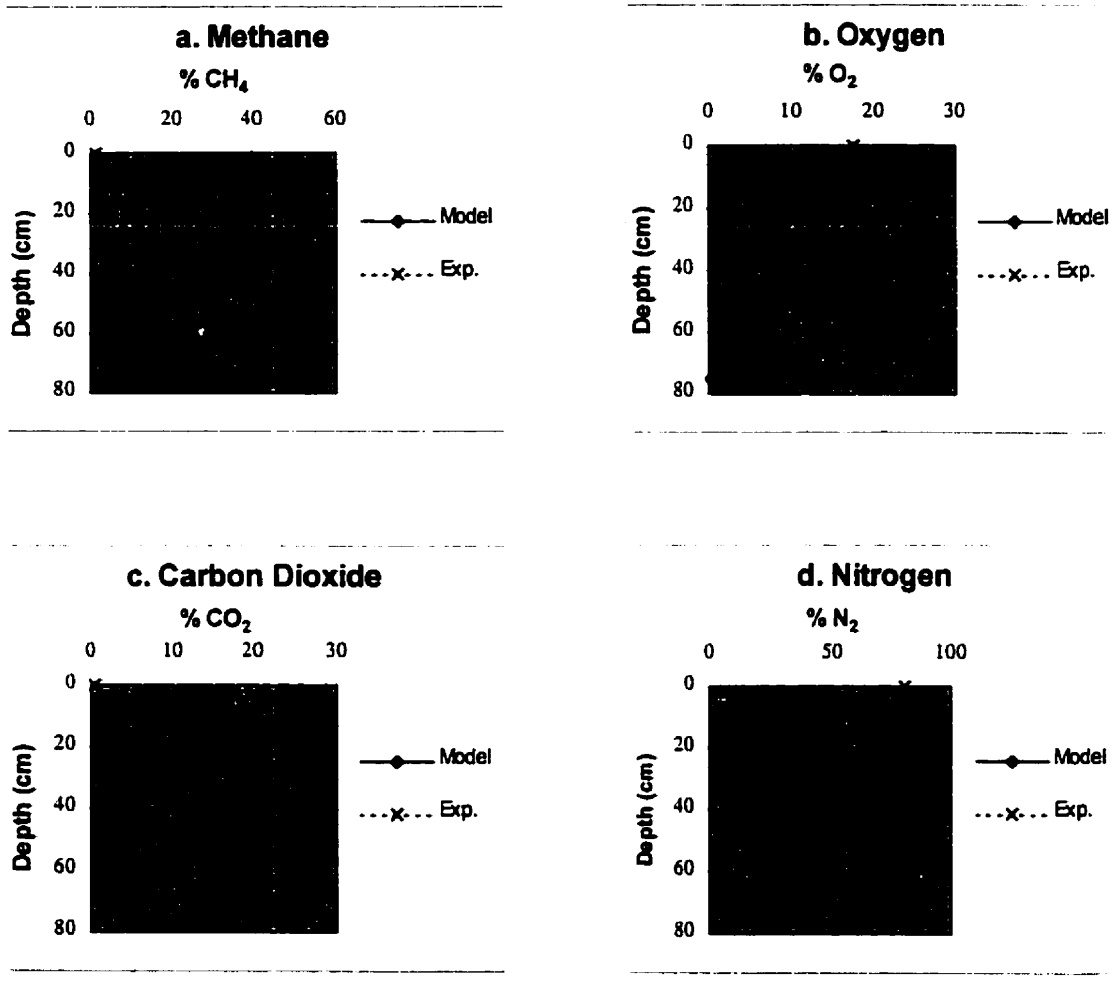

%CH_4 Oxidised (model) = 21.5%

% CH_4 Oxidised (experimental) = 25.7 %

Error = -21.6%

5.3.2 Column SB2

Model Input

As in 6.3.1.1 with the following exceptions:

- $\rho_{bulk} = 1.163$ g/cm^3
- CH_4 Flux = 328 g*m^{-2}*day^{-1}
- V_{max} values from Appendix B.2
- Moisture contents from Appendix B.2

Results:

Figure 5-3: Uncalibrated model results versus experimental results (Col. SB2)

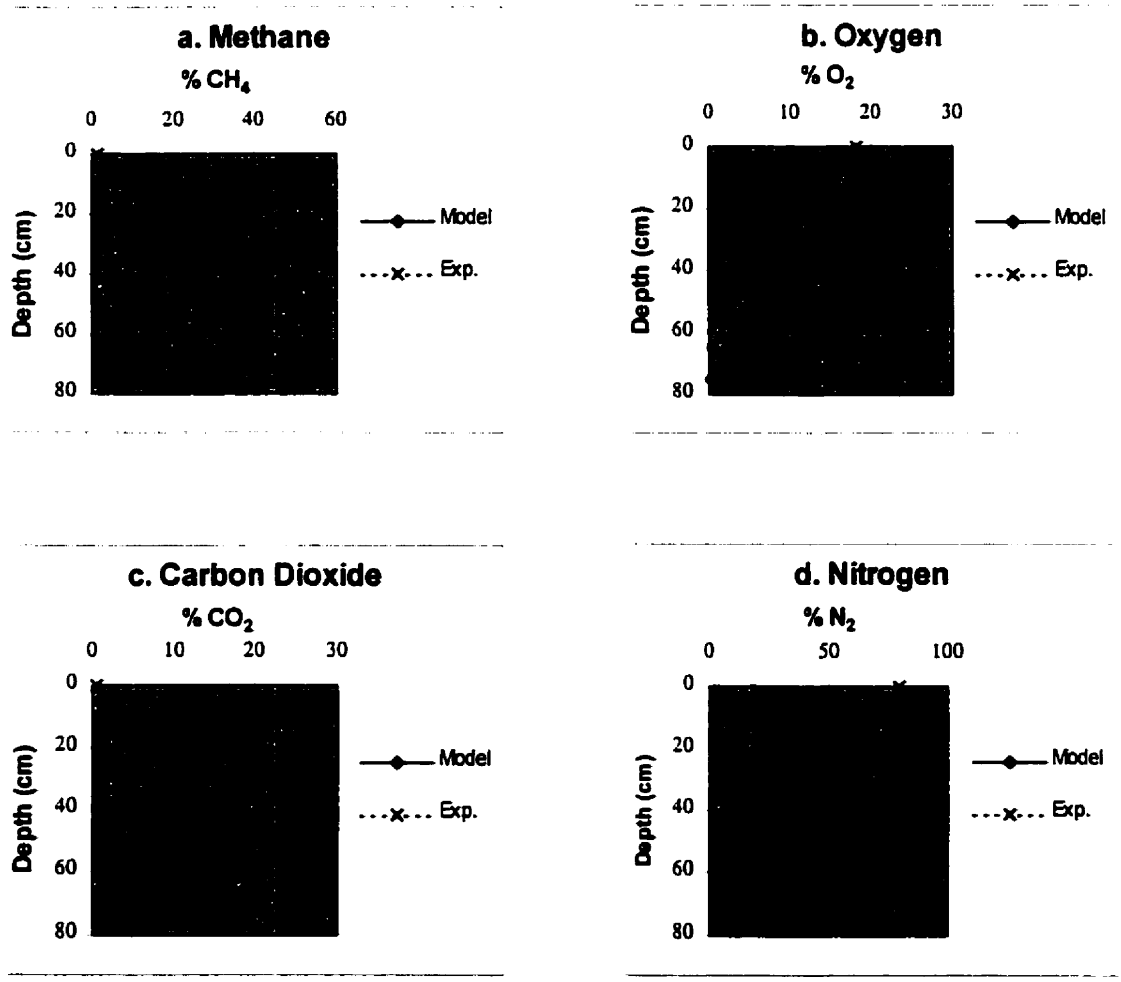

*%CH_4 Oxidised (model) = 22.6%

% CH_4 Oxidised (experimental) = 31.4%

error = -28%

Discussion

The model predicts CH_4 oxidation rates that are between 72 and 78% of those determined using incubation experiments. This can be explained by the further observation that the model-predicted O_2 concentrations were less than 0.2% for the 76cm depth, which is approximately one quarter of the experimentally measured concentrations of 0.75%. This seemingly modest discrepancy has a large impact on the over-all oxidation rate because a relatively high amount of oxidation occurs in the columns at this depth (as is evidenced by the high V_{max} values). For an O_2 half-saturation constant of K_{O2} = 1.1%, an O_2 concentration of 0.2% would result in a local oxidation rate of 15% of the V_{max} rate, whereas an O_2 concentration of 0.75% would result in a local oxidation rate of 40% of V_{max}, which would account for the model's error in predicting the overall CH_4 oxidation rate .

Notwithstanding this deviation, the model gives reasonable predictions of the N_2, O_2 and CH_4 concentration profiles. A slightly larger deviation from the measured CO_2 profile is seen, possibly due to the use of an inaccurate coefficient for CO_2 in the CH_4 oxidation stoichiometric equation.

5.4 Model Stability

5.4.1 Peclet Number

The Peclet number is a non-dimensional term which compares the characteristic time for dispersion and diffusion given a length scale with the characteristic time for advection (Steefel and Macquarie, 1996). It is defined as:

$$Pe = v^*\Delta x/D \tag{5-22}$$

Where $v=q/\phi$ is the average linear (gas) velocity and the characteristic length scale is given by the grid spacing Δx. If central difference approximations are used for the first derivative terms then at grid Peclet numbers below 2 (i.e. dispersion/diffusion and advection are either of approximately the same importance or the system is dominated by dispersion and/or diffusion), the central difference approximation is monotone. Monotonicity means that non-physical solutions (e.g. negative concentrations) are not produced.

5.4.2 Courant-Friendrich-Lewy Number

The Courant-Friendrich-Lewy (CFL) number is a parameter that gives the fractional distance relative to the grid spacing travelled due to advection in a single time step (Steefel and Macquarie, 1996).

$$CFL = v^*\Delta t / \Delta x \tag{5-23}$$

Using Fourier error analysis it is possible to show that for a forward difference in time approximation, no matter what approximation is used for the spatial derivatives, the transport equation is stable for values of the CFL < 1.

5.4.3 Diffusion Number

A similar expression to the CFL number has been derived for systems characterised by diffusive transport (Steefel and Macquarie, 1996).

$$N_D = (D^*\Delta t) / (\Delta x)^2 \tag{5-24}$$

Again, the stability constraint for an explicit formulation is that N_D be less than 1.

5.4.4 Results of Stability Analysis

5.4.4.1 Effects of Soil Permeability on Stability

Soil permeability was seen to have a significant effect on the minimum time-step required to maintain model stability, as is evident in Table 5-2.

Table 5-2: Effects of Soil Permeability on Stability

Permeabil. (m^2)	Advective CH_4 flow ($g*m^{-2}*day^{-1}$)	Diffusive CH_4 flow ($g*m^{-2}*day^{-1}$)	adv./diff. (non-dim.)	Peclet # (non-dim.)	CFL # (non-dim.)	Nd (bot. node) (non-dim.)	Nd (top node) (non-dim.)	Minimum time-step (sec)
9.72E-10	76	193	0.393782	0.151	3.20E-06	2.10E-05	1.53E-04	0.15
9.72E-11	75.2	193.5	0.38863	0.154	3.21E-05	2.09E-04	1.53E-03	1.5
9.72E-12	74.4	194.1	0.383308	0.152	3.17E-04	2.09E-03	1.53E-02	15
9.72E-13	66.6	200.4	0.332335	0.134	2.80E-03	2.09E-02	1.53E-01	150
9.72E-14	35.7	228	0.156579	0.068	7.07E-03	0.104	0.77	750
9.72E-15	7.05	253	0.027866	0.013	1.33E-03	0.104	0.77	750

For permeabilities greater than $9.72*10^{-13}$ m^2, 25% of the total mass transfer is through advection. Consequently the Peclet number is seen to govern the maximum time-step, which is a function of soil's permeability. For permeabilities less than $9.72*10^{-13}$ m^2, where diffusion is dominant, the maximum time-step is governed by the Diffusion Number, and is independent of the soil's permeability. The maximum time-step for this model is not limited by the CFL number.

5.4.4.2 Effect of Time-Step Size on Stability and Accuracy

To assess the effect that the model's time-step size has on accuracy, numerical simulations were run at time-steps varying over four orders of magnitude using the base-case model inputs given in section 5.3.1. The results are presented in Table 5-3.

Table 5-3: Effect of Time-Step Size on Stability and Accuracy (at $k=9.72*10^{-13}m^2$)

Time-step (sec)	CH_4 ox. ($g*m^{-2}*day^{-1}$)	C_{CH4} @ node1 (%)	C_{O2} @ node 1 (%)	Peclet # (non-dim.)	CFL # (non-dim.)	Nd (bot. Node) (non-dim.)	Nd (top node) (non-dim.)
0.15	87.8	35.4	0.708	0.135	2.81E-06	2.09E-05	1.53E-03
1.5	87.8	35.54	0.708	0.134	2.80E-05	2.09E-04	1.53E-03
15	87.8	35.6	0.708	0.134	2.80E-04	2.09E-03	1.53E-02
150	87.8	35.6	0.708	0.134	2.80E-03	2.09E-02	1.53E-01

As can be seen in Table 5-3, to increase computational efficiency, the maximum time-step that retains model stability can be used without a reduction in accuracy.

5.4.4.3 Effect of Spatial Discretization on Model Stability

To assess the effect that the model's spatial step-size has on accuracy, numerical simulations were run for four dz values using the base-case model inputs given in section 5.3.1. Biological oxidation was not included in these simulations. The results are presented in table 5-4.

Table 5-4: Effect of spatial discretization (dz) on stability

Dz (m)	dt (max) (sec)	Peclet # (non-dim.)	CFL # (non-dim.)	Nd# (top node)
0.1	40	0.082	1.99E-03	0.18
0.2	150	0.166	3.74E-04	0.155
0.266	275	0.22	5.16E-03	0.11
0.4	700	0.31	9.00E-03	0.12

5.5 Sensitivity Analysis

The overall responsiveness and sensitivity of certain model parameters was determined prior to calibration. The sensitivity of a model's dependent variable to a model input parameter is the partial derivative of the dependent variable with respect to that parameter (Zheng and Bennett, 1995). This partial derivative can be normalised by the parameter value so that the sensitivity coefficient with respect to any parameter is the same unit as that for the dependent variable, i.e.,

$$X_{i,k} = \frac{\partial y_i / y_i}{\partial a_k / a_k} \approx \frac{(y_i(a_k + \Delta a_k) - y_i(a_k)) / y_i(a_k)}{\Delta a_k / a_k} \qquad (5\text{-}25)$$

Here $X_{i,k}$ is the sensitivity coefficient of the model dependent variable y with respect to parameter k at observation i. The parameter value for the base case is a_k and Δa_k is a small change in it; $y(a_k)$ and $y(a_k + \Delta a_k)$ are the values of the dependent variable obtained for the base case and for the perturbed-parameter case, respectively.

Repeated forward simulation runs were performed to calculate the sensitivity coefficient for the following parameters:

1. Intrinsic permeability (k)
2. Porosity (ϕ)
3. O_2 diffusivity factor (a multiplier of the binary O_2 diffusion coefficients)
4. Relative diffusivity factor (a multiplier of the relative diffusivity, ξ_g)

The following model input parameters were used, unless otherwise stated:

- dz = 0.1 m
- Gs = 2.65 Kg/m^3 (unless otherwise stated)
- $D_{O2\text{-}CH4}$ = 1.11*10^{-5} m^2/s (unless otherwise stated)
- k = 9.72*10^{-13} m^2 (unless otherwise stated)
- K_{CH4} = 0.75%
- K_{O2} = 1.1 %
- dt = 30 sec.

The results of the sensitivity analysis are presented in Tables 5-5 through 5-9, and a chart of the sensitivity coefficients is presented in Figure 5-4.

Table 5-5: Sensitivity to permeability (k)

k (m^2)	CH_4 ox. ($g*m^{-2}*day^{-1}$)	$X_{i,k}$	C_{CH4} @ node1 (%)	$X_{i,k}$	C_{O2} @ node 1 (%)	$X_{i,k}$
9.72E-10	86.3	0.00	36.3	0.00	0.70817	0.00
9.72E-11	86.42	0.00	36.4	0.00	0.709	0.00
9.72E-12	86.5	0.00	36.3	0.00	0.708	0.00
9.72E-13	87.7	1.00	35.6	1.00	0.708	1.00
9.72E-14	92.2	-0.06	33.1	0.08	0.7	0.01
9.72E-15	100.1	-0.14	31.4	0.12	0.685	0.03

Table 5-6: Sensitivity to porosity (ϕ)

ϕ	$\%CH_4$ Ox.	$X_{i,k}$	$\%\ CH_4$ @ Node 1	$X_{i,k}$	$\%\ O_2$ @ node 1	$X_{i,k}$
0.53	15.4	2.15	51.4	-2.36	0.066	6.41
0.55	16.74	2.19	47.6	-2.26	0.09	7.13
0.57	18.13	1.00	44.1	1.00	0.12	1.00
0.59	19.52	2.19	41	-2.00	0.16	9.50
0.61	20.93	2.20	38.16	-1.92	0.205	10.09

Table 5-7: Sensitivity to O_2 diffusivity

O_2 diff. Coef.	%CH_4 Ox.	$X_{i,k}$	% CH_4 @ Node 1	$X_{i,k}$	% O_2 @ node 1	$X_{i,k}$
1	20.1	1.000	39.7	1.000	0.18	1.000
1.1	21.7	0.796	38.9	-0.202	0.23	2.778
1.2	23.3	0.796	38.1	-0.202	0.29	3.056
1.3	24.8	0.779	37.4	-0.193	0.36	3.333
1.4	26.3	0.771	36.6	-0.195	0.44	3.611
1.5	27.8	0.766	35.9	-0.191	0.53	3.889
1.6	29.2	0.755	35.3	-0.185	0.63	4.167
1.7	30.6	0.746	34.6	-0.184	0.74	4.444
1.8	31.9	0.734	34	-0.179	0.86	4.722

Table 5-8: Sensitivity to relative diffusivity (ξ_g)

ξ_g	%CH_4 Ox.	$X_{i,k}$	% CH_4 @ Node 1	$X_{i,k}$	% O_2 @ node 1	$X_{i,k}$
1	20.14	1.000	39.7	1.000	0.18	1.000
1.1	21.9	0.874	36.5	-0.806	0.24	3.333
1.2	23.6	0.859	33.6	-0.768	0.31	3.611
1.3	25.3	0.854	31.1	-0.722	0.39	3.889
1.4	27	0.852	28.9	-0.680	0.49	4.306

Figure 5-4: Sensitivity coefficients

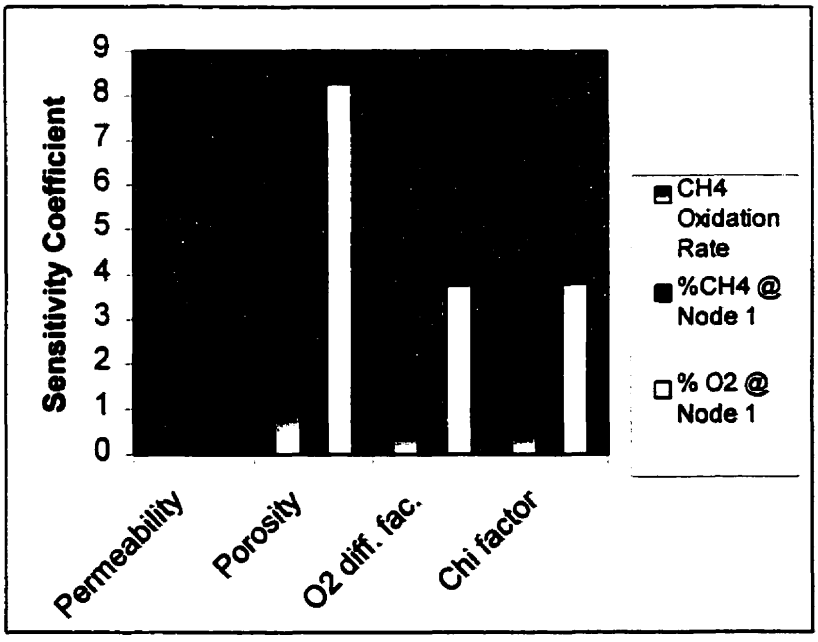

As can be seen in Figure 5-4, all of the dependent variables investigated are insensitive to the soil permeability. This is in agreement with observations found in literature which indicate that mass transfer of CH_4 landfill soil covers is governed mainly by diffusion. Thus when modelling CH_4 migration through soil covers with permeabilities greater than $10^{-12}\,m^2$ (i.e. sands or gravels) and at flux rates comparable to those found in landfills, it is possible to greatly increase computational efficiency by using a numeric value for k of $10^{-12}\,m^2$. This can be done without a reduction in accuracy.

The parameters that had the greatest effect on model output were porosity, the relative diffusivity coefficient, and the O_2 diffusivity coefficient. These are the parameters that were varied for the purpose of calibration.

5.6 Model Calibration

In calibrating a numerical model, the goal is to adjust model input parameters until model output variables match empirically observed values to a reasonable degree. In this case, conformity between model output and experimental variables was sought for both the total CH_4 oxidation rate and the gas concentration profiles. A correspondence was sought between the modelled CH_4 oxidation rate and the oxidation rate determined from batch incubation experiments because these experiments were used to determine the model's biological kinetic parameters. Model calibration was carried out by running the simulation repeatedly, and manually adjusting the input parameters selected for calibration, including the upper boundary gas concentrations.

Correspondence between the model output variables (gas profiles and oxidation rates) and experimental results was best achieved by multiplying the O_2 diffusivity coefficient by 1.15. While a reasonable correspondence was achieved for CH_4 oxidation rates by multiplying the relative diffusivity coefficient (ξ_g) by a factor of 1.15, this resulted in a substantial deviation from the experimentally observed gas concentration profiles.

5.6.1 Column SB1 Calibrated Results

The calibrated model output for a simulation of column SB1 is presented in Figure 5-5.

Figure 5-5: SB1 model output with O_2 diffusivity multiplied by 1.15

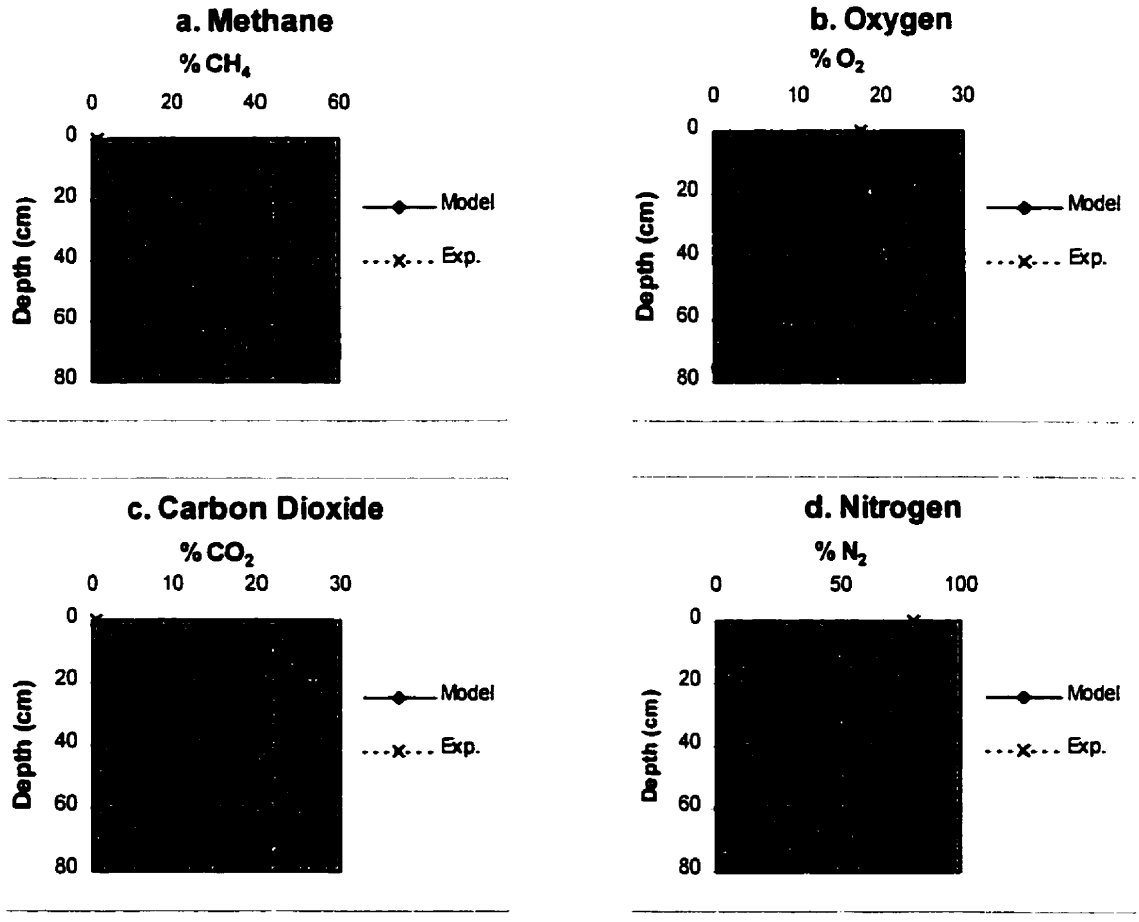

%CH_4 Oxidised (model) = 25.6%

% CH_4 Oxidised (experimental) = 25.7 %

Error = -0.4%

5.6.2 Column SB2 Calibrated Results

The calibrated model output for a simulation of column SB2 is presented in figure 5-6.

Figure 5-6: SB2 model output with O_2 diffusivity multiplied by 1.15

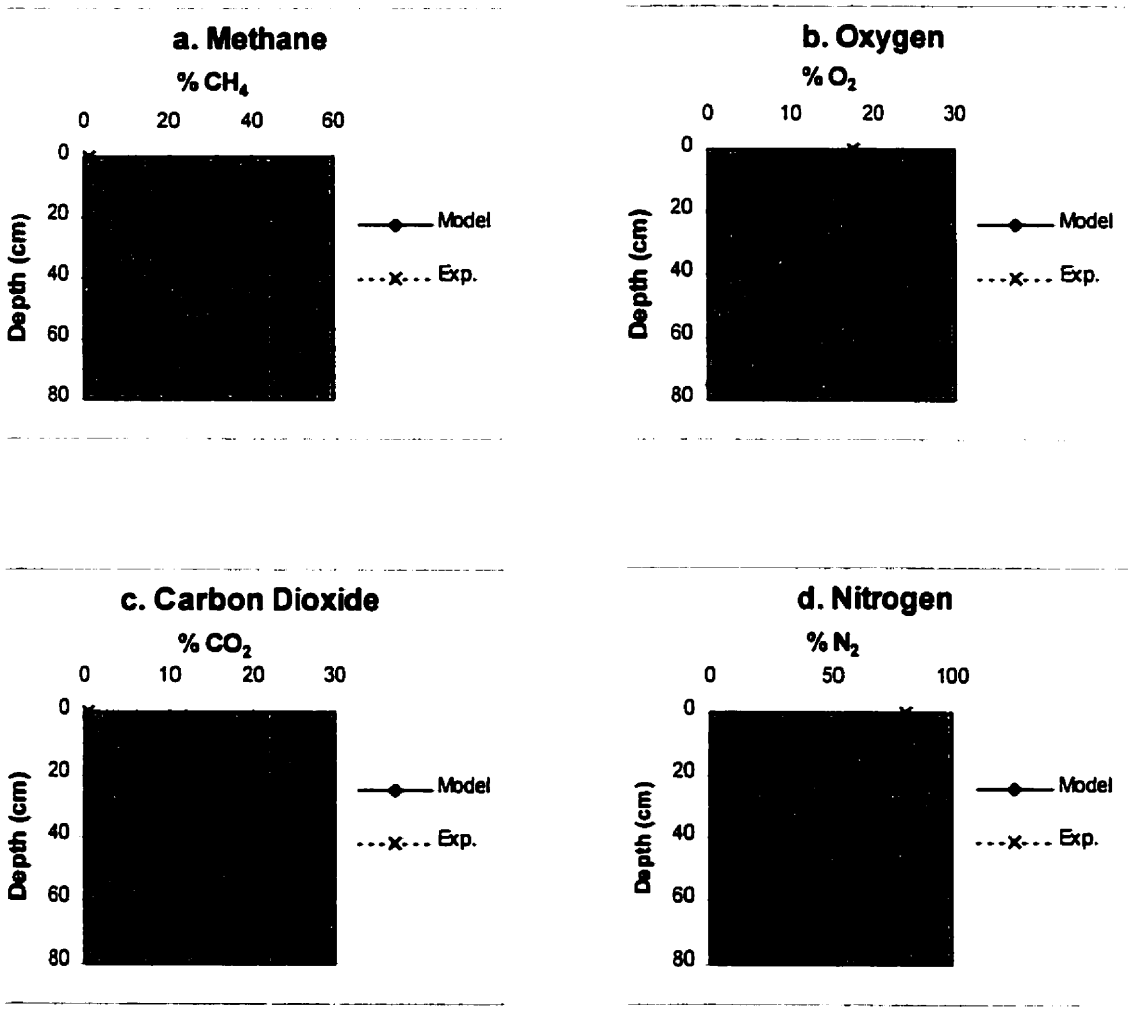

%CH_4 Oxidised (model) = 30.9%

% CH_4 Oxidised (experimental) = 31.4 %

Error = -1.6%

5.7 Model Verification

To verify a numerical model, one must demonstrate that the calibrated model is shown to be capable of reproducing a set of empirical observations independent of those used in model calibration. The model was calibrated for column SB1 and then accurately predicted the CH_4 oxidation rate for column SB2, which had a slightly higher CH_4 flow-rate and a 20% higher oxidation rate than column SB1. It was also intended that the model be verified by comparison with the observations made on column SB3. However because of the uncertainty surrounding the V_{max} values determined for that column, an attempt was made to verify the model using soil parameters and CH_4 oxidation data found in literature. de Visscher et al. (1999) recently performed soil column experiments on an agricultural soil taken from a cornfield in Belgium. Their soil was of a similar texture to the soil used for this study, but had a higher bulk density, and was purged with a 50 CH_4/ 50 CO_2 gas mixture. The parameters obtained from their study for use as model input are as follows:

Model Input Parameters

- $G_s = 2521$ Kg/m^3
- $\rho_{bulk} = 1205$ Kg/m^3
- Moisture content = 16.5% (d.w.)
- CH_4 flux = 214.4 g*m^{-2}*day^{-1}
- CO_2 flux = 214.4 g*m^{-2}*day^{-1}
- $K_{O2} = 1.23\%$
- $K_{CH4} = 0.34\%$

V_{max} values*

Depth (cm)	V_{max} (nmol*h^{-1}*g d.w.$^{-1}$)
10	828
20	3348
30	3870
40	1516

*Interpolated from the graph provided by de Visscher et al. (1999)

The model output is presented in Figure 5-7, superimposed on the gas concentration profiles observed by de Visscher et al. (1999).

Figure 5-7: Model Results Versus Experimental Results of de Visscher et al. (1999)

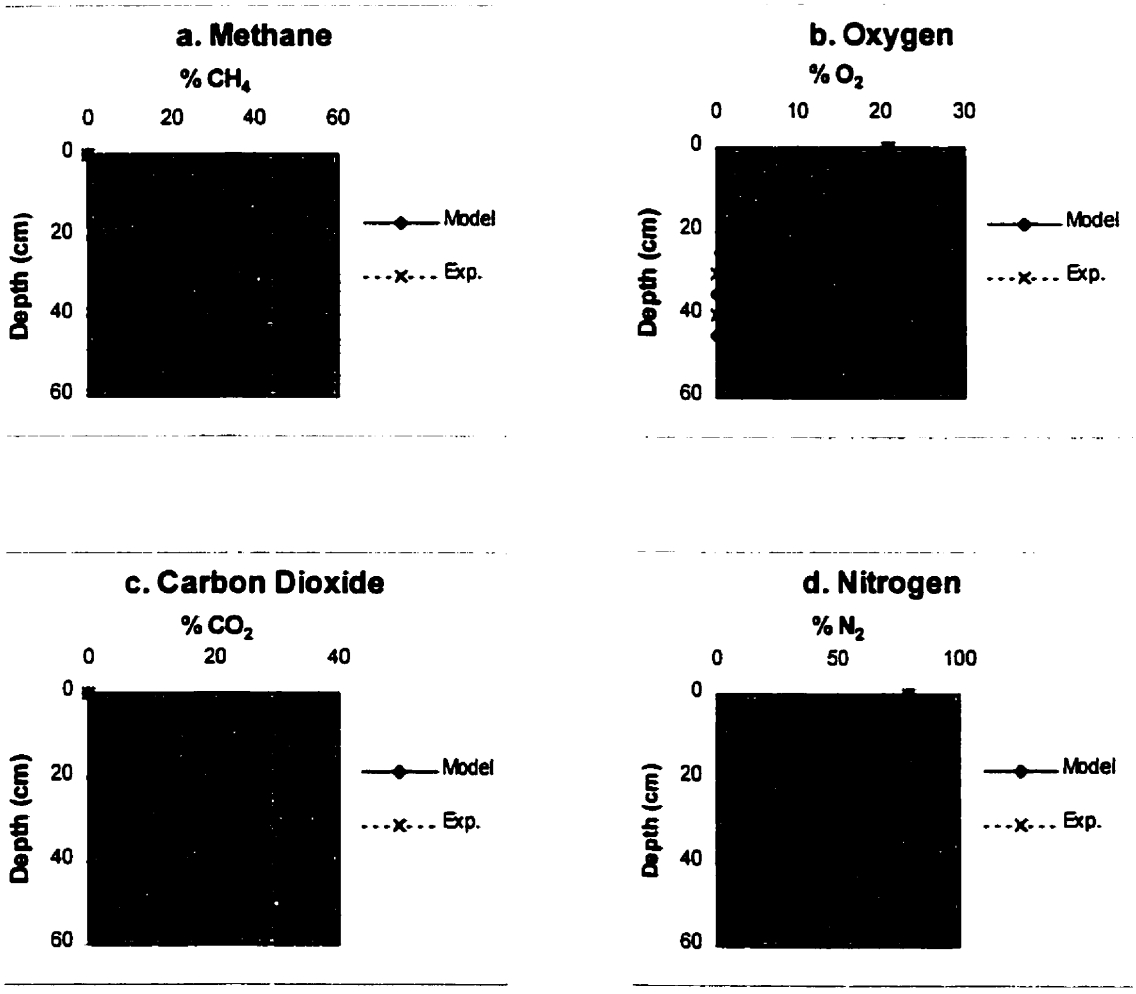

% CH_4 oxidised (model): 87.3%

% CH_4 oxidised (de Visscher et al, 1999): 80.0%

Error = 9.1%

The model successfully predicts de Visscher's experimentally observed gas concentration profiles and CH_4 oxidation rate with a reasonable degree of accuracy, thus verifying its applicability to soils with higher bulk densities and purged with a different mixture of gases than those for which it was calibrated.

5.8 Maximum CH_4 Oxidation Rate Based on Mass Transfer Limitations

Assuming that it were possible to maintain CH_4 oxidation rates as high as those reported by Nozhnikova et al. (1996), then a soil cover's overall rate of CH_4 oxidation would be limited by the rate at which O_2 could diffuse into the soil. To determine this theoretical maximum rate, a simulation was run using the soil properties from column SB1, but with Nozhnikova's CH_4 V_{max} parameter of 25000 $nmol*h^{-1}*g$ $d.w.^{-1}$ at all soil depths. The CH_4 flux was adjusted until an oxidation efficiency of 90% was achieved, which was found to be 1115 $g*m^{-2}*day^{-1}$. The results are presented in Figure 5-8.

Figure 5-8: Simulation of SB1 with V_{max} values from Nozhevnikova et al. (1999)

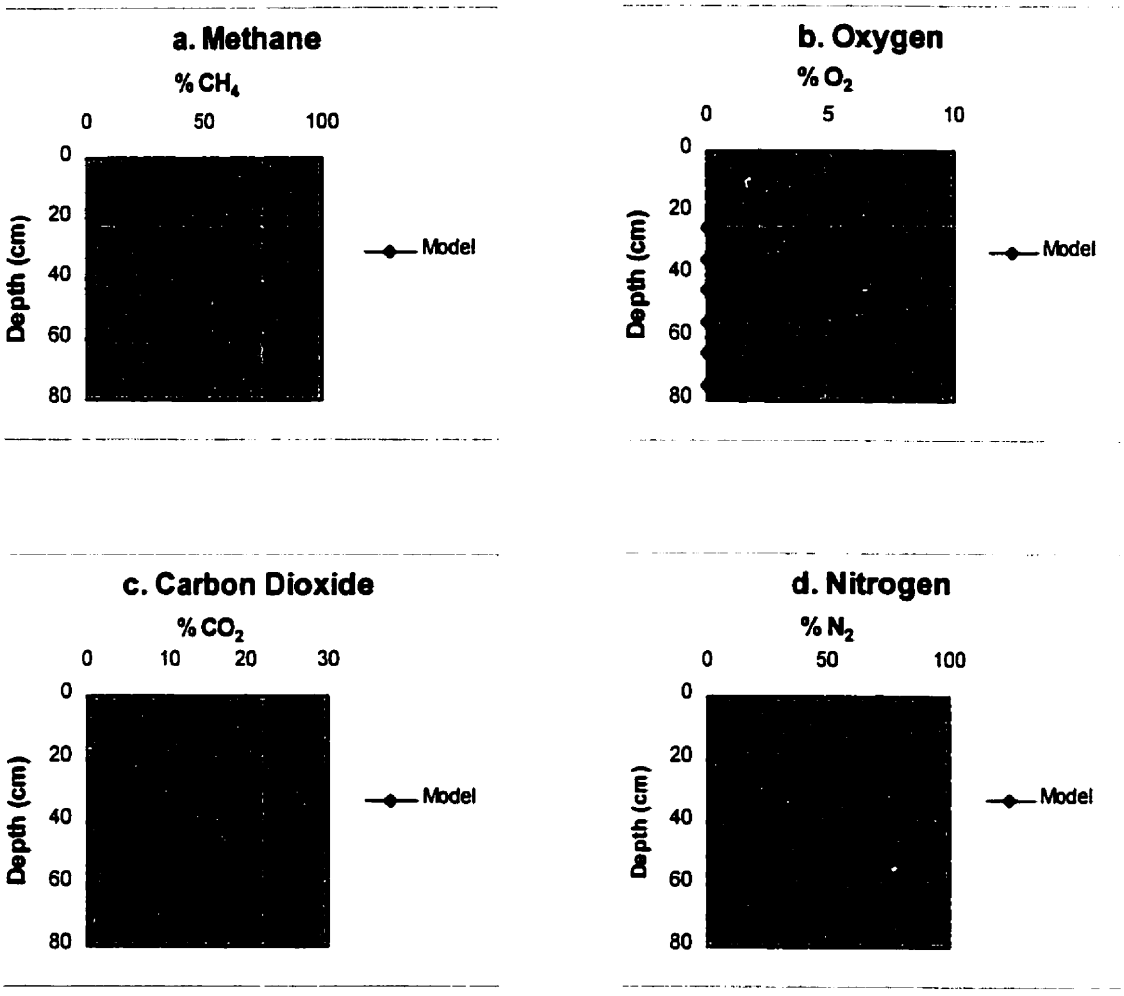

CH_4 Oxidation Rate = 990 $g*m^{-2}*day^{-1}$ (90%)

In this simulation, oxidation occurred only in the top 15cm because O_2 could not penetrate any deeper due to its rapid biological oxidation. The oxidation rate of 990 $g*m^{-2}*day^{-1}$ can be considered an upper theoretical limit on the rate of CH_4 consumption that could occur in a soil with the same physical properties as the Springbank loam, were mass transfer the only limitation on CH_4 oxidation.

Chapter 6. Conclusions and Recommendations

6.1 Conclusions

The type of soil selected for a cover influences the amount of CH_4 that can be biologically degraded in it. While the steady-state rate of CH_4 oxidation observed in the soils investigated for this study averaged 100 $g*m^{-2}*day^{-1}$, rates 60-100% higher have been observed by others (Kightley, 1996; de Vischer et al., 1999). Based on the oxidation rates reported by these authors, one could expect to treat a CH_4 gas flow-rate of 25 m^3/day in a 10mx10m passively aerated biofilter with a soil medium.

Moisture content appears to be a critical variable in limiting the CH_4 oxidation potential of a soil, as is evident in the dramatic increase in the oxidation rate of the Rocky View dark soil after increasing its moisture content from 6% to 10%. The importance of moisture content can also be seen in the moisture response curves of the Springbank loamy soil, and by the extremely low CH_4 oxidation rates observed in the top 25 cm of the Springbank soil columns, where M.C. was <7.5%.

A soil's moisture content affects both the movement of gases through the soil and microbial activity. The type of soil selected for an oxidative cover will influence the moisture content within the soil, which will be site specific, depending on climatic variables such as temperature, solar flux, average wind speed and the type of vegetative cover. For example, in a droughty environment, a soil with a higher field capacity may be desirable. Therefore, when using soil column tests to decide what soil type would afford the highest amount of CH_4 oxidation for a given climate, it is important to conduct

the experiments at soil moisture contents comparable to those the soils would have in the field. This would be a difficult task, given that a soil's moisture content varies throughout the year. For this reason, it may be necessary to employ a soil heat and moisture flux model such as BROOK90 (Czepiel, 1996b) to characterize the seasonable variability of a soil's moisture content. The output from such a model could then be used as input for the reactive-transport model developed in this study, in which relative soil gas diffusivity coefficients are a function of the soil's moisture content. It might then be a simple matter of modifying the model's V_{max} parameters by multiplying them with coefficients obtained from a normalized version of the inverted parabolic moisture response curve such as the one in Figure 4-27.

The use of soil incubation experiments for estimating in situ CH_4 oxidation rates appears to be a valid technique. By integrating V_{max} rates that were corrected for sub-saturating O_2 concentration with the Monod equation, estimates of the overall CH_4 oxidation rate for two of the three columns tested were within 12% and 19% of the CH_4 oxidation rate determined by a mass balance. The results obtained for the third soil column had an error of 100%, but this was likely due to erroneous V_{max} values, for reasons previously discussed.

A numerical reactive-transport model was developed which, given soil bulk density, particle density, moisture content and biological kinetic parameters as input, can predict gas concentration profiles and CH_4 oxidation rates with a reasonable degree of accuracy. The model was verified by reproducing the experimentally observed results of

a study by de Vischer et al. (1999), which involved a soil with higher bulk density that was purged with a different mixture of gases than those for which it was calibrated.

The use of the second Milington-Quirk model for calculating intrinsic diffusivities (Equation 5-2) for the model resulted in accurate predictions of soil column gas concentration profiles, further validating its efficacy.

The empirical relationship used by Czepiel et al. (1996b) (Equation 2-3) for predicting the maximum rate of CH_4 oxidation in a soil as a function of the in situ soil gas CH_4 was capable of predicting the V_{max} values in two of the three Springbank loam soil columns. However, it is unlikely that this relationship is universally applicable because some of the higher V_{max} values reported by others would require soil CH_4 concentrations to exceed 500%, which is impossible. Furthermore, even if the relationship were applicable for a specific soil type, the need still arises to predict the depth at which the maximum CH_4 oxidation rate will occur, as this would greatly affect the overall rate of oxidation within a soil cover.

A starting point for making such a prediction might be the observation that methanotrophs seem to thrive in micro-aerobic environments (0.5% - 2% O_2), a phenomenon that was observed in the soil columns of this study. However, a greater understanding of this phenomenon is needed, specifically, the ability to quantify the inhibitory effect that a higher O_2 concentration has on the growth of methanotrophic bacteria. Only then can equations for microbial growth be coupled with the reactive-transport model.

The fact that methanotrophs exhibit the highest growth rate in low O_2 environments also has important implications for designing actively aerated CH_4 biofilters. Rather than supplying air at a biofilter's inlet, the best approach would be to aerate the biofilter through staged inlets along its length, supplying just enough air to maintain O_2 concentrations that are close to the optimal (e.g. between 0.5 and 2%).

The maximum V_{max} determined through the batch experiments performed in this study was 1944 $nmol*h^{-1}*g$ d.w. Given that others have observed substantially higher V_{max} values, it is conceivable that CH_4 oxidation rates that are significantly higher than those observed in the laboratory soil columns of this study are attainable. If, for example, it were somehow possible to maintain the V_{max} rate of 25000 $nmol*h^{-1}*g$ d.w. observed by Nozhevnikova et al. (1999) , then based on numerical model simulations, the oxidation rates in a passively aerated soil cover could be as high as 990 $g*m^{-2}*day^{-1}$, and would occur in the top 15 cm of the soil cover.

Straka et al. (1999) has reported CH_4 oxidation rates in a passively aerated compost biofilter that are up to two orders of magnitude higher than those observed in this study. Based on mass transfer limitations and the maximum V_{max} values for CH_4 oxidation reported in literature, their reported oxidation rate of 23,760 $g*m^{-2}*day^{-1}$ seems physically impossible. Nevertheless, compost should be investigated as a potential biofilter material in laboratory column experiments to see whether the V_{max} values reported by Nozhevnikova et al. (1993) and Bender and Conrad (1992) are attainable.

6.2 Recommendations

It is recommended that experiments be performed to evaluate the V_{max} kinetic parameter as a function of soil properties such as specific surface area, organic matter content, and nitrogen content. These could be performed in an incubation chamber in which CH_4 and O_2 concentration were held constant for several weeks. Additional experiments should also be performed at variable O_2 concentrations to investigate the inhibitory effect that O_2 concentrations in excess of 2% seem to have on the development of methanotrophic populations. The relationships determined between these variables and the V_{max} parameter could then be incorporated into the reactive-transport model developed in this study, and would result in a highly useful model for designing soil covers or biofilters for optimal CH_4 oxidation.

It is also recommended that field-scale trials of surface casing vent gas treatment be considered. Even without optimization, the soil column experiments performed in this study demonstrate that significant quantities of CH_4 could be treated by simply diverting casing gas into the soil adjacent to heavy oil wells, rather than venting it directly to the atmosphere.

REFERENCES

Adams, R.S. and R. Ellis. 1969. Some physical and chemical changes in the soil brought about by saturation with natural gas. In *Proceedings of the Soil Science Society of America* **24**: 41-44.

Ademsen, A. P. S., and G.M. King. 1993. Methane consumption in temperate and subarctic forest soils: rates, vertical zonation, and responses to water and nitrogen. *Applied and Environmental Microbiology* **59**:485-490.

Alperin, M.J. and W.S. Reeberg. 1985. Inhibition experiments on anaerobic methane oxidation. *Applied and Environmental Microbiology* **50**: 940-945.

Asady, G. H. and A. J. M. Smucker. 1989. Compaction and root modifications of soil aeration. *Soil Science Society of America Journal* **53**:251-254.

Augenstein, D. And Pacey, J. 1996. *Landfill Gas Energy Utilization: Technology Options and Case Studies*. EPA-600/R-92-116; U.S. Environmental Protection Agency: Office of Air and Radiation.

Bavel, G. H. M. van. 1951. A soil aeration theory based on diffusion. *Soil Science* **72**:33-46.

Bavel, G. H. M. van. 1952. Gaseous diffusion and porosity in porous media. *Soil Science* **73**:91-104.

Bédard, C. and R. Knowles. 1989. Physiology, biochemistry, and specific inhibitors of CH_4, NH_4^+, and CO oxidation by methanotrophs and nitrifiers. *Microbiological Reviews* **53**: 68-84.

Bender, M., and R. Conrad. 1992. Kinetics of CH4 oxidation in oxic soils exposed to ambient air or high CH4 mixing ratios. *FEMS Microbiology Ecology* **101:** 261-270.

Bender, M. and R. Conrad. 1993. Kinetics of methane oxidation in oxic soils. *Chemosphere* **26**:687-696.

Bender, M., and R. Conrad. 1994. Methane oxidation activity in various soils and freshwater sediments: Occurrence, characteristics, vertical profiles and distribution on grain size fractions. *Journal of Geophysical Research* **99(D8)**:16531-16540.

Boeckx, P. and O. van Cleemput. 1996. Methane oxidation in neutral landfill cover soil: influence of moisture content, temperature, and nitrogen turnover. *Journal of Environmental Quality* **25**:178-183.

Bogner, J., and K. Spokas. 1993. Landfill methane: Rates, fates, and role in global carbon cycle. *Chemosphere* **26**:369-386.

Bogner, J., K. Spokas, E. Burton, R. Sweeney, and V. Corona. 1995. Landfills as atmospheric methane sources and sinks. *Chemosphere* **31**(9):4119-4130.

Born, M., H. Dorr and I. Levin. 1990. Methane consumption in aerated soils of the temperate zone. *Tellus* **42**(B):2-8.

Bouwman, A.F. 1990. "Exchange of Greenhouse Gases Between Terrestrial Ecosystems and the Atmosphere." Chapter 4 in *Soils and the Greenhouse Effect*; A.F. Bouwmjan, Editor. Wiley & Sons, Chichester, England.

Bruckler, L., B. C. Ball, and P. Renault. 1989. Laboratory estimation of gas diffusion coefficient and effective porosity in soils. *Soil Science* **147**:1-10.

Carlson, D.A. and C.P. Leiser. 1966. Soil beds for the control of sewage odors. *Journal of the Water Pollution Control Federation* **38**:829.

Chen and Othmer. 1962. *Journal of Chemical Engineering Data* **7**:37.

Cheney, W. and D. Kincaid. 1985. Numerical Mathematics and Computing. Wadsworth, Inc., Belmont, California.

Collin, M and A. Rasmuson. 1988. A comparison of gas diffusivity models for unsaturated porous media. *Soil Science Society of America Journal* **52**:1559-1565.

Conrad, R. 1984. Capacity of aerobic microorganisms to utilize and grow on atmospheric trace gases. In: *Current Perspectives in Microbial Ecology*. Ed. Klug, M.J. and Reddy, C.A. 461-467. American Society of Microbiology, Washington, DC.

Crill, P.M., P.J. Martikainen, H. Nykanen, and J. Silvolva. 1994. Temperature and N fertilization effects on methane oxidation in a drained peatland soil. *Soil Biology and Biochemistry* **26**:1331-1339.

Currie, J. A. 1961. Gaseous diffusion in the aeration of aggregated soils. *Soil Science* **92**:40-45.

Czepiel, P., P. Crill, and R. Harriss. 1995. Environmental factors influencing the variability of methane oxidation in temperate zone soils. *Journal of Geophysical Research* **100**:9359-9364.

Czepiel, P., B. Mosher, J. H. Shorter, J.B. McManus, C.E. Kolb, E. Allwine, B.K. Lamb, and R.C. Harriss. 1996a. Landfill methane emissions measured by enclosure and atmospheric tracer methods. *Journal of Geophysical Research* **101**: 16711-16719.

Czepiel, P.M., B. Mosher, P. M. Crill, and R. C. Harris. 1996b. Quantifying the effect of oxidation on landfill methane emissions. *Journal of Geophysical Research* **101**:16721-16729.

de Vischer, A., D Thomas, P. Boeckx and O. van Cleemput. 1999. Methane Oxidation in Simulated Landfill Cover Soil Environments. *Environmental Science and Technology* **33**:1854-1859.

Dörr, H., L. Katruff and I. Levin. 1993. Soil texture parameterization of the methane uptake in aerated soils. *Chemosphere* **26**:697-713.

Erno, B., R. Schmitz. 1996. Measurements of soil gas migration around oil and gas wells in the Lloydminster area. *Journal of Canadian Petroleum and Technology.* **35**(7):37-45.

Essaid, H.I., Bekins, B.A., Godsy, E.M., Warren, E., Baedecker, J.J., and Cozzarelli, I.M. 1995. Simulation of aerobic and anaerobic biodegradation processes at a crude oil spill site. *Water Resource Research* **31**:3309-3327.

Federer, C.A. 1995. Brook90: A Simulation Model for Evaporation, Soil Water, and Streamflow, Version 3.1, Computer freeware and documentation. For. Serv., U.S. Dep. of Agric., Durham, N.H.

Fouhy, K. 1992. Cleaning Waste Gas, Naturally. *Chemical Engineering* **99**:41-42.

Focht, D. D. 1992. Diffusional constraints on microbial processes in soil. *Soil Science* **154**:300-307.

Freijer, Jan I. 1994. Calibration of jointed tube model for the gas diffusion coefficient in soils. *Soil Science Society of America Journal* **58**:1067-1076.

Fuentes, H. R., W. L. Polzer, and J. L. Smith. 1991. Laboratory measurements of diffusion coefficients for trichloroethylene and orthoxylene in undisturbed tuff. *Journal of Environmental Quality* **20**:215-221.

Gaudy, A. F. and E. T. Gaudy. 1980. Microbiology for Environmental Scientists and Engineers. McGraw-Hill Inc, New York, NY.

Gibbs, M.J.; Bashki, V. 1996. *A Guide for Methane Mitigation Projects: Gas-to-Energy at Landfills and Open Dumps (Draft);* U.S. Environmental Protection Agency: Office of Air and Radiation.

Haber, C.L., L.N. Allem, S. Zhao and R.S. Hanson. 1983. Methyltrophic bacteria: biochemical diversity and genetics. *Science* **221**:1147-1153.

Hilger, H.A., S.K. Liehr and M.A. Barlaz. 1999. "A model to assess biofilm exopolymer effects o methane oxidation in landfill cover soils." in *Proceedings: Sardinia 99, 7th International Waste Management and Landfill Symposium*. Cagliari, Italy.

Hilger, H.A. 1999. Dept. of Civil Engineering, University of North Carolina at Charlotte. Personal Communication.

Hoeks, JU. 1972. "Effect of Leaking Natural Gas on Soil and Vegetation in Urban Areas." Report published by the Centre for Agricultural Publishing and Documentation, Wageningen, Netherlands.

Hodgson, A. S. and D. A. MacLeod. 1989. Use of oxygen flux density to estimate critical air-filled porosity of a vertisol. *Soil Science Society of America Journal* **53**:355-361.

Hoeks, J. 1972. Changes in Composition of Soil Air Near Leaks in Natural Gas Mains. *Soil Science* **113**:1-46.

Hogan, K.B. and Kruger, D.W. 1992. "Methane Reductions are a Cost-Effective Approach for Reducing Emissions of Greenhouse Gases" in *Proceedings: The 1992 Greenhouse Gas Emissions and Mitigation Research Symposium*; U.S. Dept. of Commerce NTIS, Washington, D.C.

IPCC. (Intergovernmental Panel on Climate Change) 1996a. "Summary for Policy Makers," in *Climate Change 1995: The Science of Climate Change*; J.T. Houghton, L.G. Meira Filho, B.A. Callander, N. Harris, A. Katternberg and K. Maskell, Eds.; Cambridge University Press, UK.

IPCC (Intergovernmental Panel on Climate Change). 1996b. "Radiative Forcing of Climate Change." In *Climate Change 1995: The Science of Climate Change*; J.T. Houghton, L.G. Meira Filho, B.A. Callander, N. Harris, A. Katternberg and K. Maskell, Eds.; Cambridge University Press, UK.

Isaksen, I.S.A. *Climate Change 1992: The Supplementary Report to the IPCC Scientific Assessment.* Cambridge University Press, UK.

Ishitani, H. and Johansson, T.B. 1996. "Energy Supply Mitigation Options," in *Climate Change 1995: Impacts, Adaptations and Mitigation of Climate Change.* Robert T. Watson, Marufu C. Zinyowera, and Richard H. Moss, Eds.; Cambridge University Press, UK.

Jin, Y and W. A. Jury. 1996. Characterizing the dependence of gas diffusion coefficient on soil properties. *Soil Science Society of America Journal.* **60**:66-71.

Jocksch, T., M. Watson, G. Shepartd, J. Edgson, and R. Cox. 1993. "Husky's experience at mitigation of gas migration in the Lloydminster area." Paper presented at the 5th Petroleum Conference of South Saskatchewan Section, The Petroleum Society of CIM. October 18-20, 1993. Regina, Saskatchewan.

Jones, H.A., and D.B. Nedwell. 1990. Soil atmosphere concentration profiles and methane emission rates in the restoration covers above landfill sites: equipment and preliminary results. *Waste Management and Research* **8:**21-31.

Jones, H.A., and D.B. Nedwell. 1993. Methane emission and methane oxidation in landfill cover soil. *FEMS Microbiology Ecology* **102:**185-195.

Kampbell, D.H., J.T. Wilson, H.W. Read, T.T. Stocksdale. 1987. Removal of volatile aliphatic hydrocarbons in a soil bioreactor. *Journal of Air Pollution Control Association* **37**:1236.

Keller, M., T.J. Goreau, S.C. Wofsy, W.A. Kaplanb and M.B. McElroy. 1983. Production of nitrous oxide and consumption of methane by forest soils. Geophysical Research Letters **10(12):**1156.

Kightly, D., D. Nedwell, and M. Cooper. 1995. Capacity for methane oxidation in landfill cover soils measured in laboratory-scale microcosms. *Applied and Environmental Microbiology* **61**:592-601.

King, G.M. 1990. Dynamics and controls of methane oxidation in a Danish wetland sediment. *FEMS Microbiology Ecology* **74:**309-323.

King, G.M. 1992. Ecological aspects of methane oxidation, a key determinant of global methane dynamics. *Advances in Microbial Ecology* **12:**431-468.

King, G.M., P. Roslev, and H. Skovgaard. 1990. Methane oxidation in sediments and peats of a subtropical wetland, the Florida Everglades. *Applied and Environmental Microbiology* **56**:2902-2911.

King, G.M., and A.P.S. Adamsen. 1992. Effects of temperature on methanotroph Methylomonas rubra. *Applied and Environmental Microbiology* **58:**2758-2763.

King, G.M., and S. Schnell. 1998. Effects of Ammonium and Non-Ammonium Salt Additions on Methane Oxidation by Methylosinus trichosporium OB3b and Maine Forest Soils. *Applied and Environmental Microbiology* **64:**253-257

Koschorreck, M., and R. Conrad. 1993. Oxidation of atmospheric methane in soil: Measurements in the field, in soil cores and in soil samples. *Global Biogeochemical Cycles* **7(1)**:109-121.

Kruse, C. W., P. Moldrup, N. Iversen. 1996. Modeling diffusion and reaction in soils: II. atmospheric methane diffusion and consumption in a forest soil. *Soil Science* **161**:355-365.

LaGrega, M.D., Buckingham, P.L., and Jeffrey, C.E. 1994. Hazardous Waste Management. McGraw-Hill, Inc., New York, NY.

Leson, G. 1991. Biofiltration: An innovative air pollution control technology for VOC emissions. *Journal of the Air and Waste Management Association* **41**(8):1045.

Lidstrom, M.E. and L. Somers. 1984. Seasonal studies of methane oxidation in Lake Washington. *Applied and Environmental Microbiology* **47**:1255-1260.

Martin, F. J. and C. Loehr, Raymond C. 1996. Effects of periods of non-use on biofilter performance. *Journal of the Air and Waste Management Association* **46**:539-546.

Millington, R. J. and R. C. Shearer. 1971. Diffusion in aggregated porous media. *Soil Science* **111**:372-378.

Moldrup, P., C. W. Kruse, T. Yamaguchi, and D. E. Rolston. 1996. Modeling diffusion and reaction in soils: I. a diffusion and reaction corrected finite difference calculation scheme. *Soil Science* **161**:347-354.

Moldrup, P., C. W. Kruse, D. E. Rolston and T. Yamaguchi. 1996. Modeling diffusion and reaction in soils: III. Predicting gas diffusivity from the Campbell soil-water retention model. *Soil Science* **161**:366-375.

Mohsen, M. 1980. Gas Migration and Vent Design and Landfill Sites. *Water, Air and Soil Pollution* **13**(1):79.

Nesbit, S.P., and G.A. Breitenbeck. 1992. A laboratory study of factors influencing methane uptake by soils. *Agriculture Ecosystems & Environment* **41**:39-54.

Nozhevnikova, A. A.B. Lifshitz, V.S. Lebedev, and G.A. Zavarzin. 1993. Emission of methane into the atmosphere from landfills in the former USSR. *Chemosphere* **26**:401-417.

Ottengraf, S.P.P. 1987. Biological systems for waste gas elimination. *TIBTECH* **5**:132-136.

Rappoldt, C. 1990. The application of diffusion models to an aggregated soil. *Soil Science* **150**:645-661.

Reeburg, W.S., S.C. Whalen, and M.J. Alperin. 1993. The role of methyltrophy in the global methane budget. In: J.C. Murrell and D.P. Kelly (ed.). Microbial growth on C1 compounds. Intercept Ltd., Andover, United Kingdom.

Reid, R.C. and T.K. Sherwood. 1966. The Properties of Gases and Liquids. McGraw-Hill Book Co., Inc., New York., NY.

Rich, K. 1995. *Determination of the Source of Migrating Gas from Oil and Gas Wells in the Lloydminster Area Using Stable Isotope Analyses.* Master's Thesis. Department of Earth & Atmospheric Sciences, University of Alberta.

Rolston, D. E., R. D. Glauz, G. L. Grundmann, and D. T. Louie. 1991. Evaluation of an in situ method for measurement of gas diffusivity in surface soils. *Soil Science Society of America Journal* **55**:1536-1542.

Roslev, P., and G.M. King. 1994. Survival and recovery of methanotrophic bacteria starved under oxic and anoxic conditions. *Applied and Environmental Microbiology* **60**:2602-2608.

Schmitz, R., D.V. Stempvoort, and B. Erno. 1994. "Gas migration research—working towards risk-based management." Paper presented at the 4th Annual Symposium on Groundwater and Soil Remediation. Sept. 21-23, 994. Calgary, AB.

Schmitz, R., P.B. Carlson, G.D. Lorenz, M.D. Watson, and B. Erno. 1993. "Husky Oil's gas migration research effort - an update." Paper presented at the 10th Heavy Oil and Oil Sands Symposium sponsored by the University of Calgary and the Canadian Heavy Oil Association.

Schnoor, J.L. 1996. Environmental Modeling: Fate and Transport of Pollutants in Water, Air and Soil. John Wiley & Sons, Inc., New York., NY.

Shimamura, K. 1992. Gas diffusion through compacted sands. *Soil Science* **153**:274-279.

Skopp, J. M. D. Jawson and J. W. Doran. 1990. Steady-state aerobic microbial activity as a function of soil water content. *Soil Science Society of America Journal* **54**:1619-1625.

Steefel, C.I. and K.T.B. MacQuarrie. 1996. Approaches to modeling of reactive transport in porous media. In: P.C. Lichtner, C.I. Steefel and E.H. Oelkers (ed) Reactive Transport in Porous Media – Reviews in Mineralogy Vol. 34. The Mineralogical Society of America, Washington, D.C.

Steele, D. D. and J. L. Nieber. 1994. Network modeling of diffusion coefficients for porous media: I. theory and model development. *Soil Science Society of America Journal* **58**:1337-1345.

Steele, D. D. and J. L. Nieber. 1994. Network modeling of diffusion coefficients for porous media: II. simulations. *Soil Science Society of America Journal* **58**:1346-1354.

Stein, V. B. and J. P. Hettiaratchi. 1997. " Methane oxidation in soils as a tool for reducing greenhouse gas emissions." in *Proceedings: Emerging Air Issues of the 21st Century, an International Specialty Conference*. Calgary, Alberta. CPANS, AWMA and APPEGA.

Stein, V. B. and J. P. Hettiaratchi. 1999. "Applicability of soil methanotrophy at oil and gas well sites as a greenhouse gas mitigation management strategy." In *Proceedings: Combustion Canada '99, Combustion and Global Climate Change Conference*. Calgary, Alberta. Natural Resources Canada.

Steudler, P.A., R.D. Bowden, J.M. Melillo, and J.D. Aber. 1989. Influence of nitrogen fertilization on methane uptake in temperate forest soils. *Nature* **341**:314-316.

Strosher, M. 1996. *Investigations of flare gas emissions in Alberta*. Final report to: Environment Canada Conservation and Protection, Alberta Energy and Utilities Board, and Canadian Association of Petroleum Producers. Alberta Research Council.

Swanson, W.J. and R.C. Loehr. 1997. Biofiltration: fundamentals, design and operations principles and applications. *Journal of Environmental Engineering* **123(6)**:538-546.

Tokunaga, T. K., L. J. Waldron, and J. Nemson. 1988. A closed tube method for measuring gas diffusion coefficients. *Soil Science Society of America Journal* **52**:17-23.

Topp, E. and Hanson, R.S. 1991. "Methane Oxidising Bacteria," in *Microbial Production and Consumption of Greenhouse Gases: Methane, Nitrogen Oxides, and Halomethanes*. John E. Rogers and William B. Whitman, Eds.; American Society for Microbiology, Washington D.C.

Washington, J. W., A. W. Rose, E. J. Ciolkosz, and R. R. Dobos. 1994. Gaseous diffusion and permeability in four soil profiles in central Pennsylvania. *Soil Science* **157**:65-76.

Whalen, S.C., W.S. Reeburgh, and K.A. Sandbeck. 1990. Rapid methane oxidation in a landfill cover soil. *Applied and Environmental Microbiology* **56**:3405-3411.

Whalen, S. and W. Reeburgh. 1992. Interannual variation in tundra methane emissions: a 4-year time series at fixed sites. *Global Biogeochemical Cycles* **6**:139-159.

Whitmore, A. P. 1991. A method for assessing the goodness of computer simulation of soil processes. *Journal of Soil Science* **42**:289-299.

Wilson, J. 1998. HydroQual Laboratories, Calgary. Personal Communication.

Yang, M. 1999. Controlling Methane Emissions from Heavy Oil Wells: Gas Clustering Simulation and Optimization Modeling. Master's Thesis. Department of Chemical Engineering, University of Calgary.

Young, A. 1992. The effects of fluctuations in atmospheric pressure on landfill gas migration and composition. *Water Air and Soil Pollution* **64**:601-616.

Zheng, C. and G.D. Bennett. 1995. Applied Contaminant Transport Modeling. Van Nostrand Reinhold, New York, N.Y.

APPENDIX A – Soil Column Experiment Data

Table A1: % CH_4 Oxidation in Sedge Peat

Date	# Days	% Oxidation in Column			CH_4 Flow-Rates ($g/m^2/d$)		
		PM1	PM2	PM3	PM1	PM2	PM3
Apr-01	5	10.7	10.4	12.8	310	329	157
Apr-02	6	7.7	9.6	10.6	310	327	164
Apr-03	7	7.7	6	11.1	309	324	165
Apr-07	11	7.7	6.8	12.1	310	327	166
Apr-15	19	10.6	8.4	11.9	319	341	171
May-06	40	22.7	22.5	28.6	342	329	164
May-08	42	20.7	23.5	29	319	319	164
May-13	47	26.8	30.4	35	319	310	165
May-17	51	28.3	33	45.5	342	324	182
May-20	54	26.3	32.9	40.9	319	310	167
May-22	56	29.2	36.8	47.1	319	315	169
May-25	59	30.2	38.5	59.5	319	319	181
May-28	62	29.2	37.1	54.5	323	308	173
Jun-01	66	42.1	45.2	75.6	348	319	181
4-Jun	69	40.9	43.7	65.8	323	308	171
7-Jun	72	43.5	45.6	73.4	323	319	178
15-Jun	80	47.8	47.4	88.9	342	323	175
21-Jun	86	46	46.1	85.8	323	308	175
Jun-98	90	47.5	46.9	84.3	323	319	175
Jul-99	97	45.7	43.7	91.4	319	308	181
Jul-98	108	41.5	41.5	87	342	340	184
Jul-98	115	45.6	39.3	92.8	342	346	200
Jul-98	124	46.5	39.5	92	336	340	190
Aug-98	137	40.3	36.1	88.6	325	330	190
Aug-98	146	37.5	34.9	85.3	319	319	181
Sept. 3	160	51.1	41.2	85	319	325	178
Sept. 11	168	45.5		80.9	325		
Sept. 15	172	45.5		78	325		
Sept. 30	187	30.8		71	342		164
Nov. 9	196	33		70.3	342		138
Nov. 17	204	34.7		76.4	342		156
Dec. 22	239	25.5		56.9	336		160
Feb. 22	300	30.4		55.1	325		167
Mar-99	314	24		54.2	274		153

Table A2: CH_4 Oxidation Rate in Sedge Peat (mass flux basis)

		CH_4 Oxidation ($g*m^{-2}*day^{-1}$)		
Date	# Days	PM1	PM2	PM3
Apr-01	5.0	33.2	34.2	20.1
Apr-02	6.0	23.9	31.4	17.4
Apr-03	7.0	23.8	19.5	18.3
Apr-07	11.0	23.9	22.2	20.1
Apr-15	19.0	33.8	28.6	20.4
May-06	40.0	77.5	73.9	47.0
May-08	42.0	66.1	75.0	47.6
May-13	47.0	85.6	94.2	57.7
May-17	51.0	96.7	107.0	82.7
01-May	54.0	84.0	102.0	68.2
May-22	56.0	93.2	115.9	79.7
May-25	59.0	96.4	122.9	107.7
May-28	62.0	94.3	114.3	94.3
Jun-01	66.0	146.4	144.3	136.9
04-Jun	69.0	132.1	134.7	112.6
07-Jun	72.0	140.5	145.6	130.6
15-Jun	80.0	163.3	153.1	155.4
21-Jun	86.0	148.6	142.1	150.0
25-Jun	90.0	153.4	149.8	147.4
02-Jul	97.0	145.9	134.7	165.5
13-Jul	108.0	141.8	141.3	160.2
20-Jul	115.0	155.8	136.0	185.8
29-Jul	124.0	156.3	134.5	175.1
11-Aug	137.0	130.9	119.1	168.6
20-Aug	146.0	119.7	111.4	154.4
Sept. 3	160.0	163.2	133.9	151.2
Sept. 11	168	147.8		116.2
Sept. 15	172	147.8		96.8
Sept. 30	187.0	105.2		119.4
Nov. 9	196.0	112.7		91.0
Nov. 17	204.0	118.5		92.2
Dec. 22	239.0	85.7		82.7
Feb. 22	300.0	98.8		92.2
08-Mar	314.0	65.8		82.7

Figure A1: CH_4 Oxidation in Sedge Peat (mass basis)

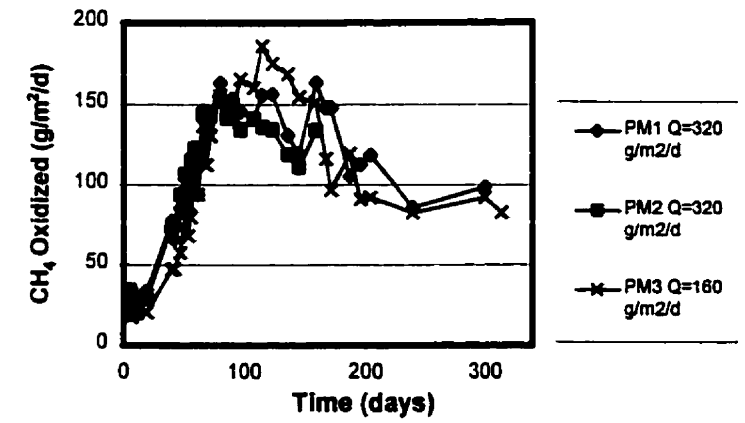

Table A3: % CH_4 Oxidation Rates in Springbank Loam

		% Oxidation in Column #			CH4 Flow-Rates ($g/m^2/d$)		
Date	# Days	SB1	SB2	SB3	SB1	SB2	SB3
May-06	6	41	40.3	41.5	339	320	169
May-08	8	40.5	35.4	36.4	319	308	155
May-13	13	46.5	42	64.2	319	310	157
May-17	17	52	46.5	77.8	339	339	166
May-20	20	51.8	47.2	86.9	319	308	163
May-22	22	54.7	49.2	91	319	320	169
May-25	25	52.5	46.9	95.8	319	302	166
May-28	28	49.9	46.3	96	316	311	219
Jun-01	32	56.2	49.3	79.4	339	310	229
04-Jun	35	51.1	45.4	77.2	319	302	219
07-Jun	38	48.4	46.5	77.4	319	308	222
15-Jun	46	47.4	47.2	71.2	339	339	229
21-Jun	52	42.7	46.3	67.2	319	310	219
25-Jun	56	39.4	45.1	69.2	324	308	222
02-Jul	63	37.5	49.6	61.3	319	310	210
13-Jul	74	26.3	43.5	49.5	342	340	184
20-Jul	81	26.8	47.5	53.1	342	346	200
29-Jul	90	30.3	42.9	49	336	340	190
11-Aug	103	23.5	35.9	44.7	319	329	212
20-Aug	112	24.5	34.3	42.4	319	329	221
Sept. 3	126	29.3	39.3	46.5	319	329	210
Sept. 9	132	38.5	45.8	62	319	329	187
Sept. 11	134	42	42.8	64.9	291	282	172
Sept. 15	138	43.2	48.3	65.2	298	298	169
Sept. 30	153	20.4	31.2	53.4	339	343	198
Nov. 9	193	27.4	36.9	55.8	305	318	177
Nov. 17	201	39.2	42.9	60.3	300	320	177
22-Dec	205	30.2	34.9	54.8	319	343	196
Feb. 22	266	32	36.6	51	319	328	183

Figure A2: % CH_4 Oxidation in Springbank Loam

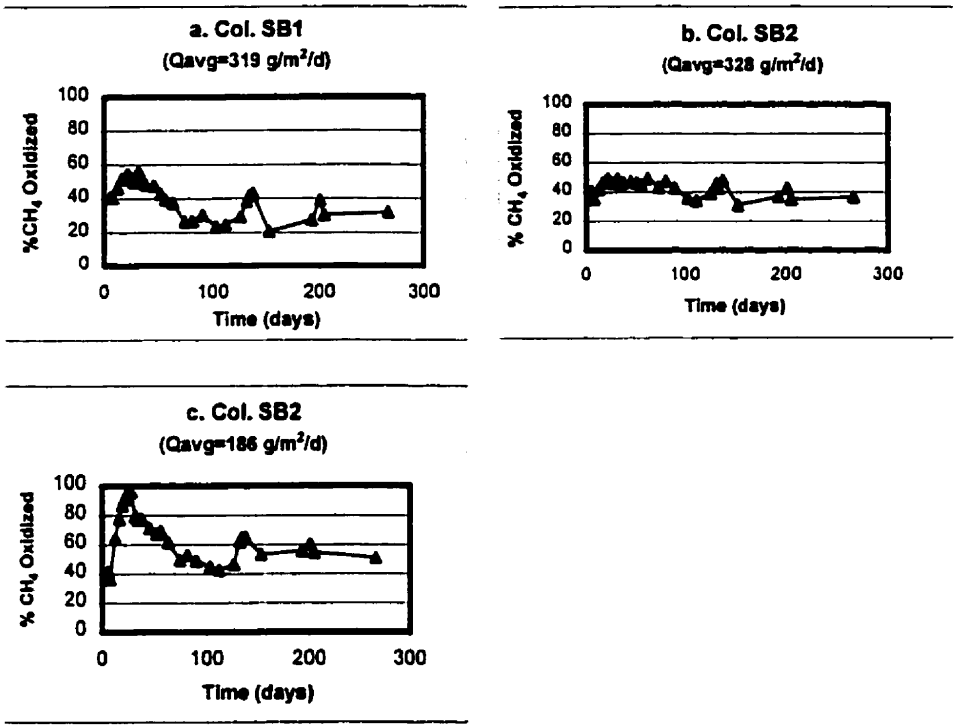

Table A4: CH_4 Oxidation in Springbank Loam (mass flux basis)

		CH_4 Oxidation ($g/m^2/day$)		
Date	# Days	PM1	PM2	PM3
May-06	6	139	129	70
May-08	8	129	109	56
May-13	13	148	130	101
May-17	17	176	157	129
May-20	20	165	145	142
May-22	22	175	157	154
May-25	25	168	142	159
May-28	28	157	144	210
Jun-01	32	191	153	182
04-Jun	35	163	137	169
07-Jun	38	155	143	172
15-Jun	46	161	160	163
21-Jun	52	136	144	147
25-Jun	56	128	139	154
02-Jul	63	120	154	128
13-Jul	74	90	148	91
20-Jul	81	92	164	106
29-Jul	90	102	146	93
11-Aug	103	75	118	95
20-Aug	112	78	113	94
Sept. 3	126	94	129	97
Sept. 9	132	123	151	116
Sept. 11	134	122	121	111
Sept. 15	138	129	144	110
Sept. 30	153	69	107	106
Nov. 9	193	84	117	99
Nov. 17	201	118	137	107
22-Dec	205	96	120	107
Feb. 22	266	102	120	93

Figure A3: CH_4 Oxidation in Springbank Loam (mass flux basis)

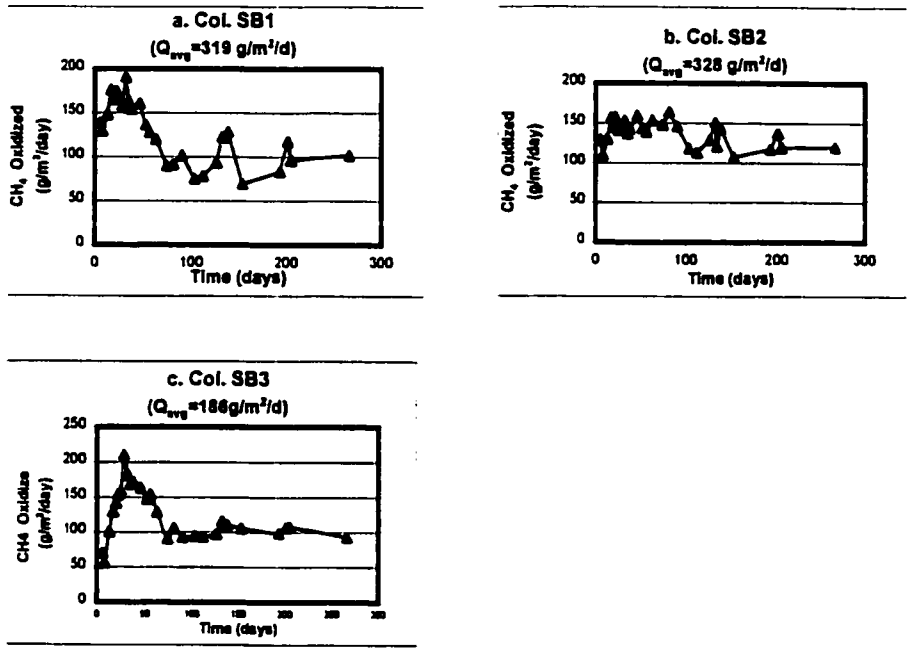

Table A5: Gas Concentration Depth Profiles - March 8,1999

a. Column PM2. Sedge Peat Q_{CH4}=325g/m^2/d

Depth (cm)	CH4 (%)	CO2 (%)	O2 (%)	N2 (%)
0	1.75	0.52	17.44	80.29
10	5.28	1.71	16.07	76.95
20	20.58	5.54	9.28	64.60
30	42.66	7.52	2.48	47.34
40	52.04	7.16	0.71	40.09
50	57.61	6.47	0.60	35.32

b. Column PM3. Sedge Peat Q_{CH4}=153g/m^2/d

Depth (cm)	CH4 (%)	CO2 (%)	O2 (%)	N2 (%)
0	0.87	0.48	17.95	80.70
2	1.50	1.53	16.75	80.21
12	2.99	3.40	14.50	79.11
22	4.68	5.47	11.75	78.10
32	7.17	8.66	8.16	76.00
42	12.14	10.80	4.58	72.48
52	15.63	10.92	3.42	70.03
62	20.13	11.94	1.89	66.05

c. Column RV1 Rockyview Dark Soil Q_{CH4}=298g/m^2/d

Depth (cm)	CH4 (%)	CO2 (%)	O2 (%)	N2 (%)
0	2.94	0.69	17.40	78.97
8	5.07	2.88	14.74	77.31
18	10.52	6.25	10.00	73.22
28	18.65	9.65	4.87	66.83
38	27.09	10.53	2.24	60.14
48	35.67	9.86	1.52	52.96
58	39.69	8.55	1.72	50.05
68	45.79	7.94	1.71	44.57
78	49.66	7.02	1.36	41.97
88	53.072	6.16	1.621	39.15

d. Column SB1. Springbank cover soil Q_{CH4}=319g/m^2/d

Depth (cm)	CH4 (%)	CO2 (%)	O2 (%)	N2 (%)
0	1.25	0.50	17.52	80.74
6	3.25	1.70	16.25	78.80
16	6.56	3.69	13.46	76.30
26	8.43	5.42	11.49	74.66
36	17.56	8.46	5.62	68.36
46	22.59	9.88	3.89	63.65
56	28.65	10.27	2.52	58.55
66	34.79	10.21	0.90	54.10
76	37.23	9.10	0.75	52.92

e. Column SB2. Springbank cover soil Q_{CH4}=328g/m^2/d

Depth (cm)	CH4 (%)	CO2 (%)	O2 (%)	N2 (%)
0	1.26	0.52	18.29	79.93
6	2.80	1.45	16.93	78.82
16	6.63	3.79	13.57	76.01
26	9.94	5.79	10.89	73.38
36	14.80	8.29	7.33	69.57
46	20.18	9.64	5.58	64.61
56	25.84	9.95	3.21	61.01
66	32.21	9.43	1.41	56.95
76	38.13	8.98	0.73	52.16
86	40.05	8.416	0.682	50.85

f. Column SB3. Springbank cover soil Q_{CH4}=183g/m^2/d

Depth (cm)	CH4 (%)	CO2 (%)	O2 (%)	N2 (%)
0	0.87	0.48	17.95	80.70
6	1.50	1.53	16.75	80.21
16	2.99	3.40	14.50	79.11
26	4.68	5.47	11.75	78.10
36	7.17	8.66	8.16	76.00
46	12.14	10.80	4.58	72.48
56	15.63	10.92	3.42	70.03
66	20.13	11.94	1.89	66.05
76	23.19	11.01	1.80	64.01
86	26.793	10.011	1.908	61.29

APPENDIX B – Batch Experiment Data

B.1 Springbank Soil Kinetic Experiments: Column SB1

Bottle 1	Blank (no soil in bottle)		
Time(h)	%CH4	%CO2	%O2
0	3.384	0.031	20.200
2.33	3.416	0.031	20.200
14.33	3.315	0.031	20.200
18.89	3.401	0.031	20.200
28.11	3.323	0.031	20.200
141.05	3.166	0.031	19.734

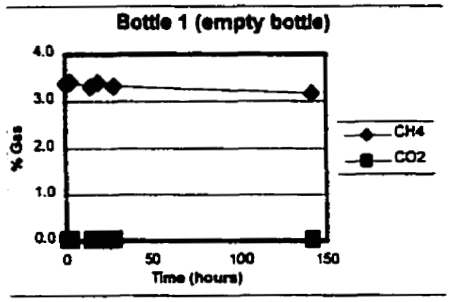

Bottle 3	6 cm depth		
Time(h)	%CH4	%CO2	%O2
0.00	3.260	0.031	19.410
2.40	3.320	0.034	19.950
14.40	3.227	0.038	20.011
18.89	3.179	0.037	18.596
28.13	3.166	0.038	18.947
141.23	2.952	0.045	18.985

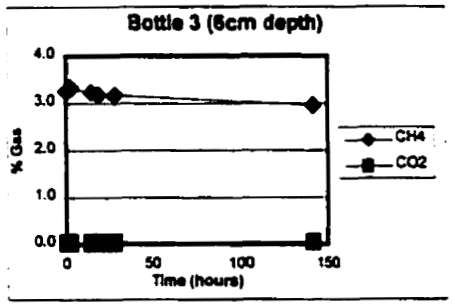

Bottle 5	16 cm depth		
Time(h)	%CH4	%CO2	%O2
0.00	3.540	0.079	19.696
1.87	3.540	0.083	19.900
13.87	3.540	0.094	20.426
18.32	3.497	0.092	19.280
27.87	3.480	0.096	19.287
141.28	3.087	0.100	18.977

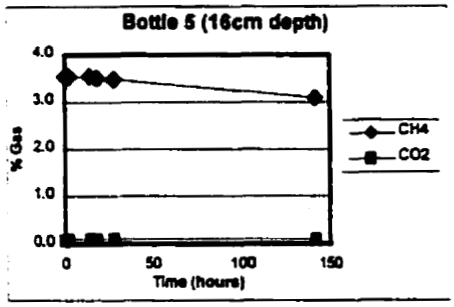

Bottle 7	26 cm depth		
Time(h)	%CH4	%CO2	%O2
0.00	2.080	0.080	20.380
2.25	2.084	0.133	19.881
14.25	2.022	0.204	20.783
18.67	2.019	0.210	19.227
28.10	2.014	0.253	19.389
141.32	1.673	0.568	18.870

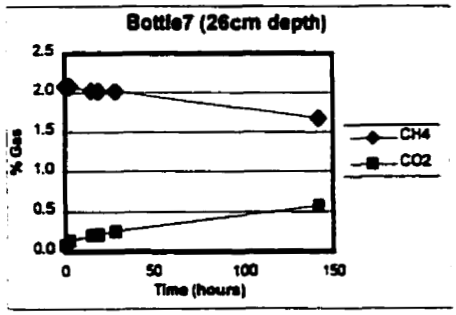

B.1 Springbank Soil Kinetic Experiments: Column SB1 (Continued)

Bottle 9	36 cm depth		
Time(h)	%CH4	%CO2	%O2
0.00	2.430	0.118	19.530
2.13	2.430	0.151	19.771
14.17	2.322	0.283	19.487
18.55	2.213	0.324	18.975
27.93	2.121	0.428	18.744
141.35	0.841	1.321	15.853

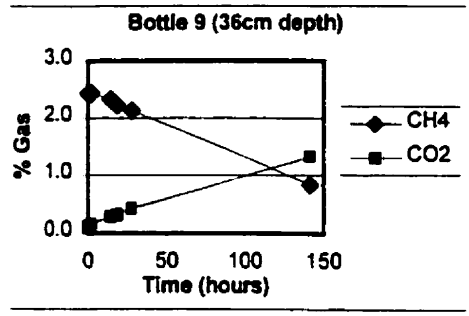

Bottle 11	46 cm depth		
Time(h)	%CH4	%CO2	%O2
0.00	2.450	0.192	19.360
1.97	2.439	0.230	19.358
13.97	2.217	0.415	19.549
18.35	2.149	0.450	18.164
27.58	2.064	0.583	18.048
141.40	0.443	1.781	15.190

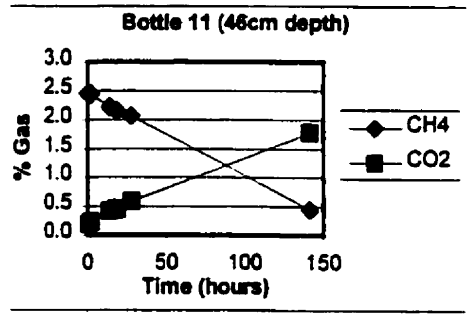

Bottle 13	56 cm depth		
Time(h)	%CH4	%CO2	%O2
0.00	3.075	0.168	19.060
1.93	3.120	0.214	19.681
13.93	2.879	0.410	18.918
18.30	2.624	0.450	17.443
27.47	2.550	0.606	18.284

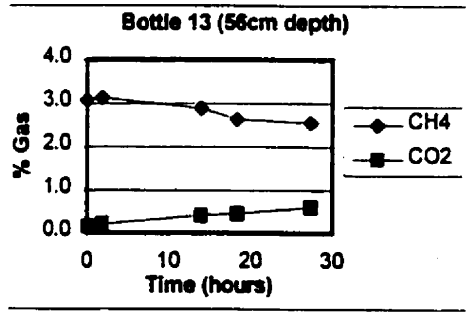

Bottle 15	66 cm depth		
Time(h)	%CH4	%CO2	%O2
0.00	2.530	0.249	19.060
1.92	2.399	0.332	18.742
13.93	1.820	0.733	18.831
18.32	1.581	0.856	17.870
27.38	1.172	1.127	17.876

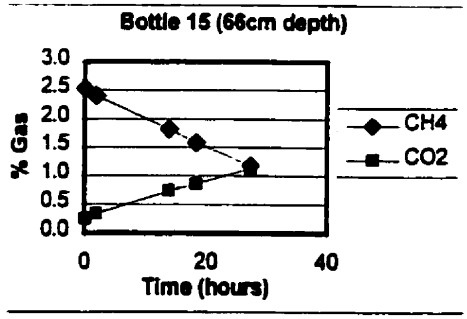

B.1 Springbank Soil Kinetic Experiments: Column SB1 (Continued)

Bottle 17	76 cm depth		
Time(h)	%CH4	%CO2	%O2
0.00	1.300	0.210	19.400
1.98	1.132	0.274	18.999
13.92	0.250	0.610	18.630
18.28	0.110	0.660	17.817
20.31	0.087	0.693	18.287
21.41	0.078	0.705	18.530
32.33	0.000	0.734	17.518

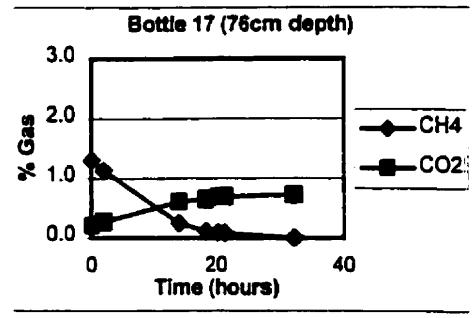

Springbank soil: Column SB1 10-Mar-99

Bottle #	Depth (cm)	Mass of bottle (g)	Mass of bottle+soi (g)	Tot. Mass 24h@104 (g)	Mass of dry soil (g)	Moisture content % dry wt.
1	0	167.424	167.428	0	0	0
3	6	167.261	177.526	177.401	10.1403	1.23
5	16	167.352	181.298	180.984	13.6321	2.30
7	26	166.785	175.265	174.677	7.8918	7.45
9	36	167.19	172.828	172.159	4.9689	13.46
11	46	167.161	173.621	172.753	5.5917	15.52
13	56	166.776	174.385	173.533	6.757	12.60
15	66	167.433	174.672	173.955	6.5227	10.99
17	76	167.326	175.09	174.429	7.1029	9.32

Reaction Rates - Column SB1, Q_{CH4}=319 g/m^2/day

Bottle #	Depth (cm)	Gas Consumption Rates (nmol * hour^{-1} * $g_{drysoil}^{-1}$)					
		CH_4	r-sqd	CO_2	r-sqd	O_2	r-sqd
3	6	32.90	0.9154	-0.82	0.8071	42.85	0.1483
5	16	4.51	0.9909	-0.81	0.4990	47.78	0.4059
7	26	15.73	0.9944	-41.78	0.9662	120.60	0.4450
9	36	208.76	0.9988	-175.73	0.9961	569.71	0.9861
11	46	234.97	0.9991	-206.49	0.9969	553.17	0.9262
13	56	311.04	0.9323	-241.85	0.9959	825.80	0.5176
15	66	767.86	0.9989	-513.66	0.9981	674.39	0.7321
17	76	1225.87	0.9997	-420.96	0.9997	690.43	0.8371

B.1 Springbank Soil Kinetic Experiments: Column SB1 (Continued)

Soil Gas Concetnrations and Reaction Rates
Column SB1, Q_{CH4}=319 g/m^2/day

Depth (cm)	% CH4	% O2	CH_4 Ox. nmol/h/g d.w.
6	3.25	16.25	6.88
16	6.56	13.46	13.13
26	8.43	11.49	16.95
36	17.56	5.62	205.74
46	22.59	3.89	234.97
56	28.65	2.52	311.04
66	34.79	0.90	767.86
76	37.23	0.75	1230.24

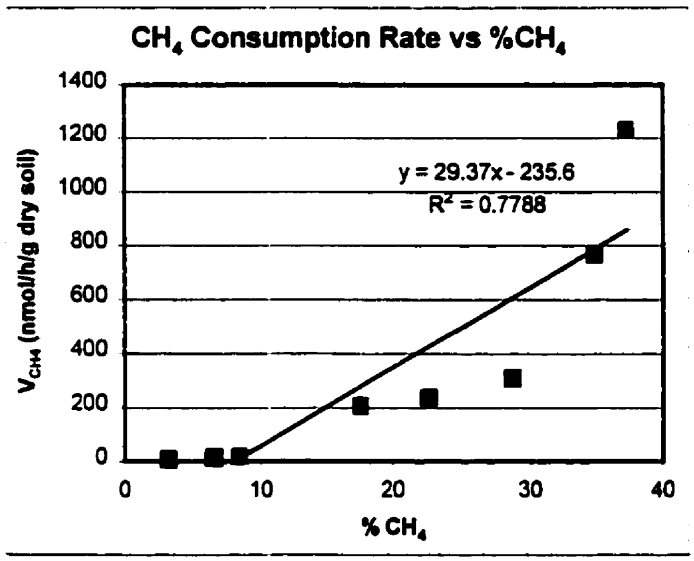

Col. SB1 Eadie Hosftee Data

% CH_4	V_{CH4} (nmol/h/g d.w	V/C (1/h g d.w.)
0	0	
1.3	1230.235	946.33
1.132	1082.725	956.47
0.25	448.4309	1793.72
0.087	143.0849	1644.65
0.039	93.96398	2409.33

Springbank Soil Oxidation Kinetics at 10% CH_4 (Col. SB1) June 22,1999

Bottle 25	56 cm depth		
Time(h)	%CH4	%CO2	%O2
0.00	10.14	0.08	22.81
1.48	9.24	0.14	20.52
3.82	7.92	0.24	18.47
6.25	7.77	0.24	18.22
23.07	7.16	0.59	17.88
50.32	5.79	1.02	16.62
69.18	4.79	1.21	16.14
239.07	0.46	3.06	10.12

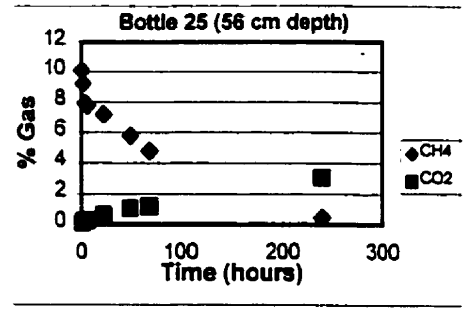

Bottle 26	56 cm depth		
Time(h)	%CH4	%CO2	%O2
0.00	8.91	0.07	21.16
1.48	8.38	0.14	19.96
3.92	7.56	0.20	18.57
6.25	7.57	0.27	18.77
23.07	6.44	0.63	17.64
50.38	5.24	1.14	16.25
69.23	4.50	1.46	15.80
239.07	0.08	3.33	9.46

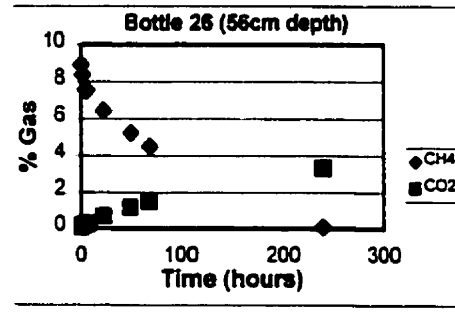

Springbank soil: SB1

Bottle #	Depth (cm)	Mass of bottle (g)	Mass of bottle+soi (g)	Tot. Mass 24h@104 (g)	Mass of dry soil (g)	Moisture content % dry wt.
19	56	167.193	177.386	176.246	9.0532	12.60
20	56	167.559	179.149	177.852	10.2925	12.60

Reaction Rates

Bottle #	Depth (cm)	Gas Consumption Rates (nmol * hour^{-1} * $g_{drysoil}^{-1}$)					
		CH_4	r-sqd	CO_2	r-sqd	O_2	r-sqd
19	56	6692.24	0.9997	-490.33	0.9998	1355.16	0.6405
20	56	3481.05	0.9998	-339.10	0.9944	786.59	0.7739
19 (2nd)	56	549.67	0.9966	-180.06	0.9884	414.02	0.9860
20 (2nd)	56	528.25	0.9858	-200.41	0.9982	575.76	0.9944

B.2 Springbank Soil Kinetic Experiments: Column SB2

Bottle 2	4 cm depth		
Time(h)	%CH4	%CO2	%O2
0.00	1.419	0.069	19.559
1.13	1.378	0.074	20.769
6.95	1.476	0.082	21.006
9.25	1.393	0.088	22.113
13.27	1.444	0.087	20.386

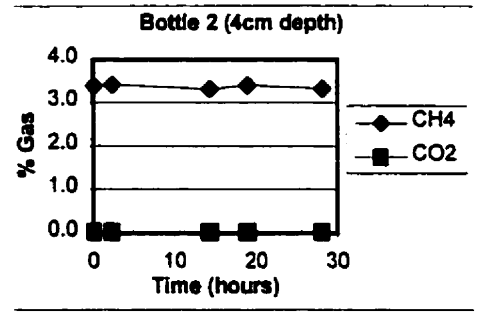

Bottle 4	14 cm depth		
Time(h)	%CH4	%CO2	%O2
0.00	1.469	0.095	19.972
1.20	1.508	0.112	20.769
6.93	1.443	0.120	19.495
9.15	1.317	0.123	19.472
13.18	1.475	0.142	20.202

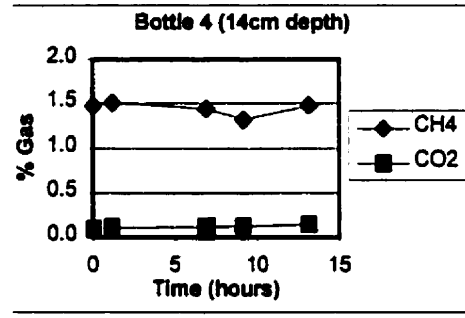

Bottle 6	24 cm depth		
Time(h)	%CH4	%CO2	%O2
0.00	1.466	0.168	20.337
1.18	1.477	0.219	20.410
6.92	1.444	0.329	20.258
9.17	1.431	0.360	19.510

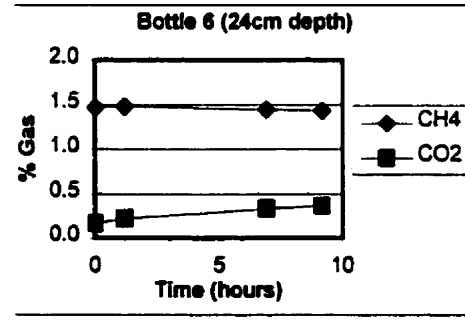

Bottle 8	34 cm depth		
Time(h)	%CH4	%CO2	%O2
0.00	1.481	0.205	20.706
1.20	1.453	0.224	20.712
6.93	1.212	0.710	19.410
9.22	1.125	0.856	19.173
13.02	0.908	1.051	17.409

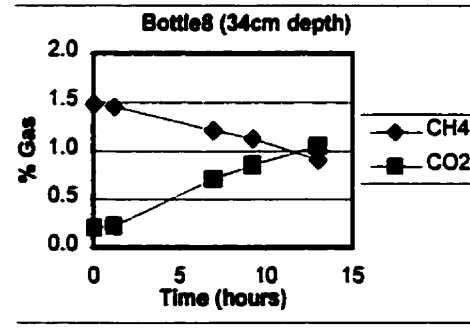

B.2 Springbank Soil Kinetic Experiments: Column SB2 (Continued)

Bottle 1	44 cm depth		
Time(h)	%CH4	%CO2	%O2
0.00	1.453	0.224	20.712
1.18	1.432	0.331	20.649
6.92	1.208	0.627	18.275
9.20	1.198	0.767	18.929
12.92	1.078	0.943	18.333

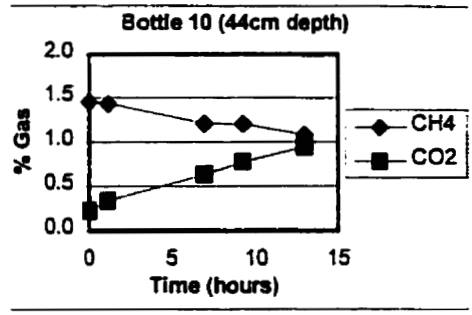

Bottle 1	54 cm depth		
Time(h)	%CH4	%CO2	%O2
0.00	1.445	0.258	19.769
1.22	1.355	0.379	19.774
6.97	0.983	0.771	19.013
9.23	0.823	0.909	18.421
12.88	0.558	1.105	17.672

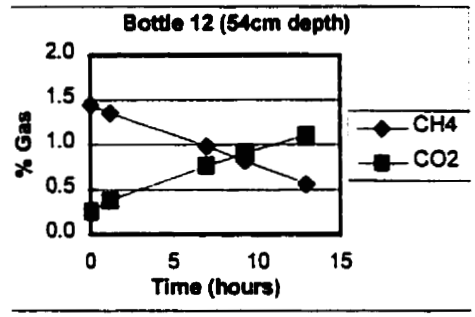

Bottle 1	64 cm depth		
Time(h)	%CH4	%CO2	%O2
0.00	1.429	0.373	20.342
1.25	1.149	0.542	19.227
6.98	0.106	1.124	16.823
9.33	0.003	1.197	17.423
12.83	0.001	1.351	16.275

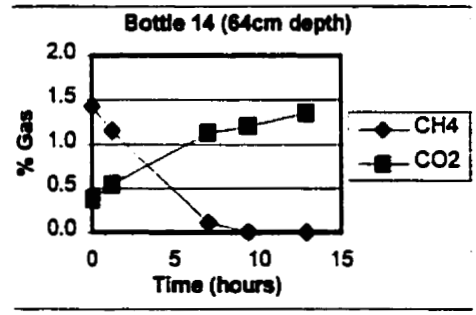

Bottle 1	74 cm depth		
Time(h)	%CH4	%CO2	%O2
0.00	1.443	0.428	19.091
1.30	1.283	0.555	18.443
7.03	0.393	1.023	17.528
9.43	0.142	1.197	17.423
12.83	0.002	1.287	16.649

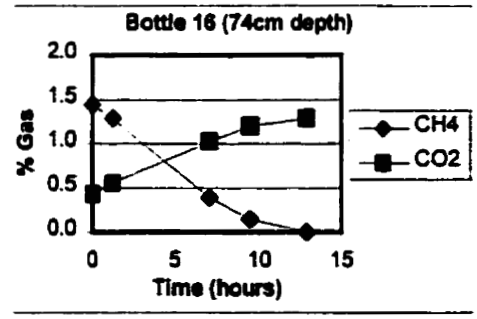

B.2 Springbank Soil Kinetic Experiments: Column SB2 (Continued)

Bottle 1	Blank		
Time(h)	%CH4	%CO2	%O2
0.00	2.234	0.086	20.412
1.33	2.205	0.083	19.928
7.08	2.150	0.085	19.351
9.55	2.222	0.093	20.275

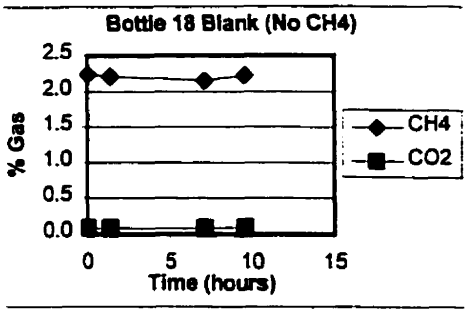

Springbank soil: Column SB2 10-Mar-99

Bottle #	Depth (cm)	Mass of bottle (g)	Mass of bottle+soi (g)	Tot.mass 4h@104 (g)	Mass of dry soil (g)	Moisture content % dry wt.
2	4	167.156	187.982	187.75	20.5931	1.13
4	14	167.365	187.266	186.834	19.4695	2.22
6	24	167.093	186.55	185.169	18.0762	7.64
8	34	167.366	185.893	183.763	16.3974	12.99
10	44	166.605	183.789	181.66	15.0546	14.14
12	54	167.69	190.116	187.559	19.869	12.87
14	64	167.467	189.08	186.609	19.1419	12.91
16	74	166.796	188.809	186.636	19.8395	10.95
18	blank	167.126	167.126	167.126	0	0.00

Reaction Rates - Column SB2, Q_{CH4}=319 g/m²/day

Bottle #	Depth (cm)	Gas Consumption Rates (nmol * hour^{-1} * $g_{dry soil}^{-1}$)					
		CH_4	r-sqd	CO_2	r-sqd	O_2	r-sqd
2	4	0.00	0.1590	-7.14	0.8916	0.00	0.1913
4	14	19.52	0.1523	-15.81	0.8961	186.12	0.1246
6	24	16.51	0.8943	-117.44	0.9808	438.67	0.6444
8	34	267.49	0.9916	-441.91	0.9886	1543.33	0.9407
10	44	194.76	0.9794	-382.30	0.9964	1402.53	0.8123
12	54	350.59	0.9994	-346.27	0.9947	865.01	0.9695
14	64	1217.32	0.9989	-578.44	0.9977	2615.14	0.9787
16	74	743.00	0.9962	-429.66	0.9989	908.49	0.9273

B.2 Springbank Soil Kinetic Experiments: Column SB2 (Continued)

Soil Gas Concetnrations andReaction Rates
Column SB2, Q_{CH4}=328 g/m^2/day

Depth (cm)	% CH4	% O2	Rate of CH4 consumption
6	2.80	16.93	0.00
16	6.63	13.57	19.52
26	9.94	10.89	16.51
36	14.80	7.33	267.49
46	20.18	5.58	194.76
56	25.84	3.21	350.59
66	32.21	1.41	1217.32
76	38.13	0.73	743.00

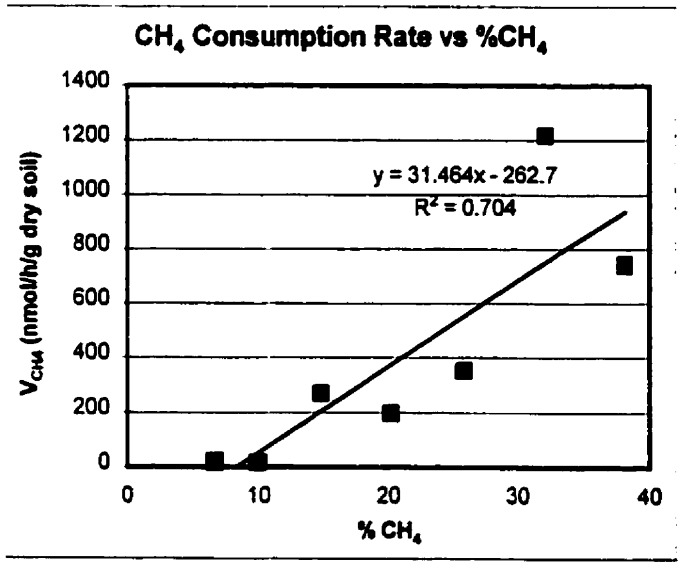

B.3 Springbank Soil Kinetic Experiments: Column SB3

Bottle 24	6 cm depth		
Time(h)	%CH4	%CO2	%O2
0.00	3.598	0.106	21.012
1.37	3.502	0.107	20.609
13.75	3.473	0.175	20.144
18.95	3.330	0.165	20.349

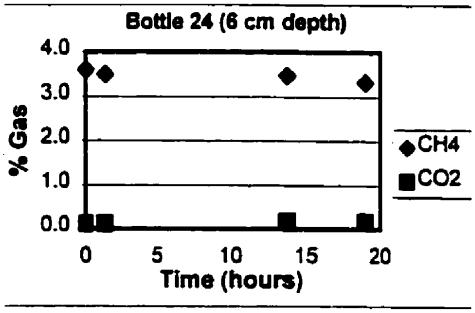

Bottle 23	16 cm depth		
Time(h)	%CH4	%CO2	%O2
0.00	3.211	0.097	20.888
1.38	3.143	0.102	21.082
13.80	3.079	0.170	20.130
18.98	3.028	0.172	20.526
37.53	2.931	0.182	20.132

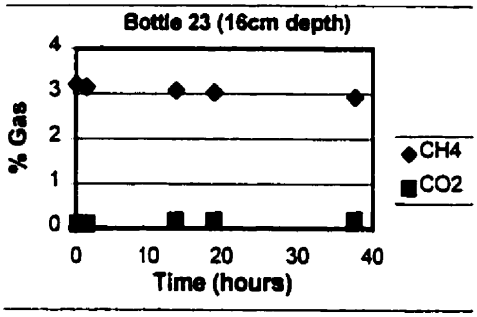

Bottle22	26 cm depth		
Time(h)	%CH4	%CO2	%O2
0.00	3.323	0.233	20.762
1.37	3.305	0.245	20.185
13.78	3.277	0.417	19.746
18.97	3.330	0.446	19.998
37.52	3.255	0.506	

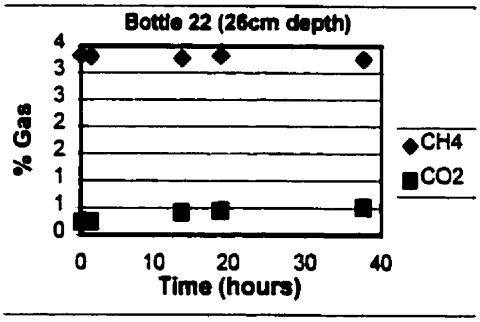

Bottle 21	36 cm depth		
Time(h)	%CH4	%CO2	%O2
0.00	3.260	0.523	20.205
1.38	2.987	0.570	19.607
13.80	2.381	1.778	17.942
18.97	2.056	2.098	17.612
37.55	0.908	3.429	15.896

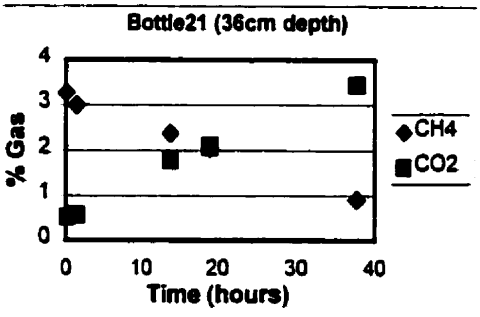

B.3 Springbank Soil Kinetic Experiments: Column SB3 (Continued)

Bottle 20	46 cm depth		
Time(h)	%CH4	%CO2	%O2
0.00	3.015	0.604	20.151
1.38	2.973	0.720	20.017
13.80	2.232	2.160	17.605
18.98	1.848	2.568	17.129
37.55	0.497	4.049	15.202

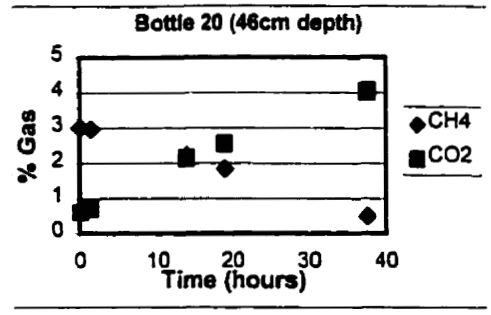

Bottle 19	56 cm depth		
Time(h)	%CH4	%CO2	%O2
0.00	2.916	0.666	19.861
1.37	2.811	0.816	18.295
13.78	1.437	2.522	16.661
18.97	0.888	2.939	16.150
37.53	0.052	4.202	14.587

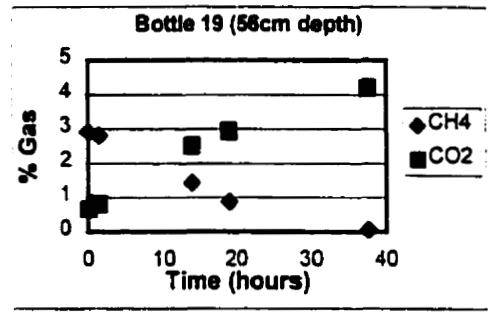

Bottle 18	66 cm depth		
Time(h)	%CH4	%CO2	%O2
0	3.6	0	20.9
6.37	1.853	0.995	19.014
7.75	1.184	1.042	18.347
20.15	0.079	2.928	15.532
25.42	0.000	3.049	15.661

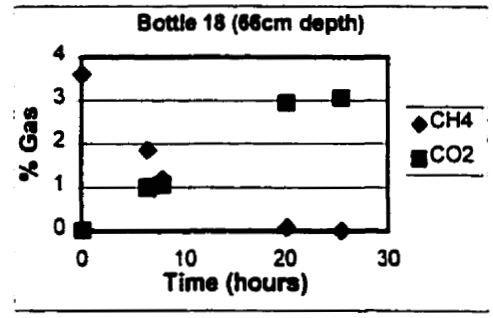

Bottle 17	76 cm depth		
Time(h)	%CH4	%CO2	%O2
0.00	3.598	0.000	20.900
6.37	1.655	1.009	18.299
7.75	1.089	1.196	17.898
20.15	0.000	2.513	15.901

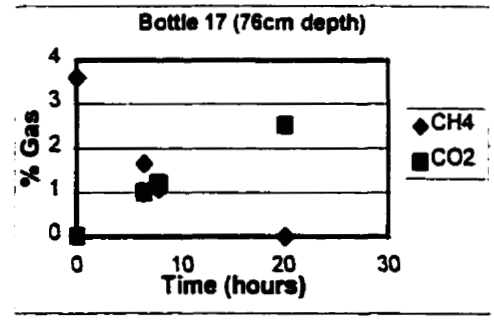

B.3 Springbank Soil Kinetic Experiments: Column SB3 (Continued)

Springbank soil: Column SB3 10-Mar-99

Bottle #	Depth (cm)	Mass of bottle (g)	Mass of bottle+soi (g)	Tot. Mass 24h@104 (g)	Mass of dry soil (g)	Moisture content % dry wt.	Initial Moisture % dry wt.
24	0	171.01	190.693	190.531	19.5208	0.83	9.4
23	6	170.855	193.099	192.157	21.302	4.42	9.4
22	16	170.566	186.618	185.777	15.2109	5.53	9.4
21	26	171.245	187.837	186.123	14.8778	11.53	9.4
20	36	171.199	186.026	184.132	12.9336	14.64	9.4
19	46	171.32	186.203	184.541	13.2217	12.57	9.4
18	56	170.754	189.563	187.546	16.7923	12.01	9.4
17	66	170.943	193.158	191.428	20.4852	8.45	9.4

Reaction Rates

Bottle #	Depth (cm)	Gas Consumption Rates (nmol * hour^{-1} * $g_{drysoil}^{-1}$)					
		CH_4	r-sqd	CO_2	r-sqd	O_2	r-sqd
24	6	57.08	0.7969	-20.02	0.8858	122.61	0.6502
23	16	33.68	0.9511	-11.68	0.7649	112.35	0.6502
22	26	9.50	0.4447	-52.16	0.8787	242.64	0.5774
21	36	423.40	0.9941	-553.86	0.9935	776.99	0.9711
20	46	545.34	0.9962	-752.03	0.9899	1090.62	0.9709
19	56	857.11	0.9494	-985.31	0.9932	1348.05	0.8873
18	66	1872.11	0.9893	-880.67	0.9837	3008.48	1.0000
17	76	1625.70	0.9976	-795.53	0.9995	2013.80	1.0000

Depth (cm)	% CH4	% O2	CH_4 Ox. Rate nmol/h/gd.w.
6	1.50	16.75	57.08
16	2.99	14.50	33.68
26	4.68	11.75	9.50
36	7.17	8.16	423.40
46	12.14	4.58	545.34
56	15.63	3.42	857.11
66	20.13	1.89	1872.11
76	23.19	1.80	1625.70

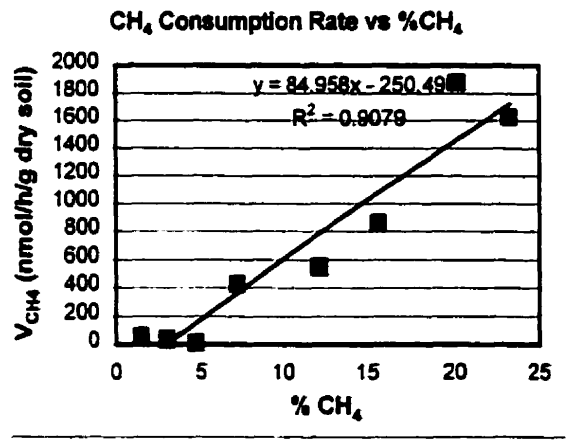

B.4. CH_4 Oxidation Rate Profiles

Column SB1 - CH4 Oxidation Rate Data Q_{CH4}=319g/m²/d

Depth (cm)	Soil [O_2] %	Uncorrected CH_4 ox. rate (nmol/h/g d.w.)	Initial jar [CH_4] (%)	Ks Correct. Vmax (nmol/h/g d.w.)	O_2 correct. ox rate (nmol/h/g d.w.)
4	16.25	6.88	3.26	8.46	7.92
14	13.46	13.13	3.54	15.92	14.71
24	11.49	16.95	2.08	23.06	21.04
34	5.62	205.74	2.43	269.23	225.15
44	3.89	234.97	2.45	306.90	239.22
54	2.52	311.04	3.08	386.78	269.38
64	0.90	767.86	2.53	995.49	448.24
74	0.75	1230.24	1.3	1939.99	785.86

K_{O2}= 1.1 K_{CH4}= 0.75

Partially (K_s) Correct. column CH_4 ox rate = 161.0 g/m²/d
Partially (K_s) Corrected column CH_4 ox eff = 50.4 %
Corrected column CH4 oxidation rate = 82.1 g/m²/d
Corrected CH4 oxidation efficiency = 25.7 %

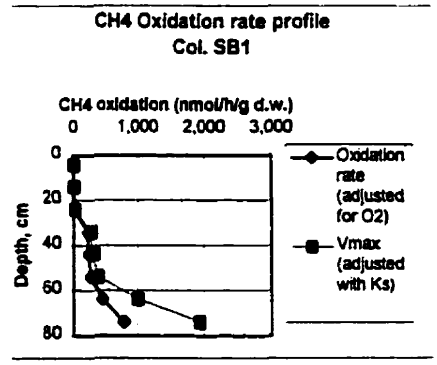

Column SB2 - CH4 Oxidation Rate Data Q_{CH4}=328g/m²/d

Depth (cm)	Soil [O_2] %	Uncorrected CH_4 ox. rate (nmol/h/g d.w.)	Initial jar [CH_4] (%)	Ks Correct. Vmax (nmol/h/g d.w.)	O_2 correct. ox rate (nmol/h/g d.w.)
6	16.93	0.00	1.42	0.00	0.00
16	13.57	19.52	1.47	29.82	27.59
26	10.89	16.51	1.47	25.23	22.92
36	7.33	267.49	1.48	407.74	354.56
46	5.58	194.76	1.45	298.98	249.73
56	3.21	350.59	1.45	538.22	400.70
66	1.41	1,217.32	1.43	1877.91	1,055.25
76	0.73	743.00	1.44	1143.39	457.23

Partially (K_s) Correct. column CH_4 ox rate = 176.4 g/m²/d
Partially (K_s) Corrected column CH_4 ox eff = 55.2 %
Corrected column CH4 oxidation rate = 104.8 g/m²/d
Corrected CH4 oxidation efficiency = 32.8 %

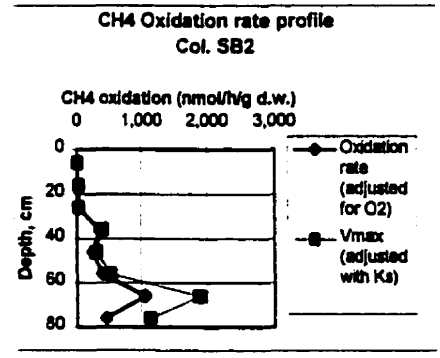

Column SB3 - CH4 Oxidation Rate Data Q_{CH4}=183g/m²/d

Depth (cm)	Soil [O_2] %	Uncorrect. CH_4 ox. rate (nmol/h/g d.w.)	Initial jar [CH_4] (%)	Ks Correct. Vmax (nmol/h/g d.w.)	O_2 correct. ox rate (nmol/h/g d.w.)
6	16.75	57.08	3.6	68.97	64.72
16	14.50	33.68	3.21	41.55	38.62
26	11.75	9.50	3.32	11.64	10.65
36	8.16	423.40	3.26	520.81	458.96
46	4.58	545.34	3.02	680.78	549.00
56	3.42	857.11	2.92	1077.26	814.92
66	1.89	1872.11	3.6	2262.14	1428.52
76	1.80	1625.70	3.6	1964.39	1218.50

Partially (K_s) Correct. column CH_4 ox rate = 270.5 g/m²/d
Partially (K_s) Corrected column CH_4 ox eff = 147.9 %
Corrected column CH4 oxidation rate = 187.1 g/m²/d
Corrected CH4 oxidation efficiency = 102.3 %

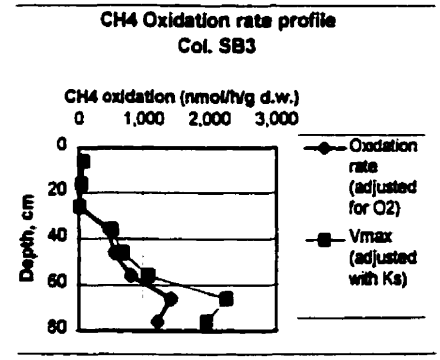

B.5 CH_4 Oxidation Rate as a Function of O_2

B.5.1 Column SB1, 35cm depth

Bottle 1	Initial O_2 = 1.754%	
Time(h)	%CH4	%O2
0.00	1.419	1.754
2.12	1.370	1.581
3.17	1.334	1.747
3.75	1.307	1.558

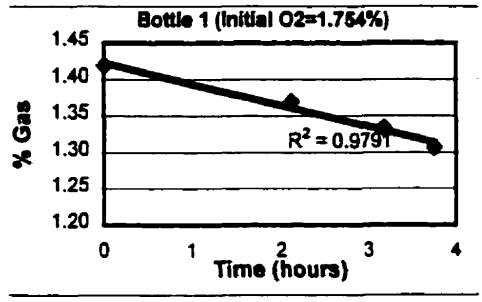

Bottle 3	Initial O_2 = 0.747%	
Time(h)	%CH4	%O2
1.73	1.363	0.630
3.32	1.337	0.534
4.27	1.333	0.507

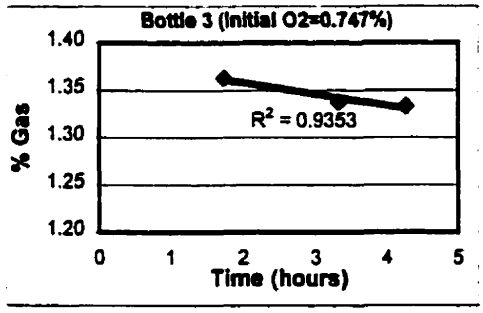

Bottle 5	Initial O_2 = 3.072%	
Time(h)	%CH4	%O2
1.63	1.354	2.805
3.27	1.319	2.657
4.22	1.309	2.695

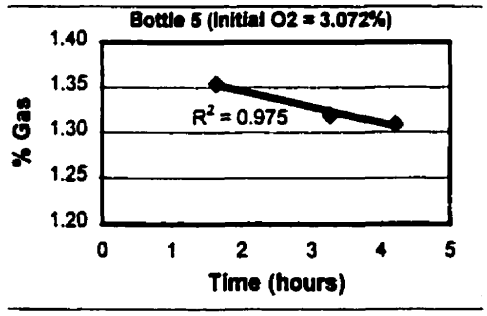

Bottle 7	Initial O_2 = 4.166%	
Time(h)	%CH4	%O2
0.00	1.396	4.166
1.55	1.349	4.038
3.27	1.285	3.761
4.25	1.308	3.906

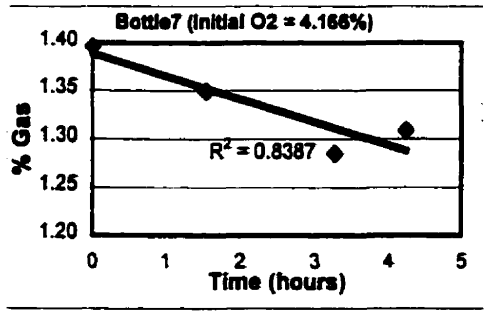

B.5.1 Column SB1, 35cm depth (continued)

Bottle 9	Initial O_2 = 7.267%	
Time(h)	%CH4	%O2
0.00	1.383	7.267
1.47	1.332	7.003
3.27	1.254	6.751
4.22	1.291	7.031

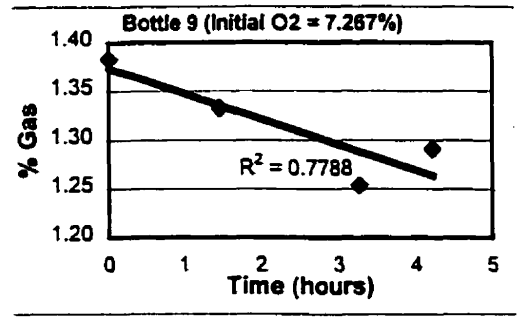

Bottle 11	Initial O_2 = 14.987%	
Time(h)	%CH4	%O2
0.00	1.375	14.987
1.27	1.356	15.616
3.25	1.275	14.782
4.22	1.232	14.436

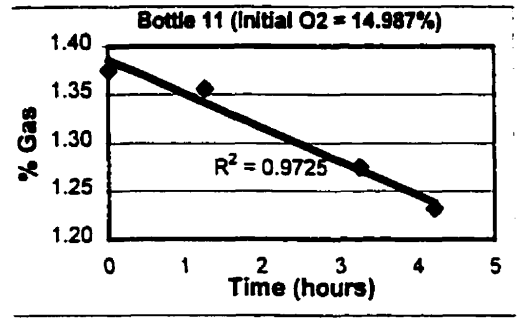

Bottle 13	Initial O_2 = 10.718%	
Time(h)	%CH4	%O2
0.00	1.354	10.718
1.37	1.344	11.010
3.27	1.250	10.270
4.22	1.239	10.285

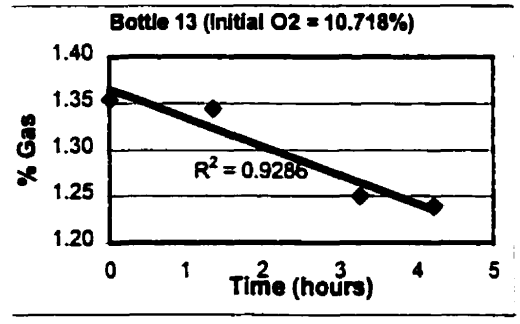

Bottle 15	Initial O_2 = 12.029%	
Time(h)	%CH4	%O2
0.00	1.369	12.029
1.30	1.338	12.242
3.27	1.273	11.645
4.23	1.259	11.634

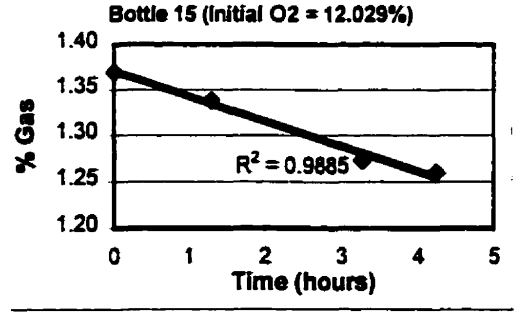

B.5.1 Column SB1, 35cm depth (continued)

Bottle 17	Initial O_2 = 11.726%	
Time(h)	%CH4	%O2
0.00	1.360	11.726
1.23	1.334	11.961
3.25	1.249	11.301
4.23	1.203	11.174

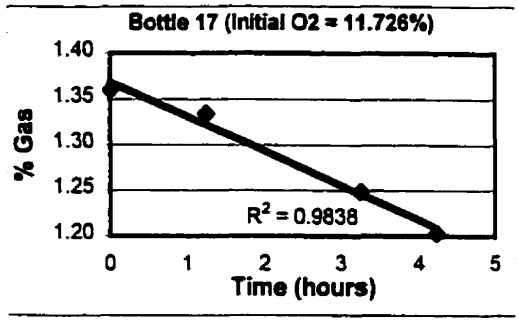

Column SB1 - 36cm depth mass data

Bottle #	Mass of bottle (g)	Mass of bottle+soil (g)	Mass of dry soil (g)
1	167.4277	177.8335	9.005179
3	167.2605	177.6508	8.991766
5	167.82	177.8404	8.671654
7	166.9186	175.9542	7.819408
9	167.4291	177.1015	8.370495
11	167.1615	176.7761	8.320475
13	166.7778	176.8839	8.745819
15	167.4395	177.5262	8.72903
17	167.3269	179.4341	10.47757

Reaction Rates & Eadie Hofstee Plot Data

Bottle #	Initial O_2 %	Gas Reaction Rates (nmol * hour^{-1} * $g_{drysoil}^{-1}$)				V_{O2}/C_{O2}
		CH_4	r-sqd	O_2	r-sqd	(1/h g d.w.)
0	0	0	1	0	1	
3	0.747	143.43	0.9353	580.11	0.9714	192
1	1.754	337.98	0.9791	390.50	0.2785	193
5	3.072	215.75	0.9750	577.71	0.6607	70
7	4.166	318.81	0.8387	1049.33	0.9680	77
9	7.267	325.77	0.7788	939.16	0.9948	45
13	10.718	370.00	0.9885	1770.53	0.6720	35
17	11.726	378.55	0.9838	1645.16	0.7396	32
15	12.029	327.67	0.9885	1543.45	0.6720	27
11	14.987	439.85	0.9725	2217.23	0.4575	29

B.5.2 Column SB1, 76cm Depth

Bottle 2	Initial O_2 = 0.782%	
Time(h)	%CH4	%O2
0.00	1.274	0.782
1.05	1.177	0.335
1.63	1.148	0.408

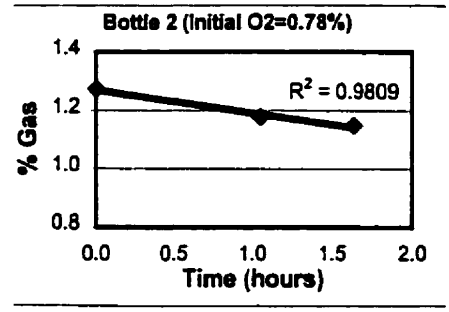

Bottle 4	Initial O_2 = 1.7%	
Time(h)	%CH4	%O2
0.00	1.160	1.700
0.97	1.073	1.566
1.63	1.009	1.382

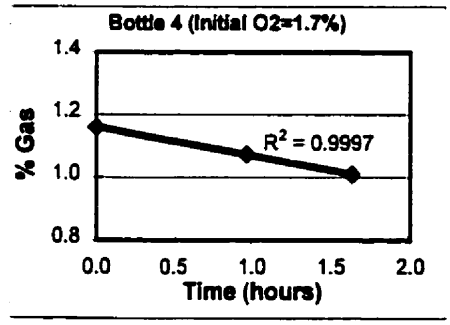

Bottle 6	Initial O_2 = 3.16%	
Time(h)	%CH4	%O2
0.00	1.238	3.156
0.83	1.107	2.828
1.58	0.973	2.454

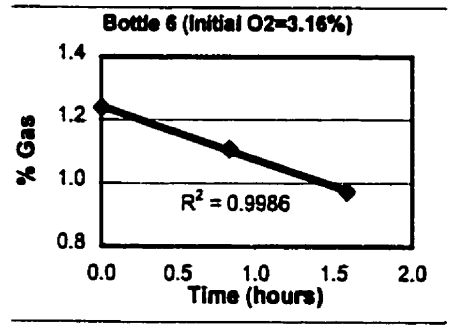

Bottle 8	Initial O_2 = 4.07%	
Time(h)	%CH4	%O2
0.00	0.902	4.072
0.65	0.821	4.195
1.55	0.648	3.557

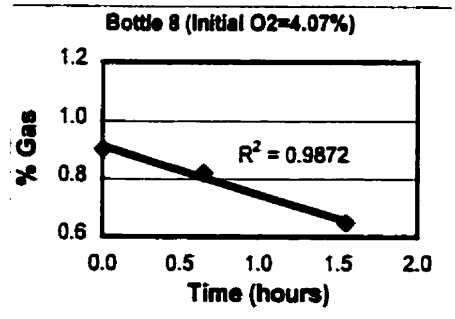

B.5.2 Column SB1, 76cm Depth (Continued)

Bottle 1	Initial O_2 = 7.20%	
Time(h)	%CH4	%O2
0.00	1.202	7.196
0.67	1.130	7.237
1.55	0.958	6.712

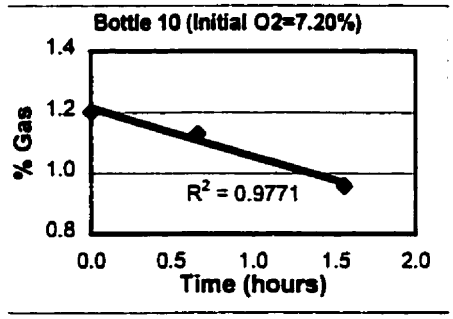

Bottle 1	Initial O_2 = 7.83%	
Time(h)	%CH4	%O2
0.00	1.206	7.831
0.50	1.094	7.444
1.57	0.942	7.414

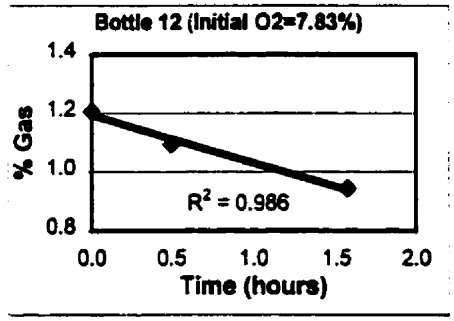

Bottle 1	Initial O_2 = 16.17%	
Time(h)	%CH4	%O2
0.00	1.191	16.174
0.42	1.114	15.785
1.58	0.950	16.320

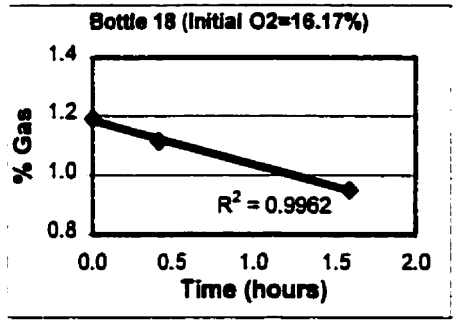

Column SB1 - 76cm depth mass data

Bottle #	Mass of bottle (g)	Mass of bottle+soil (g)	Mass of dry soil (g)
2	167.154	180.368	11.4361
4	167.504	179.917	10.7426
6	167.192	179.314	10.4904
8	167.367	179.718	10.6884
10	166.943	179.432	10.8082
12	167.959	179.501	9.98836
18	167.123	176.46	9.81104

Reaction Rates & Eadie Hofstee Plot Data

Bottle #	Initial O_2 %	Gas Reaction Rates (nmol * hour^{-1} * $g_{dry soil}$) CH_4	r-sqd	O_2	r-sqd	V_{O2}/C_{O2} (1/h g d.w.)
0	0	0	1	0	1	
2	0.782	723.41	0.9809	1530.78	0.7832	925.1
4	1.700	899.97	1.0000	1859.71	1.0000	529.4
6	3.156	1669.76	1.0000	2766.64	1.0000	529.1
8	4.072	1623.58	0.9691	2163.66	0.6077	398.7
10	7.196	1545.11	0.9702	1921.69	0.7400	214.7
12	7.831	1724.70	0.9985	1489.88	0.6944	220.2
18	16.174	1598.59	0.9955	-664.77	0.1555	98.8

B.6 CH_4 Oxidation Rate as a Function of Moisture Content

Column SB1, 35cm Depth

Bottle 7		M.C.=5%
Time(h)	%CH4	%O2
0.00	3.30	20.13
23.63	3.17	19.57
46.80	3.02	19.71
93.77	2.82	19.18

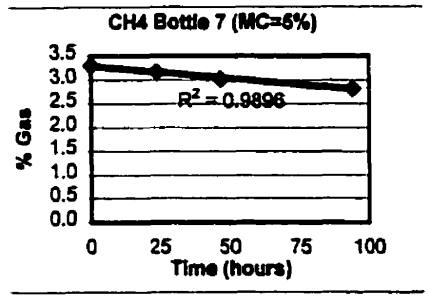

Bottle 8		M.C.=10%
Time(h)	%CH4	%O2
0.00	3.225	19.983
23.50	3.050	19.211
46.58	2.740	
93.65	1.56	16.64

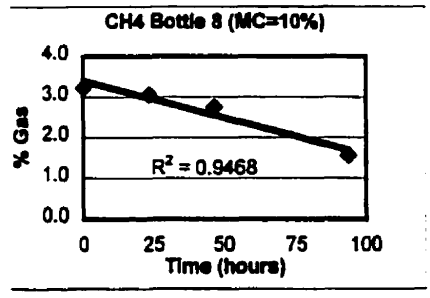

Bottle 9		M.C.=15%
Time(h)	%CH4	%O2
0.00	2.76	20.25
23.45	2.37	18.92
46.42	2.03	19.28
93.60	0.65	16.27

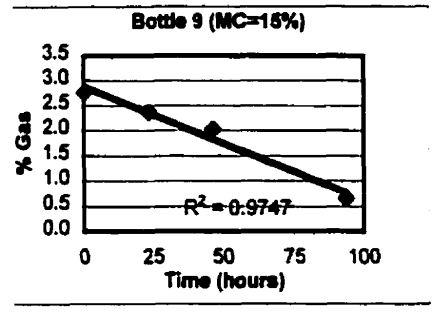

Bottle10		M.C.=1%
Time(h)	%CH4	%O2
0.00	2.47	20.72
23.43	2.43	20.68
46.32	2.29	20.89
93.58	2.21	21.00

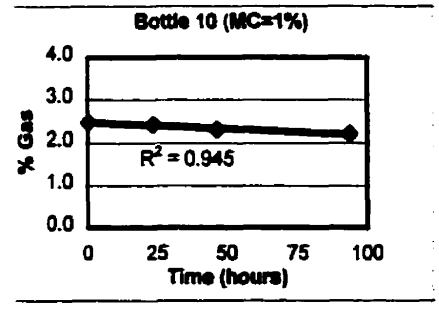

B.6 CH_4 Oxidation Rate as a Function of Moisture Content (Continued)

Bottle 11		M.C.=20%
Time(h)	%CH4	%O2
0.00	2.56	20.21
23.42	2.41	19.30
46.23	2.13	19.37
93.58	1.01	16.51

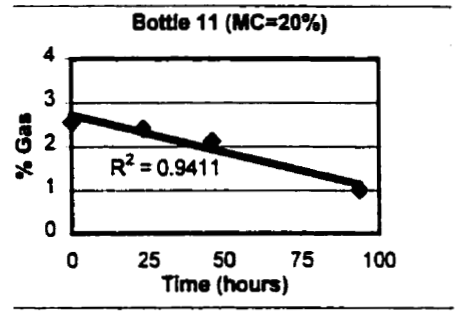

Bottle 12		M.C.=25%
Time(h)	%CH4	%O2
0.00	1.69	20.34
23.40	1.45	19.40
46.10	1.20	19.19
93.58	0.27	16.75

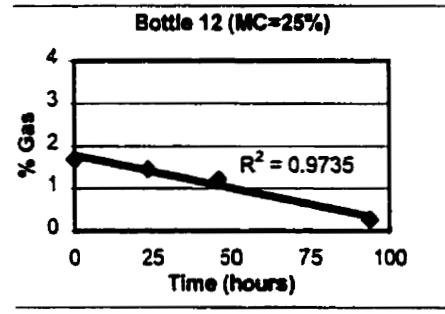

Bottle 13		M.C.=27.3%
Time(h)	%CH4	%O2
0.00	3.195	20.053
23.33	3.016	19.145
46.33	2.811	19.088
93.55	2.069	16.421

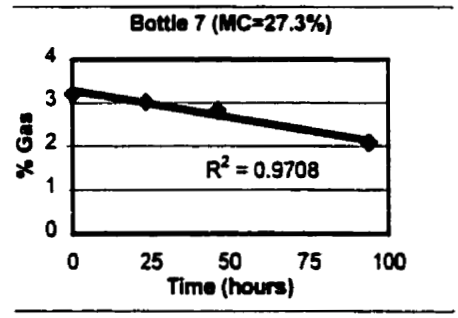

Column SB1 - 36cm depth mass data

Bottle #	Mass of bottle (g)	Mass of bottle+soi (g)	Moisture content (% dry wt)	Mass of dry soil (g)
7	166.784	176.077	6.18	8.75
8	167.37	176.577	10.71	8.32
9	167.189	176.179	15.37	7.79
10	167.383	176.873	0.49	9.44
11	167.162	176.172	23.64	7.29
12	167.69	176.65	19.05	7.53
13	166.778	177.974	27.28	8.80

CH_4 Oxidation Rate vs. M.C.

M.C. (% d.w.)	CH_4 Reaction Rate (nmol * $hour^{-1}$ * $g_{drysoil}^{-1}$)
6.18	61.12
10.71	229.89
15.37	305.15
23.64	214.01
19.05	244.31
27.28	145.40

B.7 CH_4 Oxidation Rate as a Function of Temperature

Column SB1, 35cm Depth

Bottle 1	T=40C	
Time(h)	%CH4	%O2
0.00	3.25	18.80
2.57	3.29	18.98
15.52	3.14	18.09
24.37	3.17	18.45
51.72	2.90	16.34
145.57	2.53	13.59

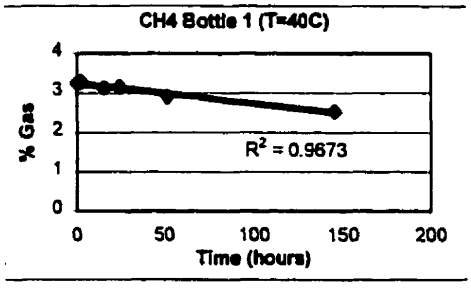

Bottle 2	T=40C	
Time(h)	%CH4	%O2
0.00	3.198	19.018
2.50	2.977	18.247
15.50	3.020	17.740
24.37	2.87	17.39
51.70	2.79	16.25
145.53	2.06	14.18

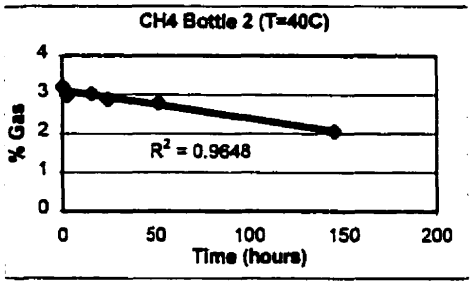

Bottle 3	T=40C	
Time(h)	%CH4	%O2
0.00	2.39	19.34
2.53	2.44	19.84
15.50	2.25	18.29
24.38	2.18	17.89
51.72	2.07	16.87
145.53	1.75	14.26

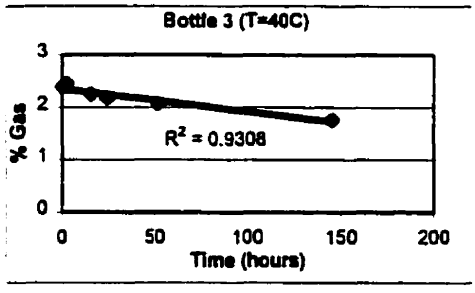

Bottle 4	T=30C	
Time(h)	%CH4	%O2
0.00	3.12	19.87
2.53	3.10	19.61
19.52	2.08	18.05
36.38	2.02	17.00
51.72	0.67	14.96

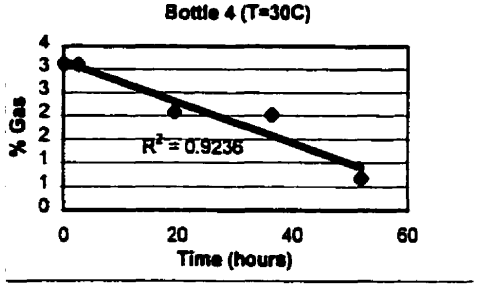

B.7 CH_4 Oxidation Rate as a Function of Temperature (Continued)

Bottle 5	T=30C	
Time(h)	%CH4	%O2
0.00	3.22	19.96
2.53	3.02	18.86
19.48	2.21	17.79
36.38	1.88	16.92
51.72	0.42	14.60

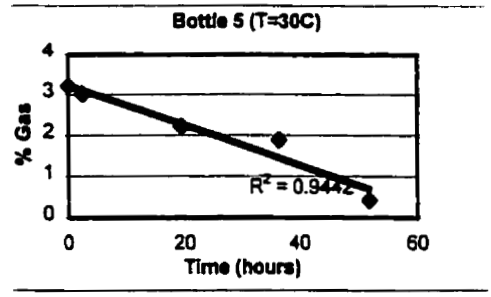

Bottle 6	T=30C	
Time(h)	%CH4	%O2
0.00	2.76	19.30
2.53	2.75	19.44
19.47	2.08	17.71
36.30	1.89	17.69
51.77	0.72	15.82

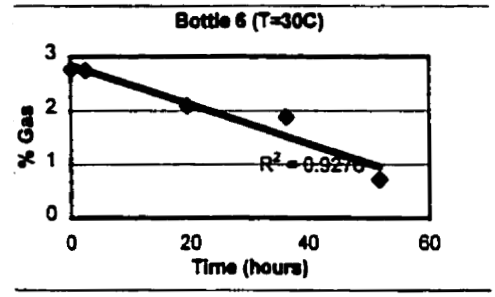

Bottle 7	T=5C	
Time(h)	%CH4	%O2
0.00	2.397	19.027
16.95	2.097	18.963
22.08	2.247	18.974
49.17	2.242	19.343
143.17	2.189	19.759

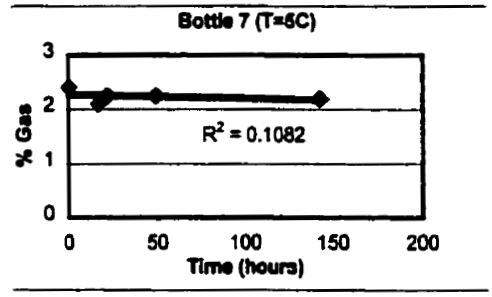

Bottle 8	T=5C	
Time(h)	%CH4	%O2
0.00	2.63	19.26
17.00	2.36	18.83
22.12	2.59	19.23
49.20	2.57	19.60
143.13	1.77	20.03

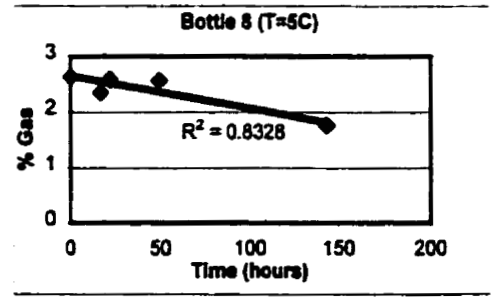

B.7 CH_4 Oxidation Rate as a Function of Temperature (Continued)

Bottle 9	T=5C	
Time(h)	%CH4	%O2
0.00	2.61	19.43
16.95	2.69	18.95
22.10	2.99	19.42
49.18	2.96	19.57
142.98	2.10	19.20

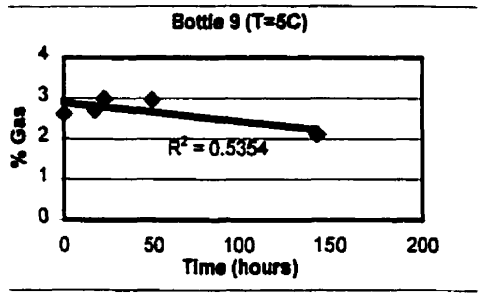

Bottle 10	T=26C	
Time(h)	%CH4	%O2
0.00	3.135	19.169
4.92	2.237	18.395
22.07	2.317	17.719
49.58	1.140	16.692

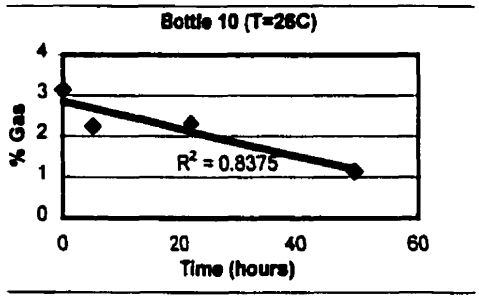

Bottle 11	T=26C	
Time(h)	%CH4	%O2
0.00	2.083	18.844
4.95	1.791	18.401
22.10	1.233	18.496
49.57	0.262	18.074

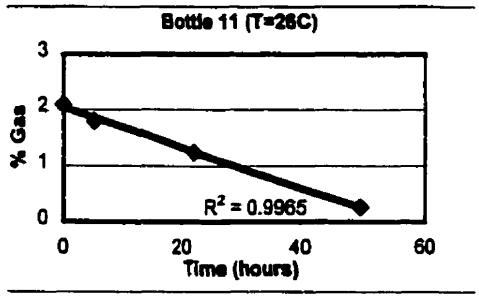

Bottle 12	T=26C	
Time(h)	%CH4	%O2
0.00	2.412	19.615
4.92	1.808	18.114
22.07	1.650	18.255
49.55	0.554	16.770

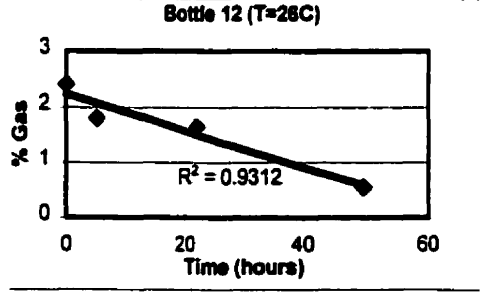

B.7 CH_4 Oxidation Rate as a Function of Temperature (Continued)

Bottle 13	T=12C	
Time(h)	%CH4	%O2
0.00	2.53	19.88
2.50	2.48	19.32
7.48	2.32	19.01
25.27	2.30	19.33
51.28	2.09	19.08
145.70	1.18	18.38

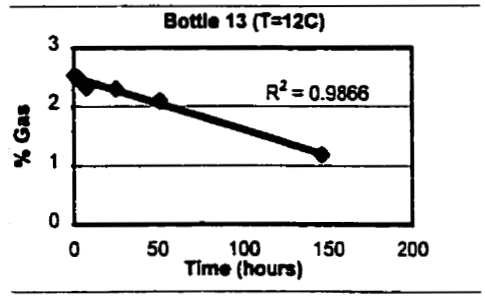

Bottle 14	T=12C	
Time(h)	%CH4	%O2
0.00	2.33	19.62
2.65	2.33	19.35
7.55	2.18	19.12
25.37	2.10	19.39
51.38	1.93	19.11
145.78	0.77	18.99

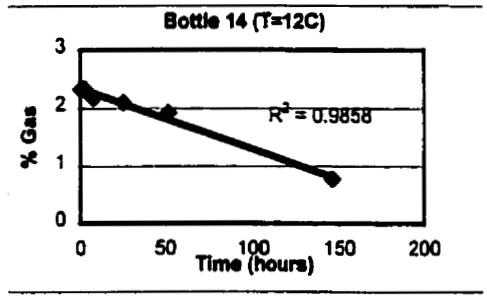

Bottle 15	T=12C	
Time(h)	%CH4	%O2
0.00	3.016	19.85
2.60	3.132	19.831
7.52	2.666	19.031
25.35	2.985	20.096
51.35	2.769	18.994
145.75	1.888	18.501

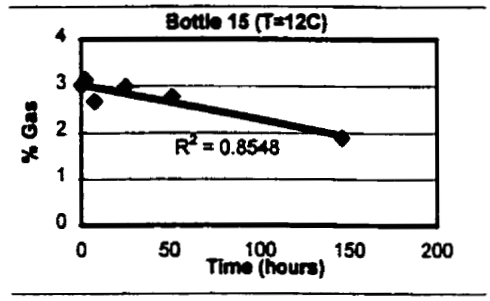

Bottle 16	Blank	
Time(h)	%CH4	%O2
0.00	2.44	20.15
2.58	2.47	20.46
7.50	2.36	19.87
25.35	2.28	20.05
51.57	2.33	20.25
145.65	2.26	21.29

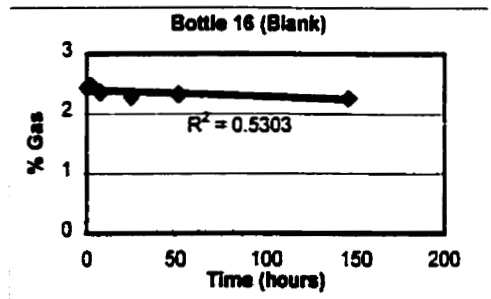

B.7 CH_4 Oxidation Rate as a Function of Temperature (Continued)

Bottle 17	Blank	
Time(h)	%CH4	%O2
0.00	2.24	19.96
2.57	2.28	20.63
7.50	2.18	19.92
25.35	2.22	20.38
51.63	2.20	20.56
145.65	2.11	20.28

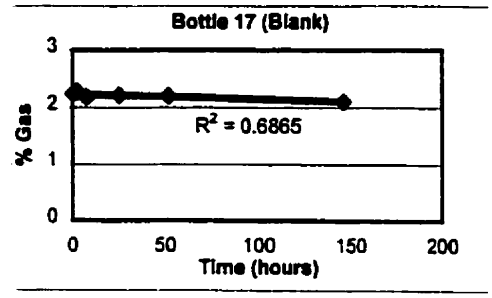

Bottle 18	Blank	
Time(h)	%CH4	%O2
0.00	3.18	20.02
2.57	3.08	20.03
7.45	2.91	19.78
25.32	3.10	20.15
51.60	3.08	20.37
145.65	2.95	20.17

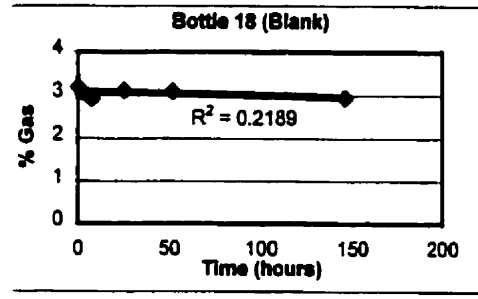

Bottle 19	T=4C	
Time(h)	%CH4	%O2
0.00	3.18	19.71
2.60	3.20	19.71
7.48	3.18	19.54
25.35	3.08	19.72
145.75	2.96	19.94

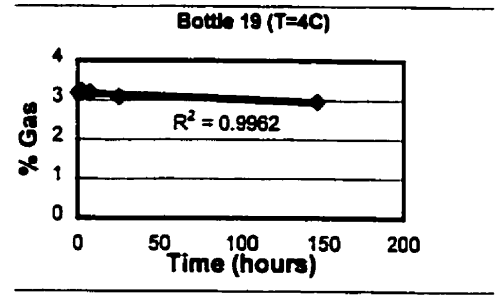

Bottle 20	T=4C	
Time(h)	%CH4	%O2
0.00	1.75	19.96
2.72	1.74	20.35
25.33	1.71	20.18
145.73	1.58	20.13

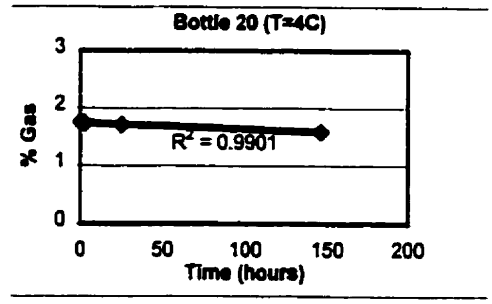

B.7 CH_4 Oxidation Rate as a Function of Temperature (Continued)

Bottle 21	T=4C	
Time(h)	%CH4	%O2
0.00	2.61	19.56
2.75	2.67	20.17
25.33	2.61	19.65
51.57	2.53	19.79
145.83	2.43	19.44

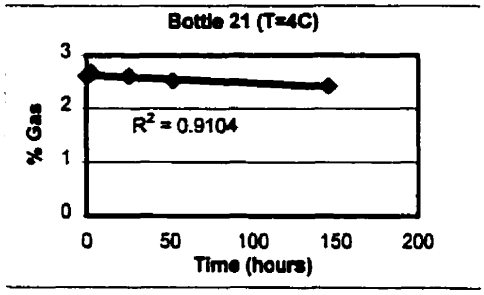

Bottle 22	T=35C	
Time(h)	%CH4	%O2
0.00	2.50	13.28
47.53	2.14	13.41
118.20	1.54	11.79

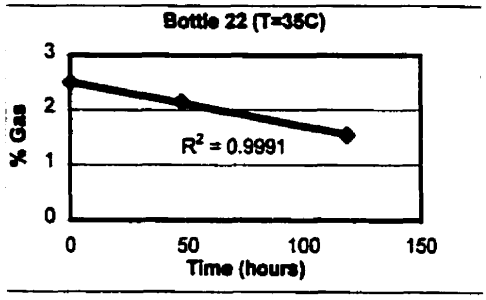

Bottle 23	T=35C	
Time(h)	%CH4	%O2
0.00	2.33	13.55
47.58	1.92	13.33
118.22	1.17	12.43

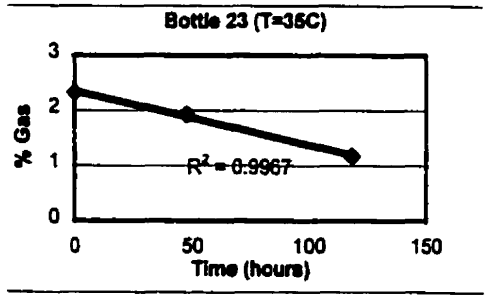

Bottle 24	T=35C	
Time(h)	%CH4	%O2
0.00	1.72	14.10
47.50	1.52	13.91
118.17	0.97	12.43

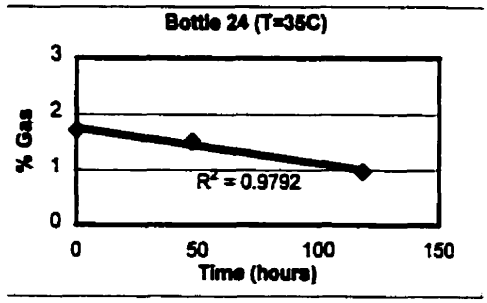

B.7 CH_4 Oxidation Rate as a Function of Temperature (Continued)

Reaction Rates

Bottle #	Temp (deg C)	Gas Reaction Rates (nmol * hour^{-1} * $g_{dryscil}^{-1}$)			
		CH_4	r-sqd	O_2	r-sqd
1	40	64.34	0.9673	468.2974	0.9673
2	40	84.31	0.9648	358.3471	0.9420
3	40	63.68	0.9308	516.21	0.9421
4	30	543.61	0.9236	1124.05	0.9859
5	30	578.03	0.9442	1059.19	0.9481
6	30	521.63	0.9276	917.55	0.9205
7	5	42.27	1.0000	352.30	1.0000
8	5	78.47	0.8328	-92.95	0.7502
9	5	61.45	0.5354	7.42	0.0172
10	26	444.21	0.8375	605.53	0.9456
11	26	487.88	0.9965	164.78	0.7284
12	26	447.95	0.9312	617.82	0.7855
13	12	99.94	0.8893	105.95	0.2526
14	12	137.51	0.9858	38.09	0.4883
15	12	105.06	0.8548	119.01	0.5661
16	BLANK	14.49	0.5303	-102.65	0.7578
17	BLANK	11.25	0.6865	-11.04	0.0253
18	BLANK	11.04	0.2189	-21.76	0.2216
19	4	18.54	0.8946	-23.20	0.7144
20	4	14.53	0.9901	2.41	0.0063
21	4	7.86	0.9901	1.30	0.0063
22	35	102.49	0.9991	168.57	0.7867
23	35	116.03	0.9967	114.85	0.9500
24	35	93.46	0.9792	212.86	0.9070

Soil Mass and Moisture Content Data

Bottle #	Mass of bottle (g)	Mass of bottle+soil (g)	Moisture content (% wt)	Mass of dry soil (g)
1	167.4231	176.7366	11.8	8.33
2	167.1579	177.0598	11.8	8.86
3	167.2625	175.308	11.8	7.20
4	167.3654	176.8195	12.1	8.43
5	167.3544	177.3022	12.1	8.87
6	167.0933	175.266	12.1	7.29
7	166.7877	175.6786	7.5	8.27
8	167.374	175.6501	7.5	7.70
9	167.191	175.6593	7.5	7.88
10	166.605	175.4329	11.8	7.90
11	167.1627	175.7514	11.8	7.68
12	167.6918	176.4253	11.8	7.81
13	166.777	175.6108	11.6	7.92
14	167.4666	176.3891	11.6	8.00
15	167.436	175.7726	11.6	7.47
16	Blank	Blank	Blank	8
17	Blank	Blank	Blank	8
18	Blank	Blank	Blank	8
19	167.1927	176.8098	11.6	8.62
20	167.5573	176.4504	11.6	7.97
21	167.5297	183.9627	11.6	14.72

Appendix C– Soil Column Drawings

Figure C1: Soil Column Top Cap Design

DATE:	Y Y	M M	D D.	TITLE: SOIL MICROCOSM TOP CAP	Page: Of:
	97	10	02		
PROJECT:	V. Stein M.Sc. Thesis				
PREPARED BY:	V. Stein			CHKD BY:	

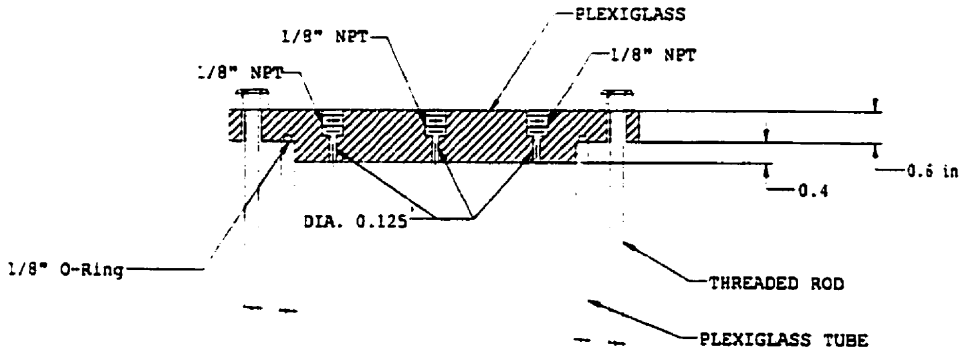

Section A-A

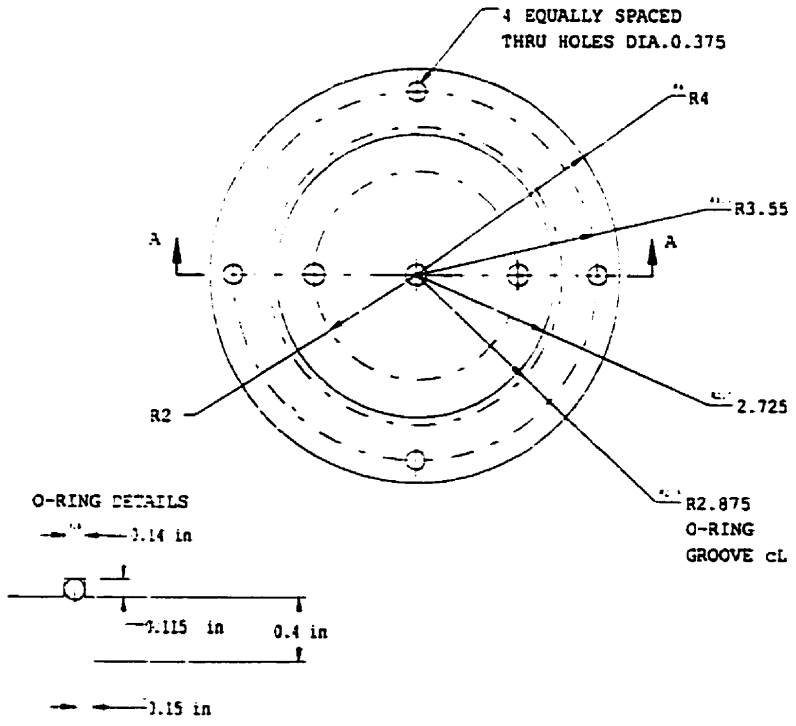

Figure C2: Soil Column Bottom Cap Design

DATE: Y Y M M D D	TITLE: SOIL MICROCOSM BOTTOM CAP	Page:	Of:
97 10 02			
PROJECT: V. Stein M.Sc. Thesis			
PREPARED BY: V. Stein	CHKD BY:		

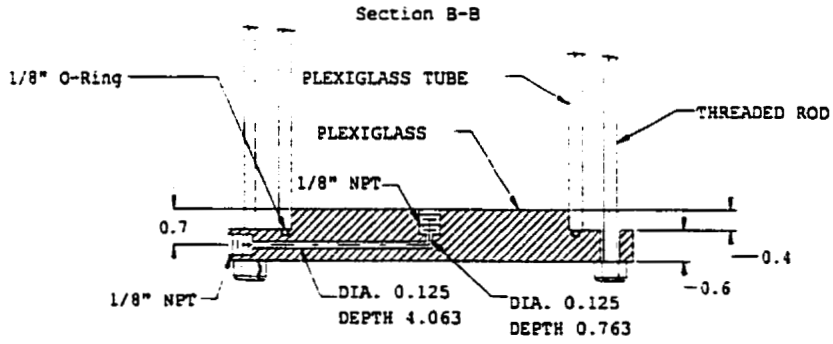

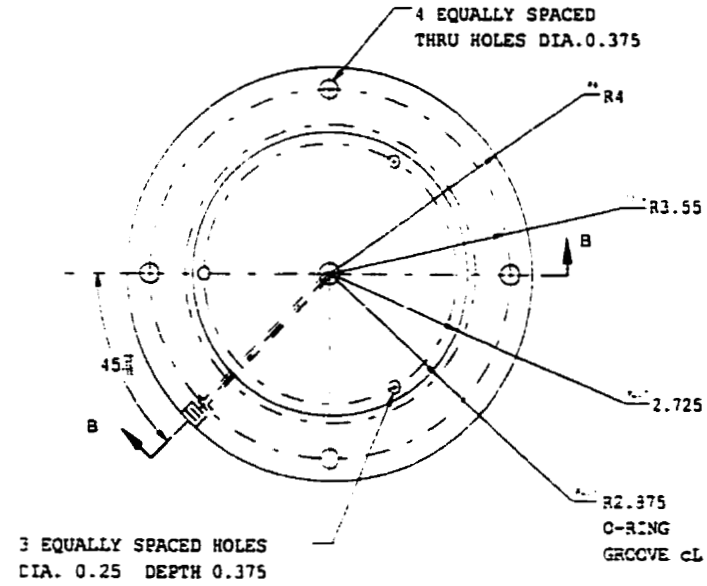

Figure C3: Soil Column Design

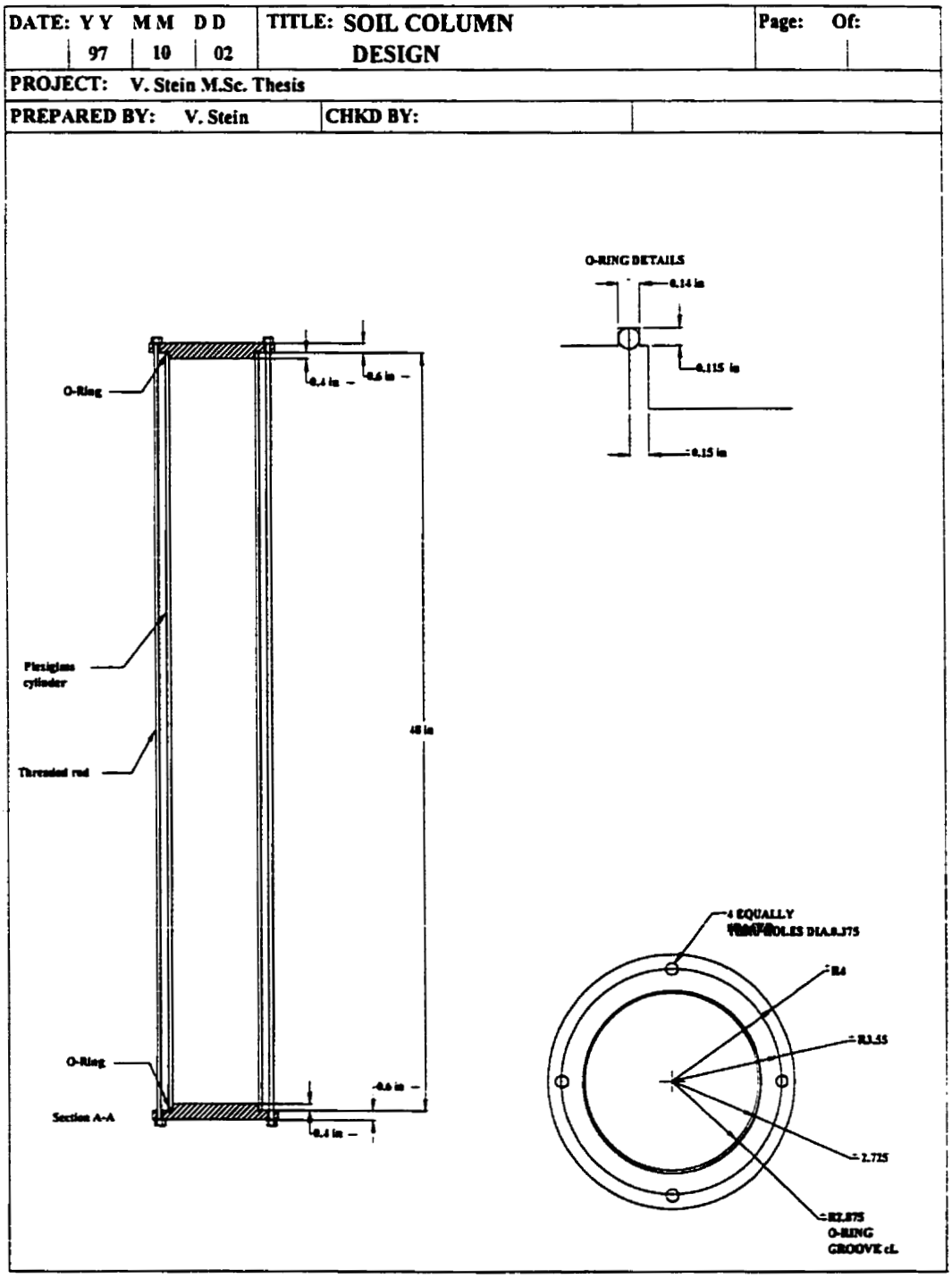

Figure C4: Soil Column Perforated Plate Stand Design

DATE:	Y Y	M M	D D	TITLE:	SOIL MICROCOSM	Page: Of:
	97	11	06		PERFORATED PLATE STAND	
PROJECT:	V. Stein M.Sc. Thesis					
PREPARED BY:	V. Stein			CHKD BY:		

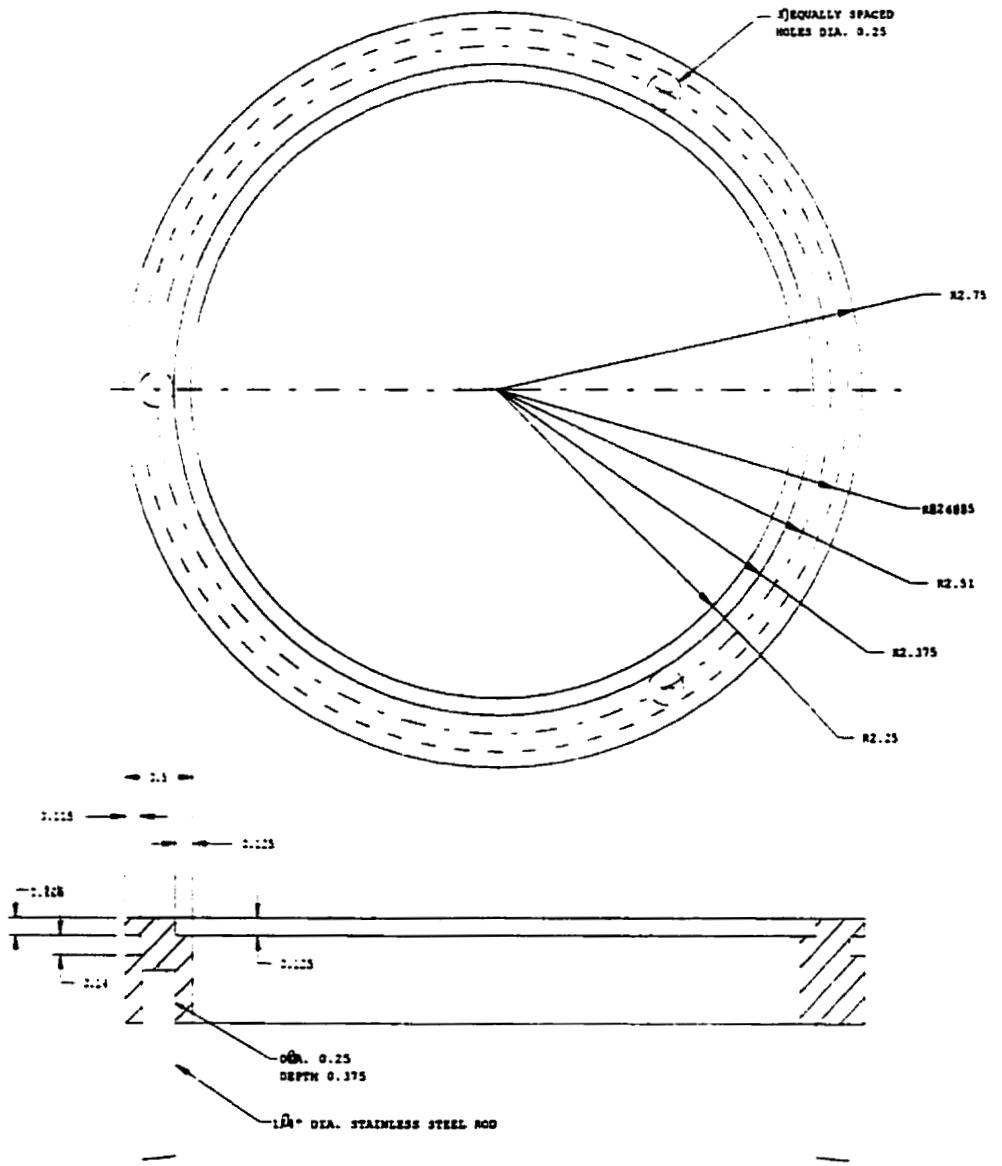

APPENDIX D – Binary Diffusion Coefficients

Binary Diffusion Coefficients (T=293K, P=1.013 bar)

Gas1	Gas2	M_1 (g/mol)	M_2 (g/mol)	Tc1 (K)	Tc2 (K)	Vc1 (m^3/kmol)	Vc2 (m^3/kmol)	D_{12} m^2/s
CH_4	CH_4	16	16	191	191	9.92E-02	9.92E-02	2.23E-05
CH_4	O_2	16	32	191	154	9.92E-02	7.34E-02	2.24E-05
CH_4	CO_2	16	44	191	304	9.92E-02	9.39E-02	1.76E-05
CH_4	N_2	16	28	191	126	9.92E-02	8.98E-02	2.18E-05
O_2	O_2	32	32	154	154	7.34E-02	7.34E-02	2.13E-05
O_2	CO_2	32	44	154	304	7.34E-02	9.39E-02	1.63E-05
O_2	N_2	32	28	154	126	7.34E-02	8.98E-02	2.09E-05
CO_2	CO_2	44	44	304	304	9.39E-02	9.39E-02	1.23E-05
CO_2	N_2	44	28	304	126	9.39E-02	8.98E-02	1.61E-05
N_2	N_2	28	28	126	126	8.98E-02	8.98E-02	2.05E-05

Diffusion Coefficients in Multi-component Mixtures

Mixture Component Ratios				D_{CH4}	D_{O2}	D_{CO2}	D_{N2}
CH_4	O_2	CO_2	N_2	m^2/s	m^2/s	m^2/s	m^2/s
0	0.15	0.25	0.6	2.07E-05	1.93E-05	1.62E-05	1.76E-05
0.25	0.1	0.25	0.4	2.03E-05	1.97E-05	1.66E-05	1.89E-05
0.5	0	0.5	0	1.76E-05	1.89E-05	1.76E-05	1.85E-05
0.5	0.01	0.1	0.39	2.08E-05	2.10E-05	1.69E-05	2.06E-05
0.02	0.19	0.02	0.77	2.18E-05	2.08E-05	1.62E-05	2.05E-05
0	0.2	0	0.8	2.19E-05	2.09E-05	1.62E-05	2.09E-05
0.25	0.15	0	0.6	2.19E-05	2.13E-05	1.65E-05	2.15E-05
0.5	0.1	0	0.4	2.19E-05	2.17E-05	1.69E-05	2.17E-05
0.75	0.05	0	0.2	2.19E-05	2.21E-05	1.72E-05	2.18E-05

APPENDIX E - Steady-State Numerical Model

This appendix presents a failed attempt at obtaining a steady-state solution to Equation 5-11, which when given a soil's mass transfer and biological kinetic parameters as inputs would output soil gas concentrations and CH_4 oxidation rates. A steady state solution was seen as desirable for its computational speed. However, a physically meaningful solution was unobtainable.

To develop this model, the derivatives in the system of transport equations are set to zero, resulting in a simple 1-D boundary value problem. The reaction terms were also set to zero in this preliminary stage of the model's development.

$$D_i \frac{d^2 C_i}{dx^2} - \frac{d(vC_i)}{dx} = 0 \tag{E-1}$$

To ensure maximum accuracy in the finite difference form of Equation E-1, a central-difference scheme is used to create finite difference approximations of both of its terms:

$$-D_i\left[\frac{C_{i,j+1} - 2C_{i,j} + C_{i,j-1}}{(\Delta x)^2}\right] + \left[\frac{C_{i,j+1/2}v_{j+1/2} - C_{i,j-1/2}v_{j-1/2}}{(\Delta x)}\right] = 0 \tag{E-2}$$

Based on figure 5-1, Equation E-2 becomes

$$-D_i\left[\frac{C_{i,j+1} - 2C_{i,j} + C_{i,j-1}}{(\Delta x)^2}\right] + \frac{\left(\frac{C_{i,j+1} + C_{i},j}{2}\right) * v_{j+1/2} - \left(\frac{C_{i,j} + C_{i,j-1}}{2}\right) * v_{j-1/2}}{\Delta x} = 0 \tag{E-3}$$

Combining Equations 5-5 and 5-6 and discretizing, the following expressions for v are obtained:

$$v_{i-1/2} = -K * R * T * \sum_{i=1}^{n} \left(\frac{C_{i,j} - C_{i,j-1}}{\Delta x} \right)$$

$$v_{i+1/2} = -K * R * T * \sum_{i=1}^{n} \left(\frac{C_{i,j+1} - C_{i,j}}{\Delta x} \right) \qquad \text{(E-4)}$$

Substitution of Equation E-4 into Equation E-3 results in a system of non-linear equations for each gas component, which may be solved using an iterative procedure in which the coefficients (in this case the v terms) are lagged. This results in a system of linear equations for each gas component, which can be solved using the equilibrium method. The systems of second order ODEs are coupled, because they share the same total pressure, and consequently the same advective flow velocities.

Lagging the coefficients in equation E-3 gives the following recurrence relationship, which is then used to generate an equilibrium matrix:

$$\left[-\frac{D_{i,j-1/2}}{(\Delta x)^2} - \frac{v_{j-1/2}}{2\Delta x} \right]^K * C_{i,j-1}^{K+1} + \left[\frac{2D_{i,j}}{(\Delta x)^2} + \frac{v_{j+1/2} - v_{j-1/2}}{2\Delta x} \right]^K * C_{i,j}^{K+1} + \left[\frac{-D_{i,j+1/2}}{(\Delta x)^2} + \frac{v_{j+1/2}}{2\Delta x} \right]^K * C_{i,j+1}^{K+1} = 0 \qquad \text{(E-5)}$$

where the K and K+1 superscripts refer to the iteration#.

Boundary Conditions

Lower boundary condition

Again, to simply the model in its initial stage of development only two gases were considered, namely methane and air. For the two-gas case, the lower boundary condition for this problem consists of a constant methane flux, and of an air flux equal to zero.

e.g. $J_{CH4} = 2.25*10^{-4}$ mol*m^{-2}*s^{-1} $J_{AIR} = 0$

This results in the following finite difference equation for CH_4 (lower boundary is at node j=1). Node 0 is a false node, which is eliminated, in the next calculation.

$$C_{CH4,1}\left(\frac{v_{1/2}+v_{1+1/2}}{2}\right)-D_{CH4}\left[\frac{C_{CH4,2}-C_{CH4,0}}{2\Delta x}\right]=J_{CH4} \qquad \text{(E-6)}$$

Combining Equations E-5 and E-6, and then eliminating the $C_{CH4,i-1}$ terms (i.e. the $C_{CH4,0}$ terms):

$$\left[\frac{2D_{CH4}}{\Delta x}+\frac{3}{2}v_{1+1/2}\right]*C_1+\left[\frac{v_{i+1/2}}{2}-\frac{2D_{CH4}}{\Delta x}\right]*C_2=2*J_{CH4} \qquad \text{(E-7)}$$

Upper boundary condition

The upper boundaries are assumed to be at constant (atmospheric) concentrations.

i.e. $C_{CH4} = 1.7$ppm

$C_{AIR} = 41.25$ mol/m^3

Steady State Solution Procedure

Solving a non-linear boundary value problem by lagging the coefficients is an iterative procedure that involves the following steps:

1. Make an initial guess of the steady state concentration profiles;
2. substitute the concentration values into the recurrence relation equations to generate an equilibrium matrix;
3. solving the resulting equilibrium matrix to obtain a new concentration profile;
4. go to step 2, repeating these iterations until the criterion for convergence is met. In this case, the solution was assumed to have converged once the change in concentrations between successive iterations was less than 5% for every node.

The algorithm for carrying out the iterative procedure was first programmed using Mathcad, and then in BASIC. By first programming the algorithm using Mathcad, and then using BASIC, it was possible to determine whether a simulation had failed to converge due to errors in the algorithm or errors in programming.

Results of the Steady-State Solution

Results Trial #1 (obtained with a constant CH_4 concentration profile for the initial guess)

The algorithm converged to an unstable solution, as is depicted in the following graphs.

Fig. 5-2a: Initial guesses for CH_4 and air concentration profiles

Parameters: $\Delta x = 0.1m$; $D_{CH4} = 7*10^{-6}m^2s^{-1}$; $D_{air} = 6.53*10^{-6}m^2s^{-1}$; $K/\mu=3.12*10^{-8}$ Ns

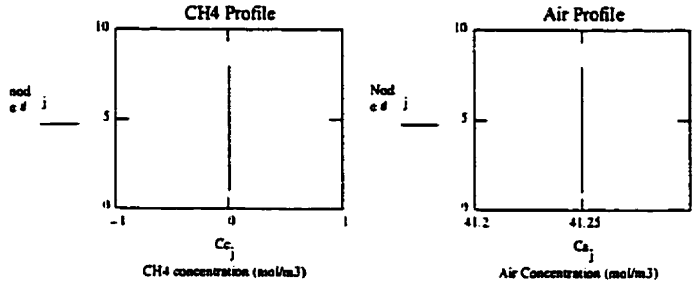

Fig. 5-2b: Concentration Profiles after first iteration (K=1)

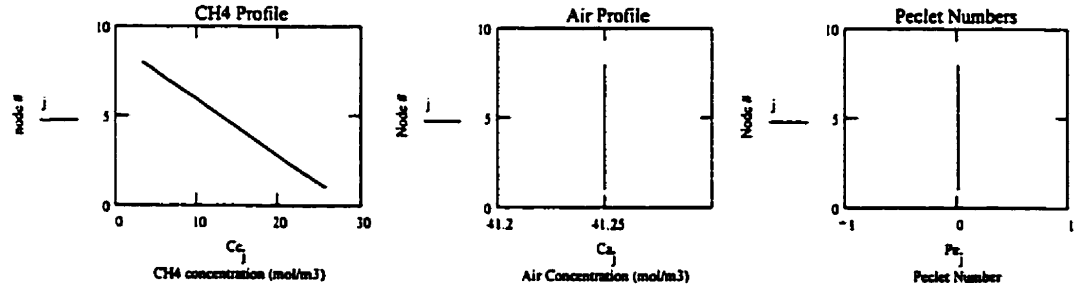

Fig. 5-2c: Concentration Profiles after 2nd Iteration

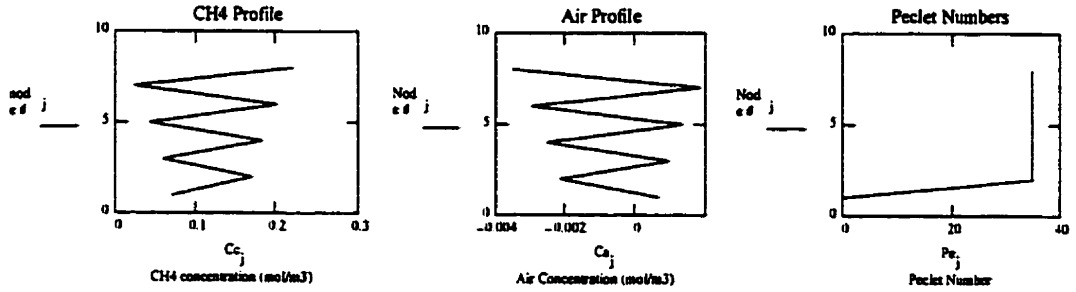

Figure 5-2d: Concentration Profiles after 5th Iteration (Convergence achieved)

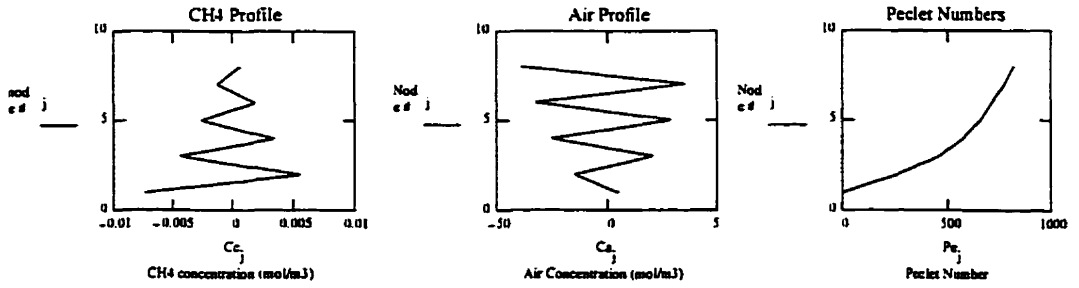

When solving a non-linear boundary value problem using the method of lagging the coefficients, a good initial guess at the solution can reduce the number of iterations, and a bad initial approximation may not converge. However every initial guess made resulted in convergence to the same physically meaningless solution. An attempt was then made to reduce the Peclet number by decreasing the node spacing from 10cm to 0.1cm. However this merely resulted in convergence to a physically meaningless solution with the same concentration magnitudes with a greater frequency in oscillations.
It is hypothesised that the non-linear nature of this problem results in the absence of a unique solution. Unfortunately, the above procedure results in convergence to the physically impossible solution.

Because the equilibrium method failed to produce a physically meaningful solution, an attempt was then made to use an explicit non-steady state method, which will converge to a physically meaningful solution provided that the time-step size is small enough or the node-spacing is sufficiently large.

APPENDIX F - CH_4 Reactive Transport Model Source Code (in BASIC)

```
'CH4ox1.bas
'Soil methane biological oxidation and transport model
'In this version, four nodes are used, with a spacing of 20 cm

DECLARE SUB ReacTran (c(), visc())
DECLARE SUB Viscocity (c(), y(), visc())
DECLARE SUB Density (c(), dens())
DECLARE SUB PrintC (c())
DECLARE SUB Diffusivity (c(), y(), D())
DECLARE SUB Plot (c())

COMMON SHARED perm(), por(), air(), xi(), temp(), db12(), db13(), db14()
COMMON SHARED db23(), db24(), db34(), n, flux(), void(), mc(), Gs, mu(), M()
COMMON SHARED cox(), dt, dz, bulk(), confac()

' Variables:
' perm() = soil's intrinsic permeability
' por() = porosity
' air() = aeration porosity
' xi() = soil's relative diffusivity coefficienty
' temp() = soil temperature
' db12,13,14,23,24,34() = binary diffusion coefficients
' n = number of nodes
' flux() = gas fluxes (1=CH4, 2=O2, 3=CO2, 4=N2)(in mol/m2/s)
' void() = void ratio
' mc() = moisture content (as a ratio of the soil's dry weight)
' Gs = soil particle density (g/m3)
' mu() = viscocity of bulk fluid
' dt = time-step size
' dz = distance between nodes (in m)
' bulk() = bulk density
' moist = soil's initial moisture content

FOR j = 1 TO n
  por(j) = 1 - (bulk(j) / (Gs * 10 ^ 6 * (1 + moist)))
NEXT j


'void ratio
FOR j = 1 TO n
   void(j) = por(j) / (1 - por(j))
NEXT j


CONST Rid = 8.314  'Universal gas constant

'assign values to variables
n = 4
dz = .2
dt = 15
```

```
Gs = 2.5
moist = .094
KO2= 0.45 ' O2 half saturation constant (in mol/m3)
KCH4 = 0.31 ' CH4 half saturation constant (in mol/m3)
DIM c(4, n + 1), perm(n), por(n), temp(n + 1), visc(n + 1), D(4, n), dens(n)
DIM flux(4), mu(4, n + 1), M(4), db12(n), db13(n), db14(n), db23(n), db24(n), db34(n)
DIM air(n), xi(n), void(n), mc(n), bulk(n), confac(n), cox(n)

'Sources/sinks
flux(1) = (5.15 / 5) * 2.24 * 10 ^ -4

'bulk density in g/m3
FOR j = 1 TO n
   bulk(j) = 1.163 * 10 ^ 6
NEXT j

'moisture content
FOR j = 1 TO n
   mc(j) = .094
NEXT j
mc(4) = .00165
mc(3) = .103
mc(2) = .135
mc(1) = .1195

'porosity
FOR j = 1 TO n
  por(j) = 1 - (bulk(j) / (Gs * 10 ^ 6 * (1 + moist)))
NEXT j


'void ratio
FOR j = 1 TO n
   void(j) = por(j) / (1 - por(j))
NEXT j


'free air space
FOR j = 1 TO n
   air(j) = (void(j) - mc(j) * Gs) / (1 + void(j))
NEXT j

'confac  factor for converting reaction rates from nmol/h/gdw to mol/m3/s
FOR j = 1 TO n
   confac(j) = 2.778 * 10 ^ -13 * bulk(j) / (1 + mc)
NEXT j

'temperature (degrees Kelvin)
FOR j = 1 TO n + 1
  temp(j) = 293
NEXT j
```

```
'intrinsic permeability of soil
FOR j = 1 TO n
  perm(j) = 9.72 * 10 ^ -13
NEXT j

'initial gas concentrations
FOR j = 1 TO n + 1
c(1, j) = 7 * 10 ^ -5
c(2, j) = 8.62
c(3, j) = .015
c(4, j) = 32.63
NEXT j

'individual gas molar masses
M(1) = 16
M(2) = 32
M(3) = 44
M(4) = 28

'individual gas viscocities
FOR j = 1 TO n + 1
  mu(1, j) = (1.935 + .0305 * temp(j)) * 10 ^ -6
  mu(3, j) = (-30.212 + .256 * temp(j) - .00035 * temp(j) ^ 2) * 10 ^ -6
  mu(4, j) = (.526 + .071 * temp(j) - .000043 * temp(j) ^ 2) * 10 ^ -6
  mu(2, j) = mu(3, j)
NEXT j

'viscocity of bulk fluid (simplification)
FOR j = 1 TO n + 1
  visc(j) = 1.694 * 10 ^ -4
NEXT j

'relative diffusivity (due to porosity and tortuosity of soil)
FOR j = 1 TO n
   xi(j) = 1 * air(j) ^ 2 / por(j) ^ .666'Millington Quirk second model
NEXT j

'Binary diffusion coefficients
FOR j = 1 TO n
  db12(j) = 2.24 * 10 ^ -5 * (temp(j) / 293) ^ 1.81 * xi(j)
  db13(j) = 1.76 * 10 ^ -5 * (temp(j) / 293) ^ 1.81 * xi(j)
  db14(j) = 2.18 * 10 ^ -5 * (temp(j) / 293) ^ 1.81 * xi(j)
  db23(j) = 1.63 * 10 ^ -5 * (temp(j) / 293) ^ 1.81 * xi(j)
  db24(j) = 2.09 * 10 ^ -5 * (temp(j) / 293) ^ 1.81 * xi(j)
  db34(j) = 1.61 * 10 ^ -5 * (temp(j) / 293) ^ 1.81 * xi(j)
NEXT j

' This is the main routine
SCREEN 2, 1
CLS
t$ = "###.##"
FOR t = 1 TO 1000000
  ReacTran c(), visc()
```

```
  IF t / 100 = INT(t / 100) THEN CLS : PRINT "t="; : PRINT USING t$; t * dt / 3600; : PRINT " hours":
PrintC c(): Plot c()
NEXT t

END



SUB Density (c(), dens())

'This subroutine calcualtes the density of the gas mixture at each node

FOR j = 1 TO n
  dens(j) = (c(1, j) * 16 + c(2, j) * 32 + c(3, j) * 44 + c(4, j) * 28) / 1000
NEXT j

END SUB



SUB Diffusivity (c(), y(), D())

'This subroutine calculates the diffusivity of the four gases for each node
'For now, a constant value will be used for each node.  An equation will
'be added at a later date
'note: gas#1=CH4, gas#2=O2, gas#3=CO2, gas#4=N2

FOR j = 1 TO n
  D(1, j) = (1 - y(1, j)) / ((y(2, j) / db12(j)) + (y(3, j) / db13(j)) + (y(4, j) / db14(j)))
  D(2, j) = (1 - y(2, j)) / ((y(1, j) / db12(j)) + (y(3, j) / db23(j)) + (y(4, j) / db24(j)))
  D(3, j) = (1 - y(3, j)) / ((y(1, j) / db13(j)) + (y(2, j) / db23(j)) + (y(4, j) / db34(j)))
  D(4, j) = (1 - y(4, j)) / ((y(1, j) / db14(j)) + (y(2, j) / db24(j)) + (y(3, j) / db34(j)))
NEXT j

END SUB


SUB Plot (c())
' This subroutine plots a graph of the concentration profiles

  DIM da(4)
  da(1) = &HFFFF
  da(2) = &HF0F
  da(3) = &H1111
  da(4) = &H1F11
  LINE (230, 80)-(230, 180)
  LINE (430, 80)-(430, 180)
  FOR i = 1 TO 4
    FOR j = 1 TO n
    x1 = INT(c(i, j) * 200 / 41.27 + 230)
    y1 = INT(-100 * j * dz + 180 + INT(dz * 100))
    x2 = INT(c(i, j + 1) * 200 / 41.27 + 230)
    y2 = INT(-100 * (j + 1) * dz + 180 + INT(dz * 100))
```

```
    LINE (x1, y1)-(x2, y2), , , da(i)
    NEXT j
  NEXT i
END SUB


SUB PrintC (c())
DIM cp(4, n)

'prints table of concentrations

'convert concentrations from mol/m3 to %
FOR i = 1 TO 4
  FOR j = 1 TO n
    cp(i, j) = 100 * c(i, j) / (c(1, j) + c(2, j) + c(3, j) + c(4, j))
  NEXT j
NEXT i

tit$ = "node    % CH4     % O2     % CO2      % N2    CH4 ox(ml/min)"
tmp$ = "  #    ##.#####   ##.#####   ##.#####   ##.#####    ###.####"
PRINT tit$
FOR j = n TO 1 STEP -1
  PRINT USING tmp$; j; cp(1, j); cp(2, j); cp(3, j); cp(4, j); cox(j)
  tot = tot + cox(j)
NEXT j
coxp = 100 * tot / (flux(1) * 22295)
PRINT
PRINT "%CH4 Oxidized = "; coxp
PRINT
PRINT "node   Dsoil/Dair"
FOR j = n TO 1 STEP -1
  PRINT j; "    "; xi(j)
NEXT j

END SUB


SUB ReacTran (c(), visc())
'This subroutine calculates the changes in gas concentrations due to
'advection, diffusion and microbial oxidation using a predictor-
'corrector method to solve the differential equations

'Variables:
' D(i,j)=Diffusivity of gas i at node j
' dens(j) = density at node j (in g/m3)
' P(j) = Pressure at node j (in Pa)
' Q(i,j) = molar flux of gas i into node j
' y(i,j) = molar fraction of gas i at node j
' r(i,j) = production rate of gas i at node j due to biological reaction
'       (mol/s/m3)
' vm(i,j) = vmax of gas i at node j in nmol/h/g d.w.

DIM D(4, n), dens(n), P(n + 1), Q(4, n + 1)
```

```
DIM y(4, n + 1), r(4, n), r1(4, n), r2(4, n), cs(4, n + 1), vm(4, n)

'Calculate mole fractions
FOR i = 1 TO 4
  FOR j = 1 TO n + 1
    y(i, j) = c(i, j) / (c(1, j) + c(2, j) + c(3, j) + c(4, j))
  NEXT j
NEXT i

Viscocity C(), y(), visc()
Diffusivity c(), y(), D()


'Calculate densities and pressures
FOR j = 1 TO n + 1
'  dens(j) = (c(1, j) * 16 + c(2, j) * 32 + c(3, j) * 44 + c(4, j) * 28) / 1000
  P(j) = Rid * temp(j) * (c(1, j) + c(2, j) + c(3, j) + c(4, j))
NEXT j

' Vmax kinetic parameters for CH4
vm(1, 4) = -10
vm(1, 3) = -111
vm(1, 2) = -272
vm(1, 1) = -924


FOR j = 1 TO n
'  IF c(2, j) < 1.24 THEN vo2 = c(2, j) / 1.24 ELSE vo2 = 1
  vo2 = c(2, j) / (c(2, j) + KO2)
  VCH4 = c(1, j) / (KCH4 + c(1, j))
  r(1, j) = vm(1, j) * vo2 * VCH4 * confac(j)
  r(3, j) = vm(3, j) * vo2 * VCH4 * confac(j)
  r(2, j) = 1.5 * r(1, j)'oxygen
  cox(j) = -r(1, j) * 22295 * dz ' n.b. converts from mol/m3/s to ml/min
  r(4, j) = 0
  r(3, j) = -.8 * r(1, j)  'carbon dioxide
NEXT j


'Calculate fluxes
Q(1, 1) = flux(1)
'note e.g. Q(1,2) refers to the flux of gas 1 into node 2
FOR i = 1 TO 4
cs(i, n + 1) = c(i, n + 1)
  FOR j = 2 TO n
    Q(i, j) = -((D(i, j) + D(i, j - 1)) / 2) * (c(i, j) - c(i, j - 1)) / dz
    k = ((perm(j) + perm(j - 1)) / 2) / ((visc(j) + visc(j - 1)) / 2)
    Q(i, j) = Q(i, j) - k * ((c(i, j) + c(i, j - 1)) / 2) * (P(j) - P(j - 1)) / dz
  NEXT j
  Q(i, n + 1) = -D(i, n) * (c(i, n + 1) - c(i, n)) / (dz / 2)
  k = perm(n) / visc(n + 1)
  Q(i, n + 1) = Q(i, n + 1) - k * c(i, n + 1) * (P(n + 1) - P(n)) / (dz / 2)
NEXT i
```

```
FOR i = 1 TO 4
  FOR j = 1 TO n
    r1(i, j) = r(i, j) / air(j) + (Q(i, j) - Q(i, j + 1)) / (dz * air(j))
    cs(i, j) = c(i, j) + dt * r1(i, j)
  NEXT j
NEXT i

FOR j = 1 TO n
'  IF cs(2, j) < 1.24 THEN vo2 = cs(2, j) / 1.24 ELSE vo2 = 1
  vo2 = cs(2, j) / (cs(2, j) + KO2)
  VCH4 = cs(1, j) / (KCH4 + cs(1, j))
  r(1, j) = vm(1, j) * vo2 * VCH4 * confac(j)
  r(3, j) = vm(3, j) * vo2 * VCH4 * confac(j)
  r(2, j) = 1.5 * r(1, j)'oxygen
  cox(j) = -r(1, j) * 22295 * dz ' n.b. converts from mol/m3/s to ml/min
  r(4, j) = 0
  r(3, j) = -.8 * r(1, j)  'carbon dioxide
NEXT j



'Calculate fluxes
Q(1, 1) = flux(1)
'note e.g. Q(1,2) refers to the flux of gas 1 into node 2
FOR i = 1 TO 4
  FOR j = 2 TO n
    Q(i, j) = -((D(i, j) + D(i, j - 1)) / 2) * (cs(i, j) - cs(i, j - 1)) / dz
    k = ((perm(j) + perm(j - 1)) / 2) / ((visc(j) + visc(j - 1)) / 2)
    Q(i, j) = Q(i, j) - k * ((cs(i, j) + cs(i, j - 1)) / 2) * (P(j) - P(j - 1)) / dz
  NEXT j
  Q(i, n + 1) = -D(i, n) * (cs(i, n + 1) - cs(i, n)) / (dz / 2)
  k = perm(n) / visc(n + 1)
  Q(i, n + 1) = Q(i, n + 1) - k * cs(i, n + 1) * (P(n + 1) - P(n)) / (dz / 2)
NEXT i

FOR i = 1 TO 4
  FOR j = 1 TO n
    r2(i, j) = r(i, j) / air(j) + (Q(i, j) - Q(i, j + 1)) / (dz * air(j))
    c(i, j) = c(i, j) + dt / 2 * (r1(i, j) + r2(i, j))
  NEXT j
NEXT i

END SUB


SUB Viscocity (c(), y(), visc())
'This subroutine calculates the viscocity of the gas mixture at each node.

DIM th(4, 4)

FOR j = 1 TO n + 1
  FOR i = 1 TO 4
    FOR k = 1 TO 4
```

```
      th(i, k) = (1 + (mu(i, j) / mu(k, j)) ^ .5 * (M(k) / M(i)) ^ .25) ^ 2
      th(i, k) = th(i, k) / (2.8284 * (1 + M(i) / M(k)) ^ .5)
    NEXT k
  NEXT i
NEXT j

FOR j = 1 TO n + 1
visc(j) = 0
  FOR i = 1 TO 4
    FOR k = 1 TO 4
      IF k <> i THEN sum = sum + th(i, k) * y(k, j) / y(i, j)
    NEXT k
    visc(j) = visc(j) + mu(i, j) / (1 + sum)
    sum = 0
  NEXT i
NEXT j

END SUB
```